AD NUMBER

AD820688

NEW LIMITATION CHANGE

TO

Approved for public release, distribution unlimited

FROM

Distribution authorized to U.S. Gov't. agencies and their contractors; Administrative/Operational Use; Sep 1967. Other requests shall be referred to Director, Air Force Aero Propulsion Lab., Wright-Patterson AFB, OH 45433.

AUTHORITY

AFAPL ltr, 12 Apr 1972

AFAPL-TR-67-116

HIGH TEMPERATURE HYDROCARBON FUELS RESEARCH IN AN ADVANCED AIRCRAFT FUEL SYSTEM SIMULATOR ON FUEL AFFB-8-67

Harold Goodman
Royce Bradley
Theodore Sickles

NORTH AMERICAN AVIATION, INC./LOS ANGELES DIVISION

TECHNICAL REPORT AFAPL-TR-67-116

SEPTEMBER 1967

AIR FORCE AERO PROPULSION LABORATORY
RESEARCH AND TECHNOLOGY DIVISION
AIR FORCE SYSTEM COMMAND
WRIGHT-PATTERSON AIR FORCE BASE, OHIO

NOTICE

When Government drawings, specifications, or other data are used for any purpose other than in connection with a definitely related Government procurement operation, the United States Government thereby incurs no responsibility nor any obligation whatsoever; and the fact that the Government may have formulated, furnished, or in any way supplied the said drawings, specifications, or other data, is not to be regarded by implication or otherwise as in any manner licensing the holder or any other person or corporation, or conveying any rights or permission to manufacture, use, or sell any patented invention that may in any way be related thereto.

Copies of this report should not be returned unless return is required by security considerations, contractual obligations, or notice on a specific document.

HIGH TEMPERATURE HYDROCARBON FUELS RESEARCH IN AN ADVANCED AIRCRAFT FUEL SYSTEM SIMULATOR ON FUEL AFFB-8-67

Harold Goodman
Royce Bradley
Theodore Sickles

FOREWORD

This report was prepared by North American Aviation, Inc./ Los Angeles Division under Contract No. AF33(615)-3228 which bears the Budget Program Sequence Numbers 6(63 304801 62405214) and 5(68 0100 61430014). This contract is monitored by the Air Force Aero Propulsion Laboratory with Mr. Alan E. Zengel as Air Force Project Engineer. The North American Aviation Program Manager is Mr. Harold Goodman; Project Engineer is Mr. Royce P. Bradley; and assisting Mr. Bradley is Mr. T. G. Sickles.

This report covers the first fuel series of Phase II which was conducted from 3 January 1967 to 3 May 1967. This report was submitted by the author on 14 August 1967.

Publication of this report does not constitute Air Force approval of the report's findings or conclusions. It is published only for the exchange and stimulation of ideas.

Arthur V. Churchill

ARTHUR V. CHURCHILL, Chief
Fuels, Lubrication and Hazards Br.
Support Technology Division

ABSTRACT

At elevated temperatures hydrocarbon jet fuels tend to form deposits which decrease heat exchanger efficiency and plug screens and filter elements. A small-scale device is required which has been demonstrated to be applicable to all qualities of hydrocarbon jet fuels and will quantify this tendency in terms meaningful to fuel system designers. In this report, the thermal stability of a fuel (AFFB-8-67) is quantified in terms of amount of deposit in an airframe and engine fuel system simulator. The data obtained from this first fuel series indicate that an expression, derived herein, in terms of time and temperature may predict the amount of deposits formed in any engine system using fuel AFFB-8-67.

Presently, the fuel's tendency to form deposits is determined by visual ratings of color. Two methods for determining the amount of deposits formed in a tube are discussed and a very favorable comparison results. A relationship is shown herein between these calculated values and the color of the deposits. It is shown that at certain levels of deposit thickness a color scale is insensitive to the amount of deposits. In addition to fuel testing in the simulator, fuel AFFB-8-67 was tested in the Standard, Gas, Research, Modified and Micro Cokers, Minex, Thermal Precipitation Apparatus, 5 ml Bomb, and Esso's Standard Screening Unit.

Comparisons made to data obtained in small-scale tests and the FAA-SST Data Correlation Study indicate that a static system (i.e., an "empty" wing tank) does not rank fuels the same as a dynamic system (i.e., engine system). Therefore, a dual type (static and dynamic) thermal stability device may be indicated. It was also indicated that the comparison criteria used in many of the small-scale tests yield breakpoints (initial deposition temperatures) 100 to 200°F below that indicated in the fuel system simulator.

This effort is continuing with the testing of additional fuels and a Fuel Series Report will be released two months after completion of each fuel tested. The applicability of the above findings to these fuels will be reported therein.

TABLE OF CONTENTS

ILLUSTRATIONS

ILLUSTRATIONS

SECTION I

INTRODUCTION

In an effort to investigate advanced hydrocarbon fuel performance with respect to thermal stability under simulated high Mach number flight conditions, this program was initiated to furnish an aircraft airframe and engine fuel system simulator and subsequently conduct a fuels research program. The simulator is to provide generalized performance data on various advanced fuels that will be used to correlate small-scale thermal stability laboratory tests and provide information on design criteria for future supersonic aircraft.

Phase I of this program consisted of the design, installation, and checkout of an advanced aircraft fuel system simulator. A detailed report on this phase can be found in Reference 2. The FAA-SST Fuel System Test Rig, discussed in Reference 4 was modified during this phase to increase the fuel system simulation capability to the speed regime of interest. Upon completion of this task, performance tests were conducted, and the simulator was found to fulfill the design profile requirements set forth by the Air Force.

Phase II, reported herein, then commenced with the first fuel series of testing on fuel AFFB-8-67. This consisted of two test series each consisting of 100 simulated mission profiles or test cycles. The results of the testing performed indicate the presence of deposits in the wing tank, engine manifold, and engine nozzle. Concurrently, the fuel was tested in various small-scale thermal stability test devices. The results of the simulator and small-scale devices were compared. Additionally, the data obtained on the FAA-SST Fuel System Test Rig was analyzed with respect to that obtained on fuel AFFB-8-67 so that the comparison to small-scale tests would be more inclusive.

SECTION II

FUEL TESTED

Approximately 96,000 gallons of the first test fuel arrived at W-PAFB on 20 December 1966 and were loaded into four 25,000 gallon underground storage tanks. These tanks had been cleaned and lined with a protective coating conforming to MIL-C-4556B prior to receipt of the fuel. The transfer pumps are copper-free and the transfer tubing is stainless steel and aluminum. The test fuel is designated as AFFB-8-67 and is a blend of 30% Ashland regular JP-5 jet fuel and 70% Ashland thermally stable jet fuel. The fuel was purchased to pass the Standard Coker (Reference 1) at 375/475 and fail at 425/525. The fuel had been analyzed by the supplier prior to shipment and by a W-PAFB laboratory after storage. The results are shown in Table I.

As fuel was required, it was delivered to the test site in a 4000 gallon trailer. Approximately 92,500 gallons of the fuel, ranging in temperature from 12 to 74°F were used for simulator and small-scale testing. This fuel was used between 1 December 1966 and 3 May 1967. A total of fifty 55-gallon, epoxy-phenolic coated drums were then filled with AFFB-8-67 directly from the underground storage tanks. On 27 April 1967 these drums of fuel were shipped to the Air Force Fuel Bank for future use.

TABLE I - AFFB-8-67 FUEL ANALYSIS

	Ashland Tests	Specification	W-PAFB Tests
API Gravity	46.8	39-51	46.6
Distillation, °F - IBP	330	-	330
10%	346	[illegible]0 max.	351
20%	352	[illegible]	356
50%	369	450 max.	374
90%	445	-	450
FBP	497	550 max.	502
Recovery, %	98	-	98
Residue, %	1	1.5 max.	1
Loss, %	1	1.5 max.	1
Existent Gum, mg/100 ml	0.6	7 max.	.4
Total Potential Gum, mg/100 ml	1.9	14 max.	-
Sulfur, Weight %	0.019	0.3 max.	-
RSH, %	<0.001	0.003 max.	0.0
Freeze Point, °F	-66	-54 max.	-70
Aniline Point, °F	150	-	146
Aniline-Gravity Constant	7020	-	6803
Heat of Combustion, BTU/Lb.	18,655	18,400 min.	-
Viscosity @ -30°F, cs	5.65	15 max.	6.07
Aromatics, volume %	8.9	20 max.	11.5
Olefins, volume %	1.5	-	1.3
Saturates, volume %	89.6	-	-
Smoke Point, mm	29	25 min.	26
Flash, °F, PM	124	110-150	115
Corrosion at 212°F, 2 hours	1b	1	negative
WSIM	74	-	-
H2O Tolerance	1	± 1	-
Thermal Stability (Standard Coker)	400/500/6	425/525/6	450/550/6
ΔP, In. Hg. at 300 min.	0.2	0.4	3.4
Preheater Code	1 (Pass)	3 (Fail)	5 (Fail)

SECTION III

SIMULATOR TEST CYCLES

SUMMARY OF TEST PROCEDURE AND RESULTS

Two test series, each consisting of 100 simulated environmental test cycles, were conducted on fuel AFFB-8-67 in the Advanced Aircraft Fuel System Simulator shown in Figure 1. The fuel flow rate, tank pressure, and dry tank skin temperature profiles were the same for each test series and are shown in Figures 2, 3, and 4, respectively. The component fuel-out temperatures for the two test series are shown in Figure 5. The only difference between these two test series environments were the fuel temperatures out of the manifold and nozzle. The nozzle temperature nearly coincides with the manifold temperature. The manifold and nozzle were replaced between the first and second test series so that these components were subjected to the above environments for 100 test cycles each. All other components were tested for 200 test cycles.

The following is a brief synopsis of the operational procedure and results. Prior to each test cycle, the fuselage tank and the wing tank were filled with fresh fuel to 95 percent capacity. Altitude simulation and inerting of the fuel tanks were automatically controlled through the tank vent system. A vacuum pump was utilized in this system to reduce the internal pressure of each tank, and a nitrogen supply was provided to inert the vapor space during simulated descent. The fuel in the fuselage tank was heated from approximately 60°F at the start of the test cycle to 220°F at the end of the test cycle by radiation heaters to simulate aerodynamic heating. Simultaneously, the upper and lower wing tank skin was heated to a temperature of 500°F also simulating aerodynamic heating. Vibration simulation was provided by utilizing a vibrator on each tank. The fuel was pumped from the tanks through a 74 micron airframe filter and an airframe heat exchanger.

The airframe heat exchanger system rejected heat to the fuel at a specified rate. This resulted in an average increase in temperature of 25°F and 69°F for the acceleration and cruise conditions, respectively. The fuel entering the engine fuel system was pressurized and heated by the engine pump and bypass system. The average increase in temperature across the pump was 5, 10, and 10°F during acceleration, cruise, and deceleration conditions, respectively. The high pressure fuel flow was then regulated by a manual flow control valve and filtered by a 2 micron engine filter. The fuel was further heated by the engine heat exchanger system so that an average increase in temperature of 25°F and 60°F was obtained during the acceleration and cruise conditions, respectively. The fuel then passed through a heated manifold where average temperature increases of 42°F and 85°F were produced

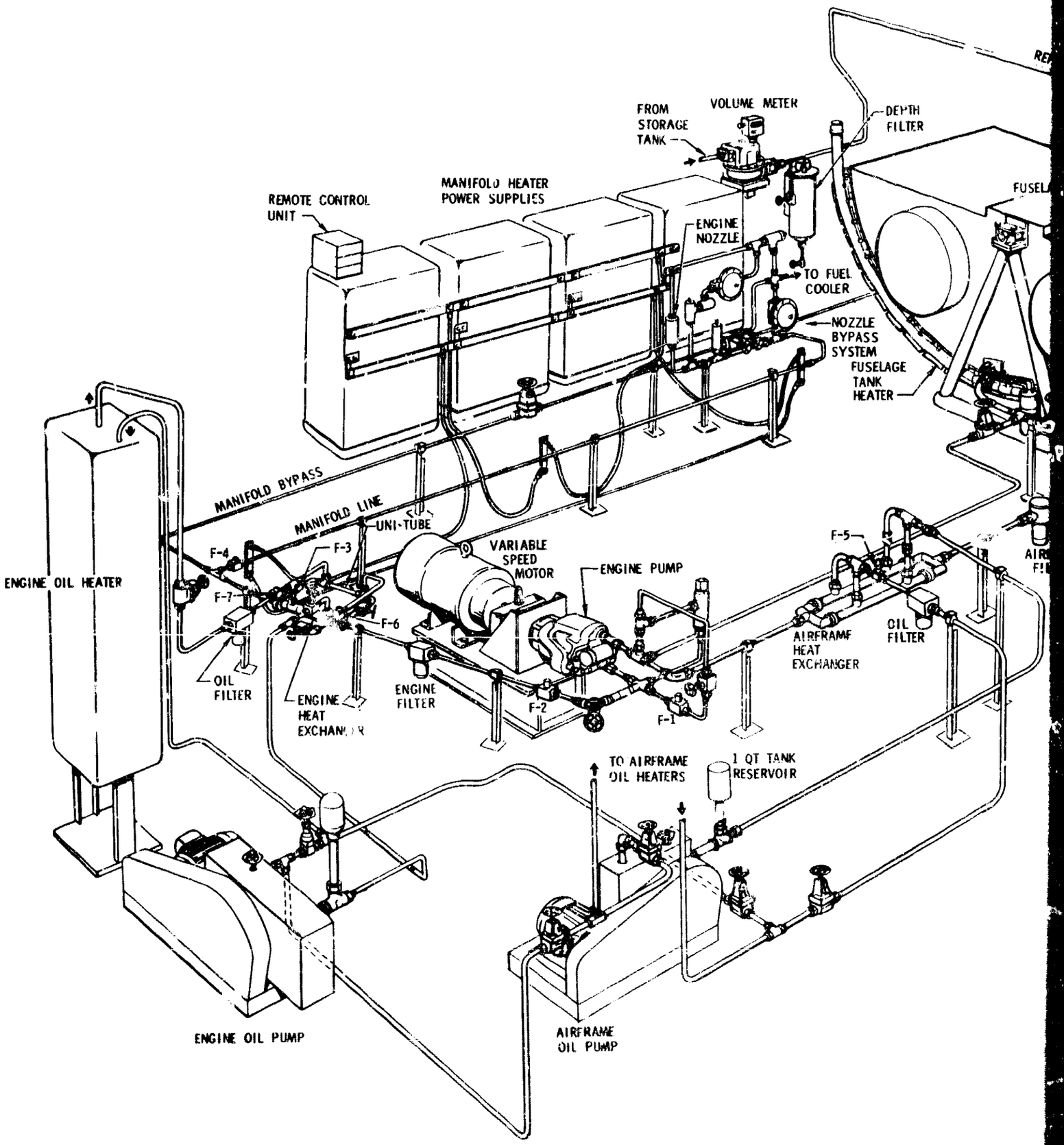
FROM STORAGE TANK
VOLUME METER
DEPTH FILTER
REMOTE CONTROL UNIT
MANIFOLD HEATER POWER SUPPLIES
ENGINE NOZZLE
TO FUEL COOLER
NOZZLE BYPASS SYSTEM
FUSELAGE TANK HEATER
MANIFOLD BYPASS
MANIFOLD LINE
UNI-TUBE
F-4
F-3
F-5
VARIABLE SPEED MOTOR
ENGINE PUMP
ENGINE OIL HEATER
F-7
F-6
OIL FILTER
ENGINE HEAT EXCHANGER
ENGINE FILTER
F-2
F-1
AIRFRAME HEAT EXCHANGER
OIL FILTER
TO AIRFRAME OIL HEATERS
1 QT TANK RESERVOIR
ENGINE OIL PUMP
AIRFRAME OIL PUMP

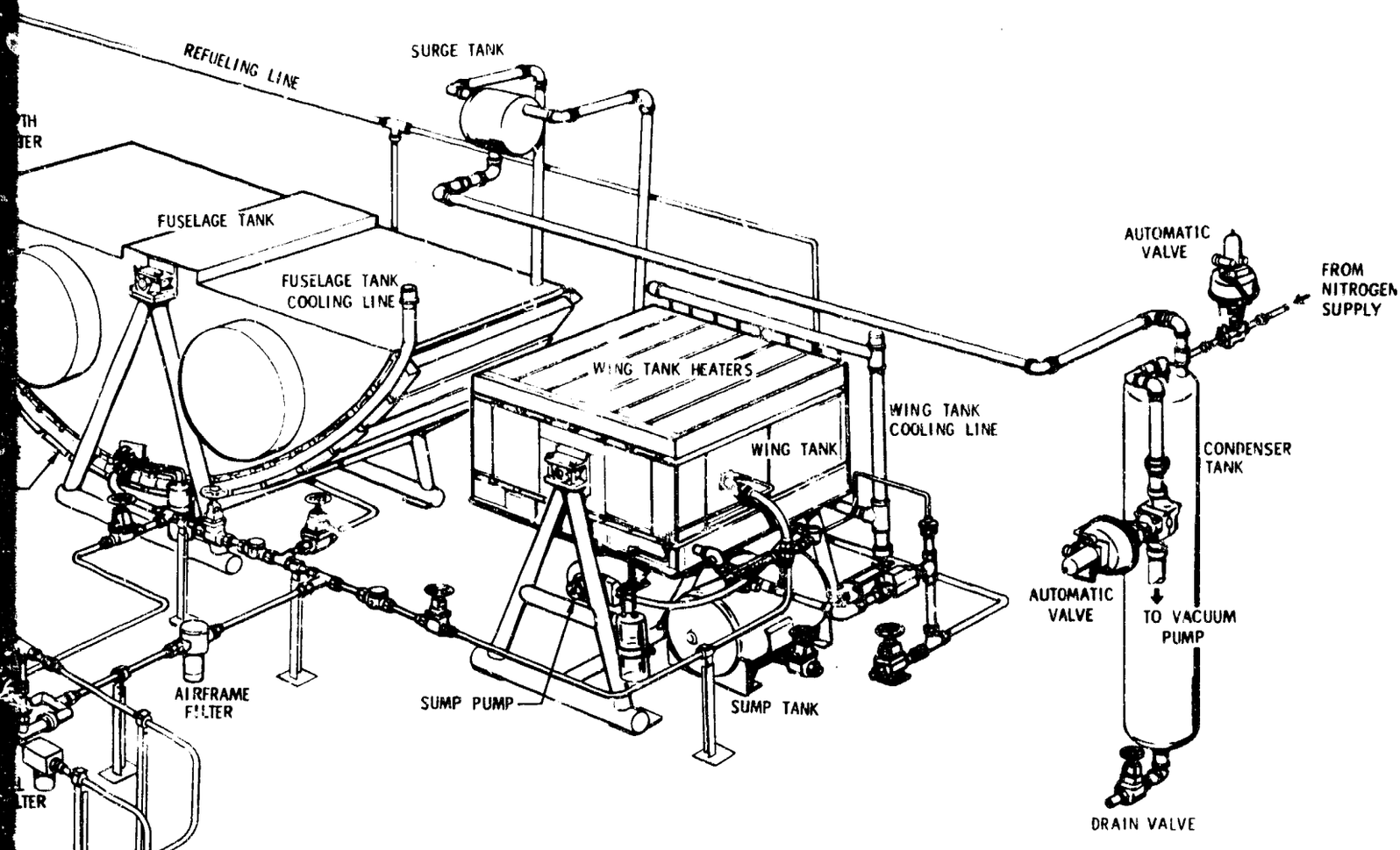

FIGURE 1 ADVANCED AIRCRAFT FUEL SYSTEM SIMULATOR

2

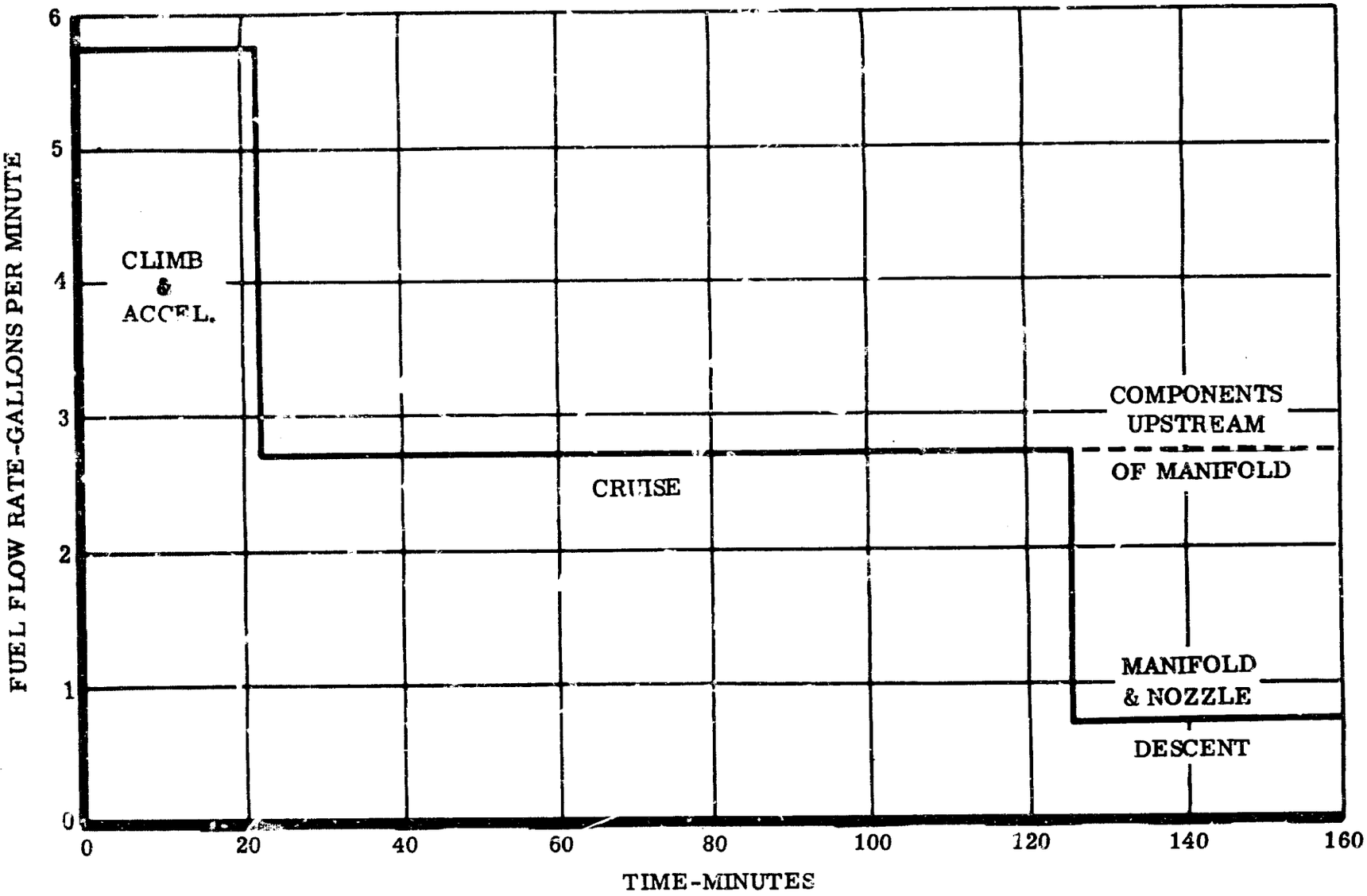

FIGURE 2 - FUEL FLOW RATE SCHEDULE

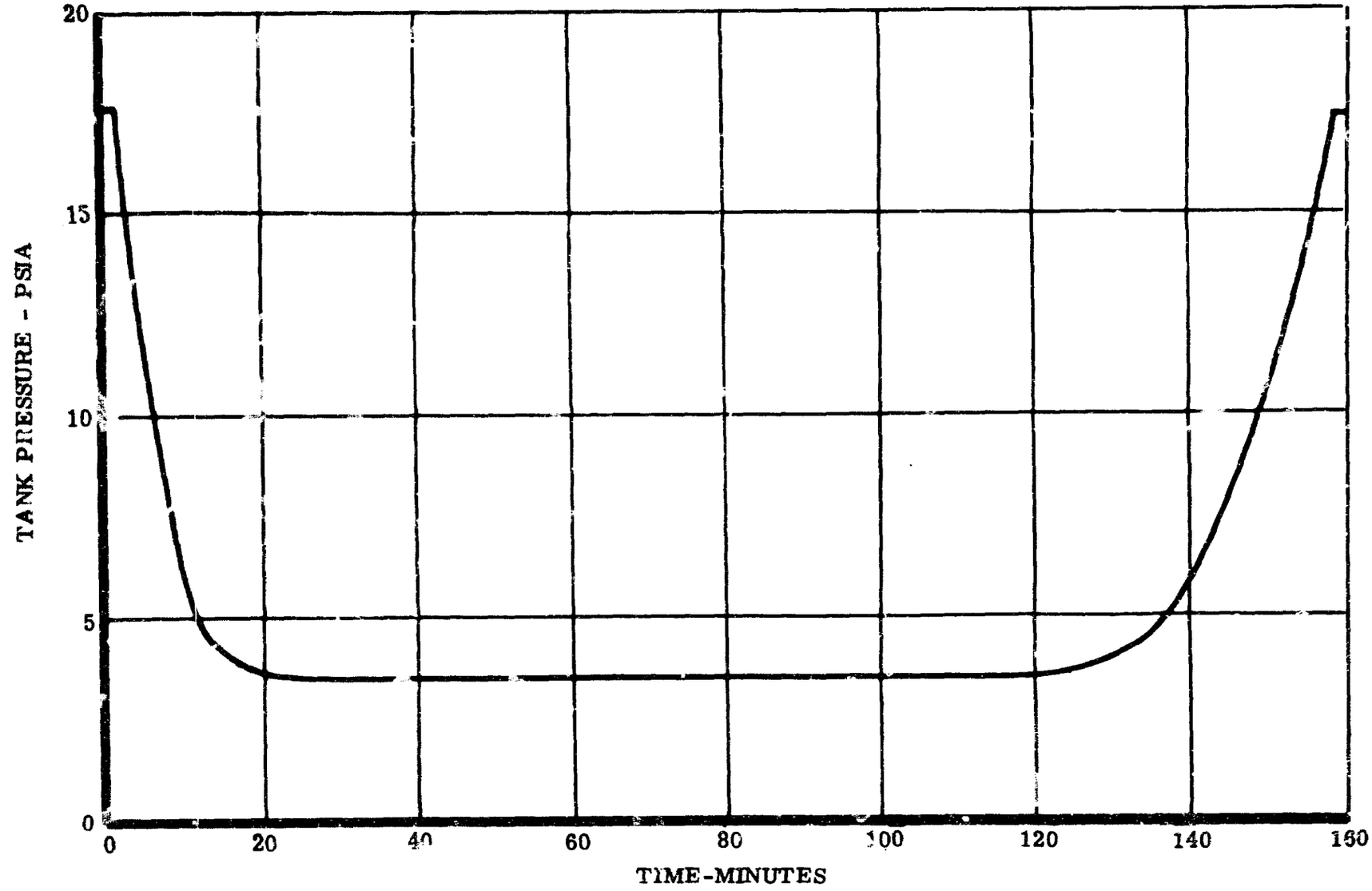

FIGURE 3 - TANK PRESSURE SCHEDULE

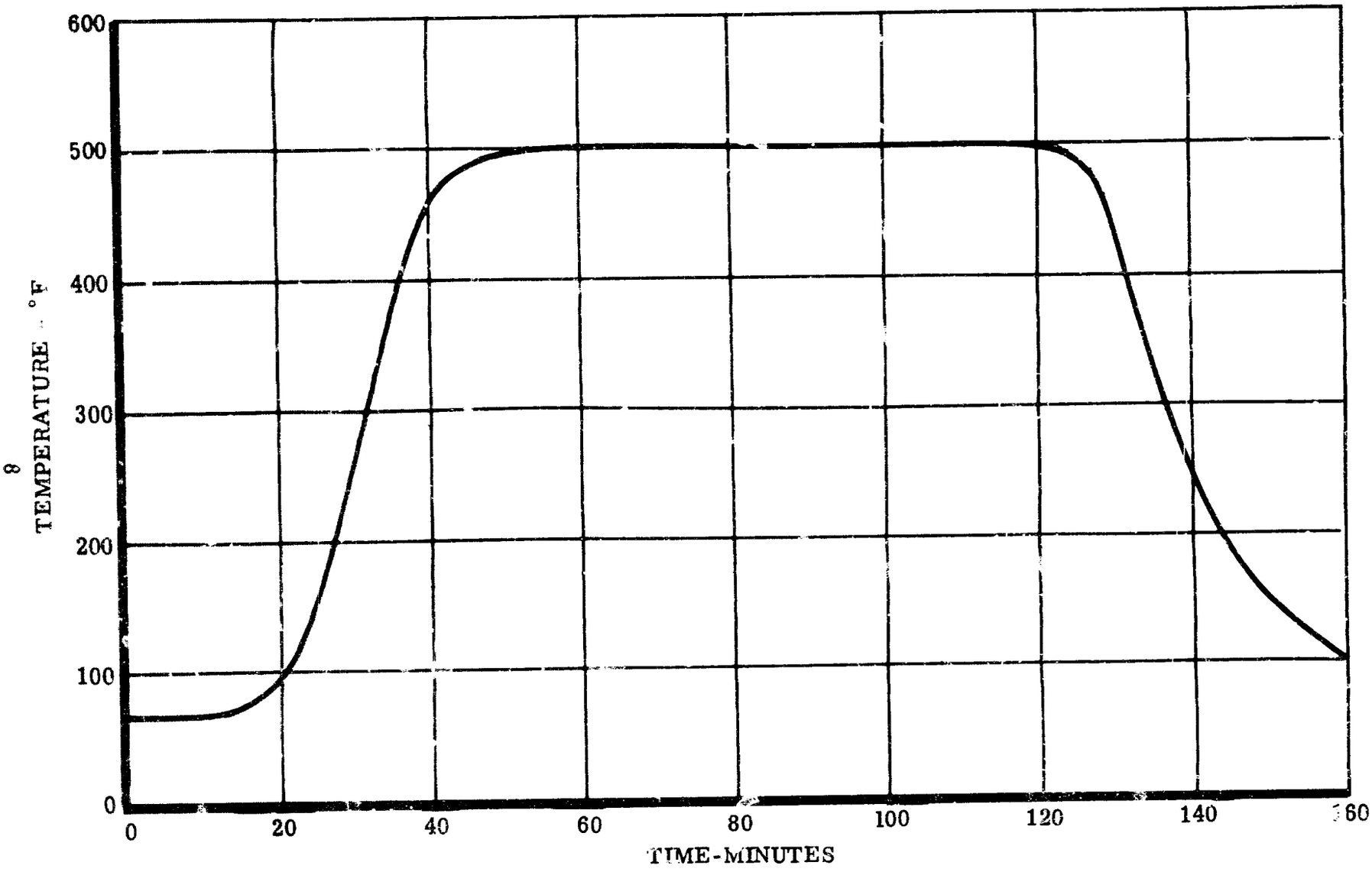

FIGURE 4 - DRY TANK SKIN TEMPERATURE

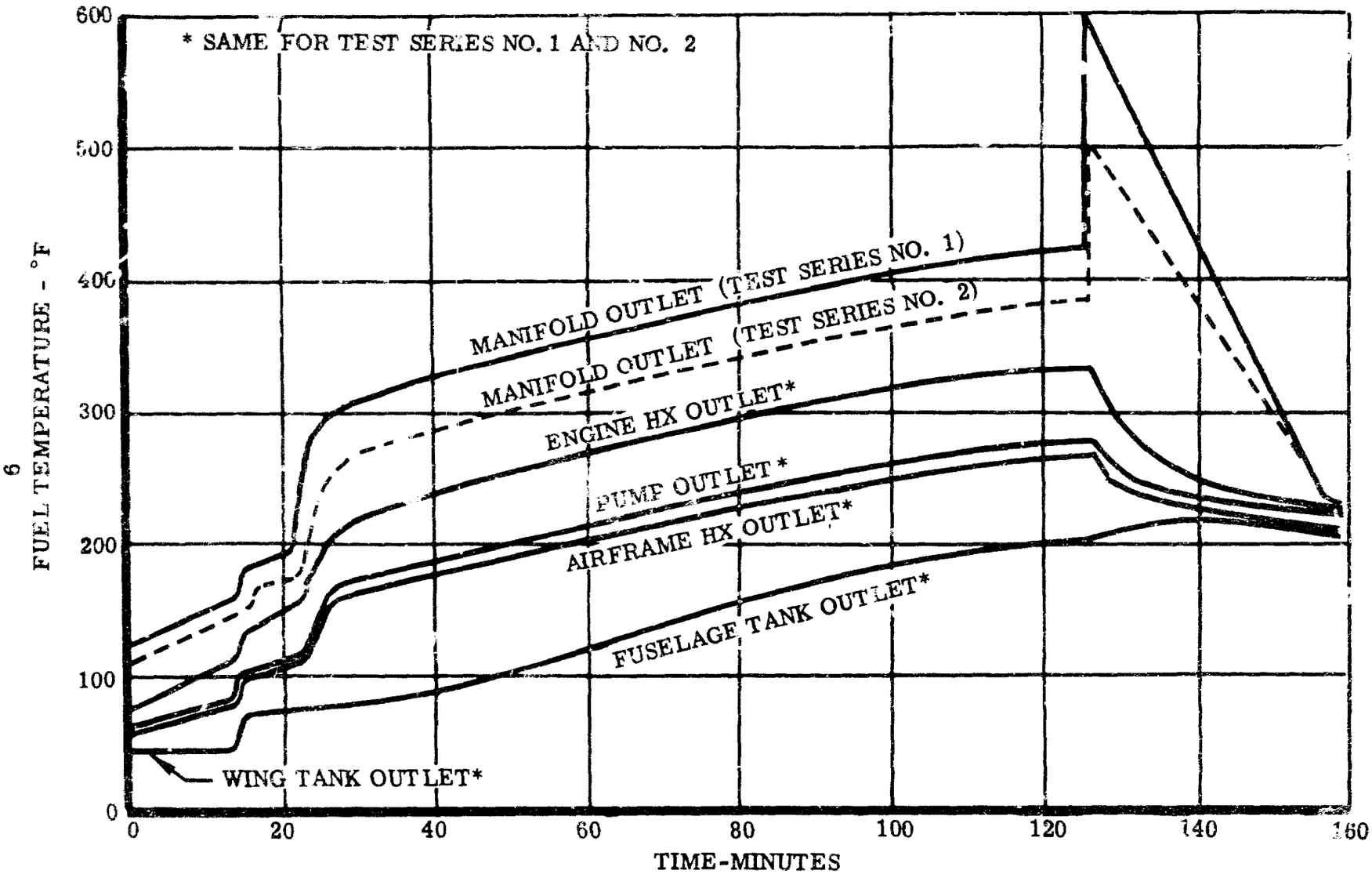

FIGURE 5 - COMPONENT FUEL TEMPERATURE

for the acceleration and cruise conditions of the first test series, respectively. The average temperature increases for the second test series were 25 and 51°F. At the beginning of descent conditions, the engine and airframe heat exchanger heating systems were de-energized. Also at descent three-quarters of the fuel passing through the engine exchanger was returned to the fuselage tank. The remaining fuel passed through the heated manifold where the fuel-out temperature rapidly increased to 600°F for the first test series and 500°F for the second test series. The heat input was then slowly decreased simulating descent cooling of the manifold line. The fuel exiting the manifold line, passed through the nozzle where temperature increases of 2 and 8°F were attained for the cruise and descent conditions, respectively. During and at the completion of each test series, the simulator was inspected and the data was analyzed. The components which showed evidence of decreased performance were the first and second test series engine filter and engine manifold and the first test series engine nozzle.

A summary of the significant results of the 200 test cycles is as follows: Visual inspection of the simulator showed that a portion of the fuselage internal surfaces had a very slight discoloration. The vent area had a fainter discoloration. The entire wing tank was discolored, and deposits were predominantly on the bottom of the tank. These deposits were as thick as 1/16 inch. Deposits were also evident in the vent area. The airframe filter was slightly discolored; however, no increase in pressure drop was evident. The airframe heat exchanger was unchanged in color, pressure drop, and heat transfer efficiency. The engine pump internal parts were in excellent condition, and a very light tan, powdery deposit was observed on the inlet fitting. The engine filter element was replaced 18 times in the 200 test cycles. This frequent replacement was attributed to debris. The engine heat exchanger pressure drop and heat transfer efficiency did not significantly change. The fuel side of the tubes was discolored at the inlet and contained deposit at the outlet.

The manifolds used in each test series contained measurable deposits. The calculated thickness ranged from .04 to .36 mils and .02 to .17 mils for the first and second test series, respectively. This was further evidenced by a measured decrease in heat transfer efficiency during the test series. The engine nozzles used in each test series contained deposits; however, an increase in pressure drop was measured only during the first test series.

TEST PROCEDURE AND RESULTS

The following is a detailed discussion of the test cycle procedure and results. The results are expressed in terms of component performance degradation, calculated deposit thickness, and color scale ratings. It is considered that the use of a color scale for quantifying the fuel degradation in the simulator is far inferior to measurements of performance degradation and deposit. However, the CRC Lacquer Rating Scale, Reference 3, was used so that comparison can be made to previous fuel testing results on the SST Fuel System Test Rig, Reference 4. This scale is not the same scale used in Coker tests.

Wing Tank

Operational Procedure - Prior to each test cycle, the wing tank was filled with fresh fuel ranging in temperature from 12 to 74°F, through a totalizing flowmeter to 95% of its capacity based on the fuel density at a temperature of 70°F. This quantity, 636 pounds, was used for each test cycle within a repeatability tolerance of less than 1%. After the tank was filled, the test cycle commenced by energizing the boost pump, establishing a fuel flow of approximately 5.8 gallons per minute out of the wing tank and automatically reducing the internal pressure of the wing tank in accordance with the required pressure schedule, Figure 3. At 14 minutes after start-up, the wing tank and probe heaters were energized in accordance with the heating schedule ascertained during the initial test cycles. One of the probes was controlled to produce the same temperature profile as the dry wing tank skin (500°F). The second probe was controlled to a maximum temperature of 425°F simulating the sides of the wing tank, and the third probe was allowed to slowly increase in temperature (to 350°F) duplicating the lowest temperature in the wing tank. In order to duplicate the environment and fuel puddle conditions of the bottom of the wing tank, a dish and disk were fixed to the bottom of the tank. At 15.0 ± 0.3 minutes after test start-up, the airframe fuel pressure diminished, indicating that the fuel depth in the wing tank was approximately 1 inch and the pump was cavitating. This condition was immediately followed by a decrease in fuel flow.

At this time the fuselage pump was energized, the wing pump de-energized, and the wing tank fuel dump valve opened. Most of the remaining fuel in the wing tank then drained through the valve into a 321 stainless steel sump tank, and the fuel dump valve was closed 28 minutes later. The wing tank attitude was calibrated to cause 1200 ml of fuel to remain in the tank after it was drained. During the cruise condition, which commenced 22 minutes after test start-up, the temperature of the dry heated portion, wing tank skin, was increased and stabilized at a temperature of 490 ± 10°F. Though 500°F was the profile temperature, a mean control value of 490°F was used so that 500°F would not be exceeded. A temperature-time history of the wing tank vapor for a typical test cycle is shown in Figure 6.

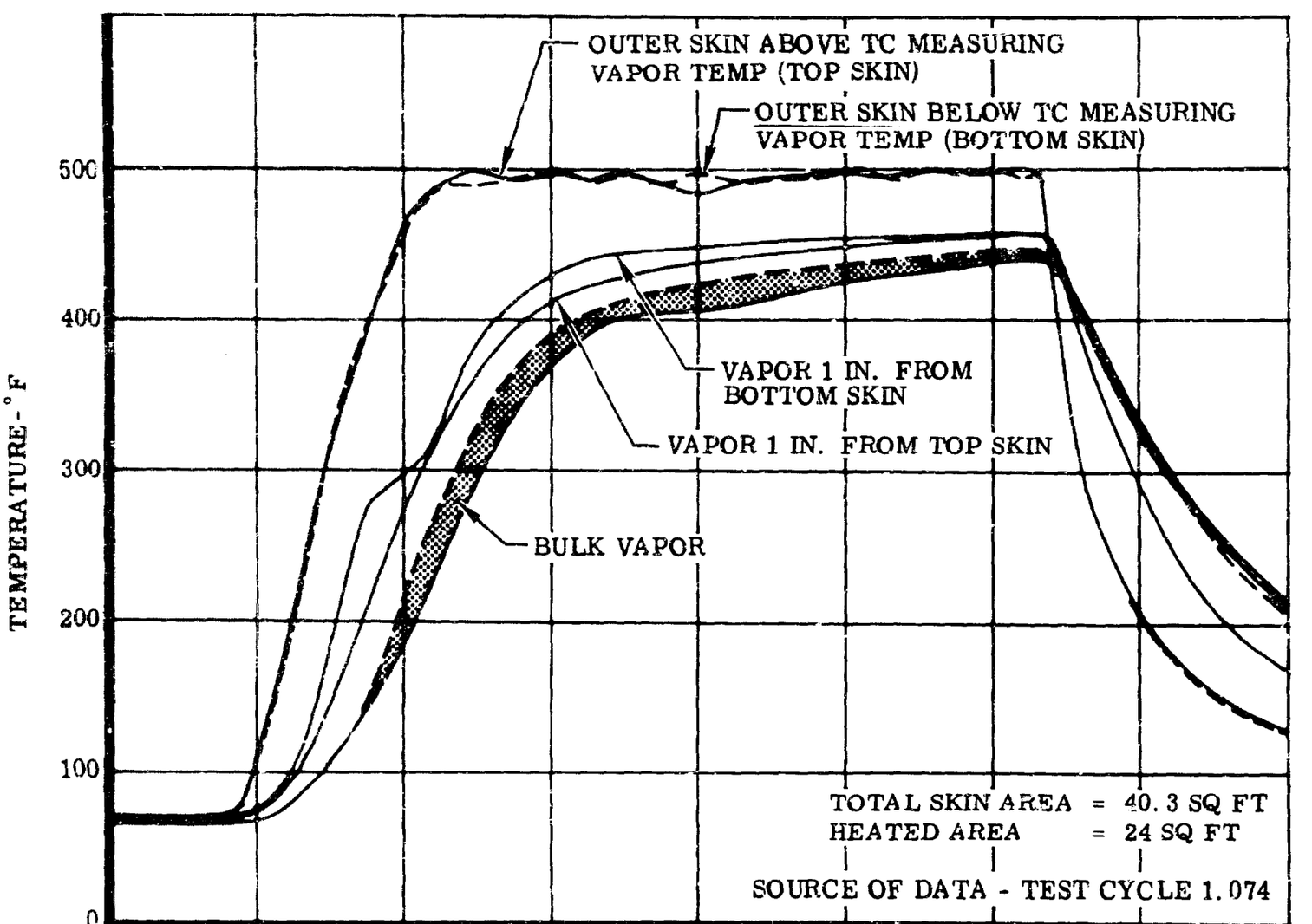

Figure 6. Time-Temperature History of Vapor in Wing Tank

At 126 minutes after test start-up, simulated aerodynamic cooling and vibration were commenced. The vibrator (input frequency of 7000 cpm and input force of 2.7 g's) was shut off at 136 minutes and cooling continued through the end of the test cycle.

Results - The wing tank was opened after selected test cycles to visually examine the deposits in the wing tank and on the probes. The probes were rated with a Tuberator (Reference 1). However, it became evident that the Tuberator rating was misleading with respect to these specimens. One of the probes having deposits which were so thick that they were flaking off the tube, rated lower with the Tuberator than a tube with a much thinner deposit. Tabulated below are the visual ratings under sunlight made without the Tuberator and using the CRC Lacquer Rating Scale, Reference 3.

Rating After Test Cycle	Unheated Probe (340°F Max.)	400°F Probe	500°F Probe
1.021	2	2	2
1.048	2-3	2	2
1.072	Light brown with black spots	Light stain	Stain
1.090	7	3-4	6
2.010	7-8	3-4	7
2.035	7-8	3-4	6
2.069	8-9	5-6	7-8
2.100	9	5-6	7-8

The deposits on the 400°F and 500°F probes were always observed as a stain with the 500°F probe darker than the 400°F probe. Starting at test cycle 2.010 or after 110 test cycles, the 340°F probe was observed to have a thick coating of deposits rather than being stained in appearance. After 2.036 the deposits were noted to be rough in appearance; after 2.070 the deposits were starting to flake off, and after 2.100 the deposits were flaking off quite easily. An unheated titanium (Ti-6Al-4Va) probe was mounted in the tank after test cycle 2.036. It could not be rated with the CRC Lacquer Rating Scale since the stain, though slight, was different in color from the scale. However, there appeared to be no significant difference between the amount of deposits on the aluminum and titanium probes on the basis of equal number of test cycles.

The entire wing tank was rated five times during the two test series by making a sketch of the tank showing the location, area, and rating of the deposits. These visual examinations are summarized as follows:

Rating After Test Cycle	Sides	Vent Area	Tube Trusses	Bottom - Dry Areas	Bottom - Puddle Areas
1.048	3-4	7-8(9)	-	5-6(3-4)	9 (7-8)
1.100	3-4(5-6)	7-8(9)	3-6	7-8(5-6)	9 to 1/32" thick
2.035	3-4	7-8(9)	4-6	7-8(5-6)	"
2.069	3-4	7-8(9)	4-6	9	"
2.100	5-6(7-8)	8-9	4-6	9 (7-8)	Up to 1/16" thick (9)

The ratings given are first the rating of the greatest area followed by the rating of a smaller area in parenthesis. The sketch made of the wing tank after test cycle 2.100 is shown on Figure 7. The discolorations of the top and sides of the tank were rainbow in appearance and very thin. The entire top of the tank was rated as 6-7 on the CRC Lacquer Rating Scale and very closely matched the stain of the 500°F probe. The stain of the 400°F probe closely matched the sides of the tank. The discoloration the struts varied from the same color as the top and bottom of the t in the areas adjacent to the top and bottom of the tank, to the same color as the sides of the tank at the middle of the struts. The center support bar was very dark, almost as dark as the dry portions of the tank bottom. The discoloration of the support bar indicates that fuel condensed on the bar and dripped from the bottom of the bar. The phenomenon of condensation accelerating deposition was also found in other wing tank deposit programs (References 4 and 5). The deposits on the 300°F probe were more brown in appearance than any specific area of the tank. A photograph of the probes is shown in Figure 8. The wing tank disk was the same color as the dry portions of the wing tank bottom. The dish was the same color as the fuel puddle areas, but there was only a slight indication of deposit blistering in the dish. A photograph of the dish and disk is shown in Figure 9.

The puddle areas of the tank were covered with brown-black deposit that was very rough and appeared blistered, as shown in Figure 10. However, the deposit was very hard and very adherent to the tank. Temperature measurements of the areas that had rough and blistery deposit indicate that these were puddle areas. The temperature increased more slowly than the dry skin temperature profile, and at 300°F the temperature remained constant for approximately 10 minutes (apparently until the fuel above the thermocouple had vaporized) and then more rapidly increased to 500°F.

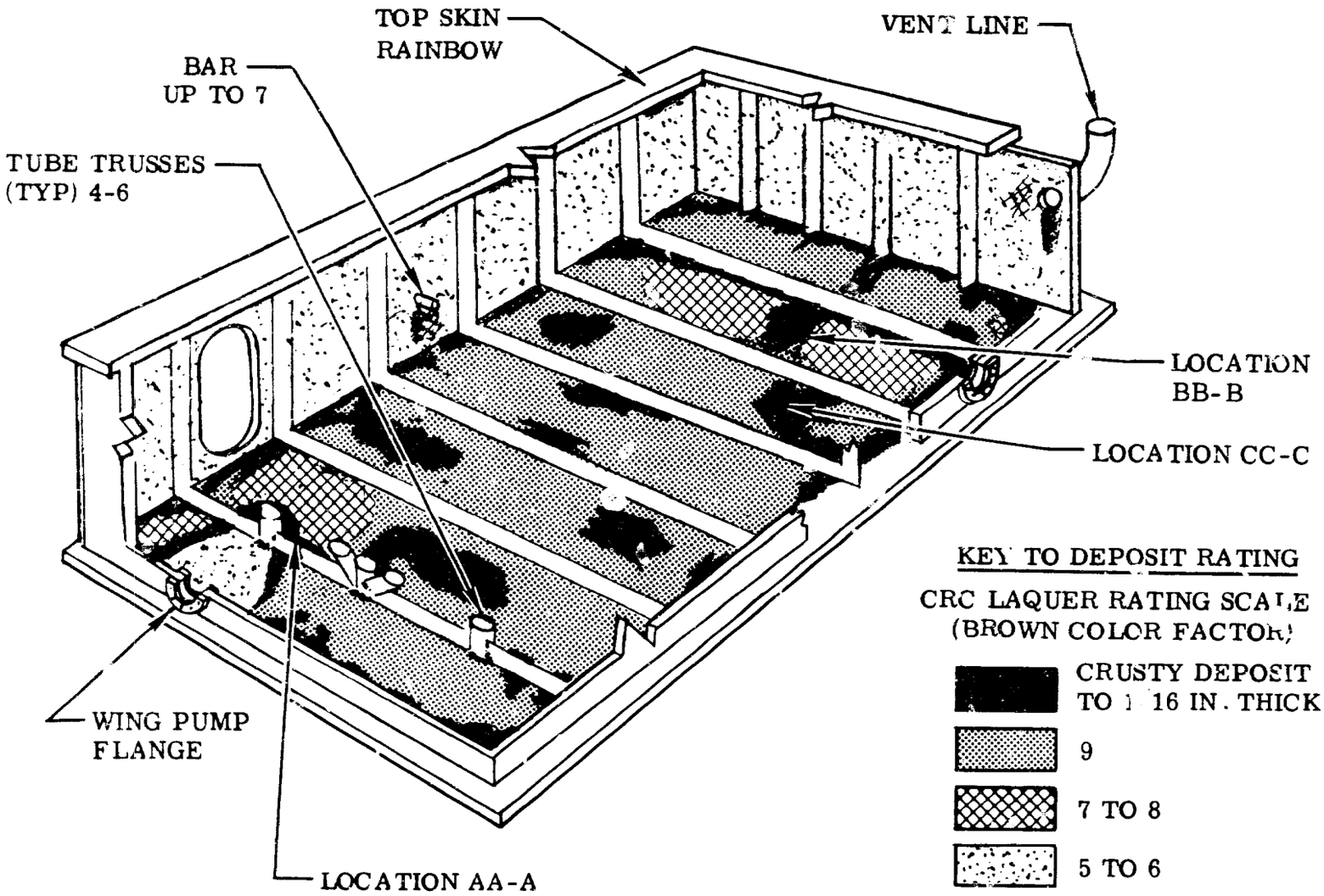

Figure 7. Wing Tank Deposits

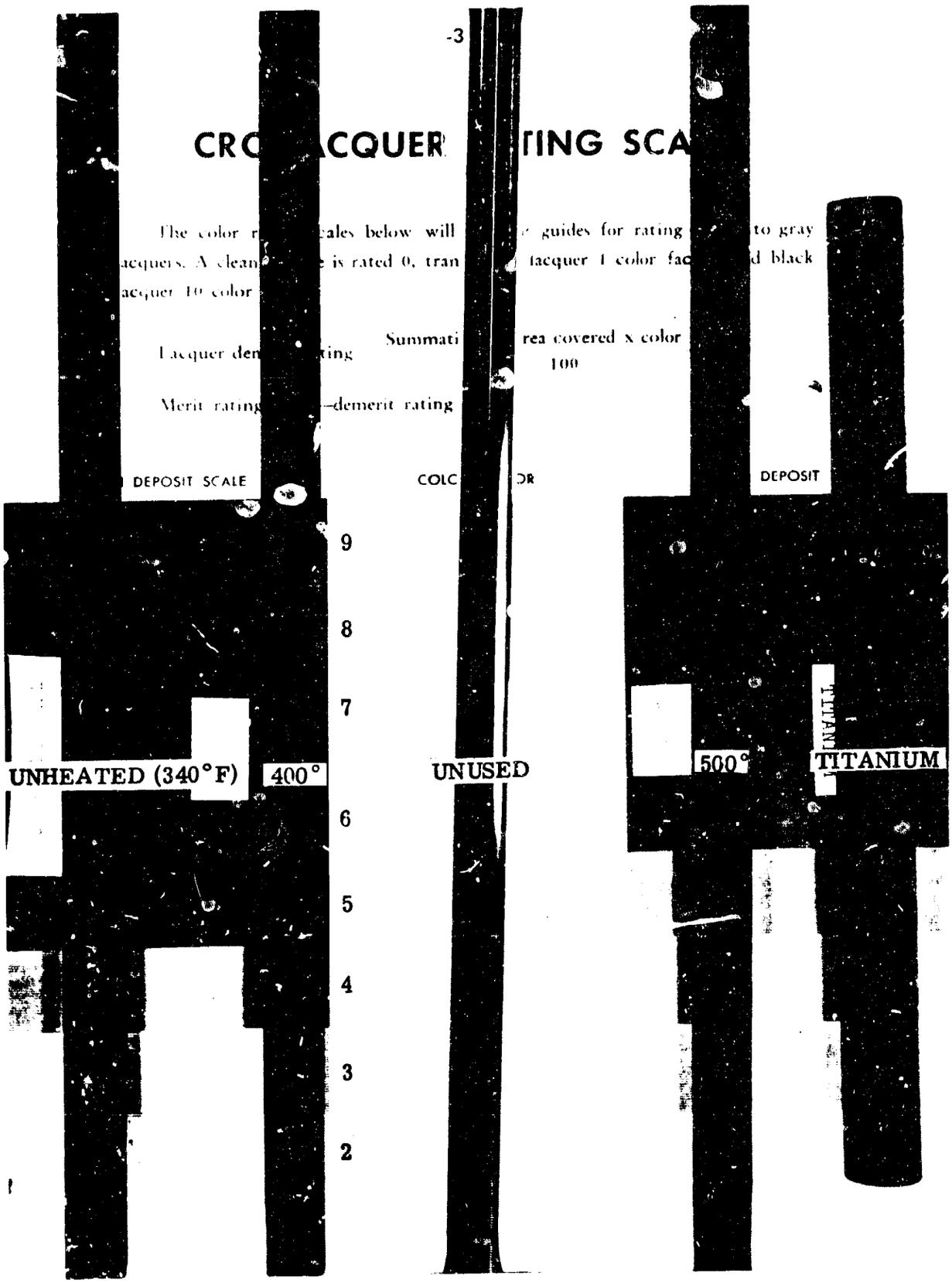

Figure 8. Wing Tank Probes

CRC LACQUER RATING SCALE

The color rating scales belo[w] [i]des for rating brown to gray lacquers. A clean surface is [r]ated [1]0 color factor, and black lacquer 10 color factor.

Lacquer demerit [f]actor = [c]olor factor

Merit rating [=]

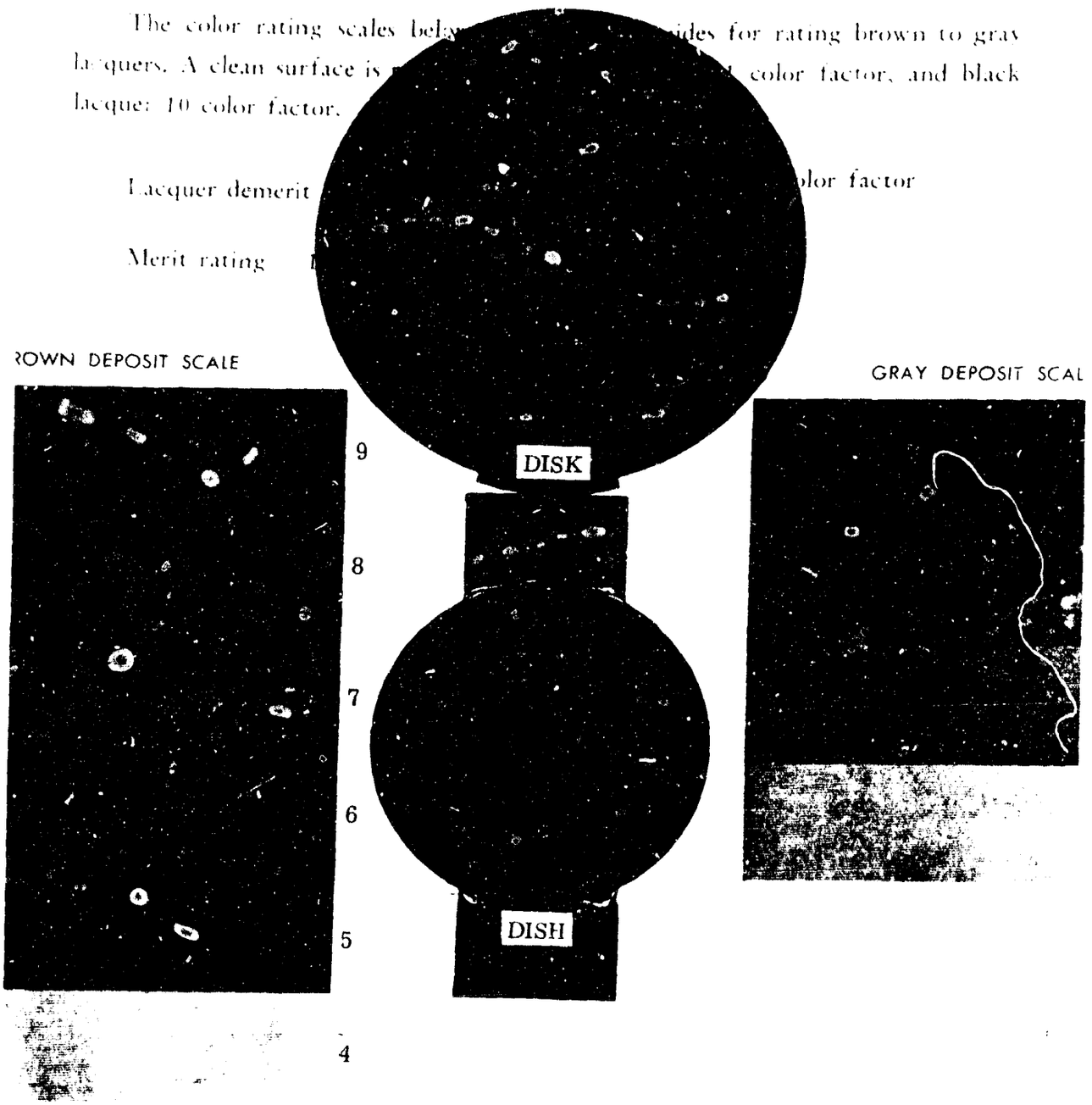

Figure 9. Wing Tank Dish and Disk

Figure 10. Ving Tank Deposits

The color of the puddle area deposits under the boost pump (see Figure 11) was a rust-brown. The difference in color of these deposits compared to other areas may be attributed to the condensing of fuel vapor on the outer housing of the boost pump cooling coil and the dripping of the condensate on the bottom of the tank. Deposit analysis results showed the amount of iron to be .01% indicating that the material was not rust. The area around the vent was black and had a powdery appearance. The horizontal portion of the vent line contained a loose gritty material.

Prior to cleaning the wing tank in preparation for the third test series, plaster casts were made of the deposits at three locations on the bottom of the tank; these locations are shown in Figure 7. The material used was Puritan Potter's Plaster. Plaster casts were made again of these locations after the wing tank was cleaned. A dial indicator was then used to measure the difference in the casts for each location on a measurement grid consisting of 3/8 inch lines. The maximum deposit thickness measured at the three locations is as follows:

Location	Maximum Deposit Thickness, Inches
AA-A	.048 (peaks as high as .062")
BB-B	.[illegible]9
CC-C	.027

A sample of the puddle area deposits and vapor was taken after test cycles 1.048, 1.100, and 2.100. The results of these analysis are included in References 6, 7, and 8. The deposit analysis results are shown in Table II. Comparing these results to those obtained on wing tank deposits in the past, Reference 4 indicates that these deposits with the exception of those from the booster pump area have a much higher quantity of sodium and silicon. Assuming no errors were made in the analyses these materials may be attributed to insufficient flushing of the wing tank after the tank was cleaned for the first test series. The tank was first "sand-blasted" with salt and then soda lime glass. If the flushing operation which followed was not effective, then high values of sodium, silicon, and calcium are understandable. Assuming that the cleaning operation was the source of this material, the total carbon and hydrogen in the actual fuel deposit can be corrected from 17.6 to 44% Further agreement to previous deposit analysis is evident from the larger ratio of carbon to hydrocarbon in the sample.

TABLE II - WIMC TANK DEPOSIT ANALYSIS*

TEST CYCLE	1.048**	1.100***			2.100	
		BLACK	BROWN	GRAY	PUDDLE AREA	BOOSTER PUMP AREA
Sodium	30%	2.0%	1.0%	10-20%	2.0%	<0.01%
Silicon	20	0.5	5.0	8	0.3	0.04
Calcium	10	0.1	0.2	0.8	0.8	2.0
Aluminum	1.0	0.2	0.1	0.6	0.15	0.01
Magnesium	0.8	0.04	0.2	1.0	0.3	0.02
Iron	0.5	0.3	0.2	5.0	1.0	0.01
Copper	0.2	0.02	-	-	0.1	0.005
Lead	0.1	0.02	-	-	0.25	0.005
Chromium	0.05	0.03	-	-	0.2	<.01
Nickel	0.03	0.01	-	-	0.1	<.005
Titanium	0.03	0.01	0.2	2.0	0.02	<.01
Manganese	0.01	NR	NR	NR	0.03	<0.001
Zirconium	<0.01	NR	NR	NR	NR	NR
Molybdenum	0.001	NR	NR	NR	NR	NR
Silver	<0.001	NR	NR	NR	0.04	0.005
Cobalt	NR	-	-	0.03	NR	NR
Boron	NR	-	.1	0.8	0.01	<0.005

*Estimated percent determined by Emission Spectrographic Analysis
**Combustion of this sample followed by gas chromatographic analysis indicated 16.4% carbon, 1.2% hydrogen.

***Observation under microscope revealed three types of samples: Black-brittle or charred material, Brown - dark material under brownish sponge, Gray - malleable dark material

NR = Not Reported

Figure 11. Wing Tank Deposits (Boost Pump Area)

Fuselage Tank

Operational Procedure - Prior to each test cycle, except for the first test cycle of the first test series, the fuselage tank initially contained an average fuel reserve of 66 gallons remaining from the previous test cycle. Fresh fuel ranging in temperature from 12 to 75°F was pumped into the tank through a totalizing flowmeter and the fuselage tank level control valve until the level control valve closed. The level control valve was mounted at a height of approximately 33 inches in the fuselage tank, which permitted it to shut off the fuel flow when the fuel quantity was 384.4 ± 1 gallons. This quantity is 95 percent of the fuselage tank capacity. The weight ratio of residual fuel to fresh fuel at the start of a test cycle was 0.19.

After the tank was filled and pressurized with nitrogen to 2 psig, the test cycle commenced, and the internal pressure of the fuselage tank was automatically reduced in accordance with the pressure schedule. At 14 minutes after start-up, the fuselage tank heaters were energized in accordance with the heating schedule ascertained during the initial test cycles. This heating schedule was established to produce the required fuselage fuel-out temperature and was used for all test cycles, with the exception of those test cycles wherein the fuel temperature at the beginning of the cycles was greater than 85°F. For these test cycles, the heat input to the wetted areas of the fuselage tank was discontinued for a maximum of 20 minutes in order to duplicate the temperature profile.

At 15.0 ± 0.3 minutes after start-up, when the wing tank fuel diminished, the fuselage pump was energized. As a given section of the heated fuselage tank skin became unwetted, the temperature of that section approached 500°F. The heating schedule provided for heating of the fuel tank until 100 minutes after test start-up. De-energization of the heaters at 100 minutes instead of 126 minutes, the start of descent, was necessary to minimize the fuselage fuel-out temperature during descent in order to approximate the overall design profile requirements, Reference 2. During the time from 100 to 126 minutes, the unwetted fuselage tank skin decreased from 500 to 400°F. Based on past testing, Reference 4, this deviation from the fuselage tank temperature profile requirements is considered to have little or no effect on the results. At 126 minutes after test start-up, the vibration (input frequency 7000 cpm at 2.5 g's) was actuated and tank cooling commenced.

The vibration excitation period was 10 minutes, the tank cooling continued for one hour after test completion, and then the fuselage tank was refueled.

A time-temperature history of the fuel and vapor in the fuselage tank is shown in Figure 12.

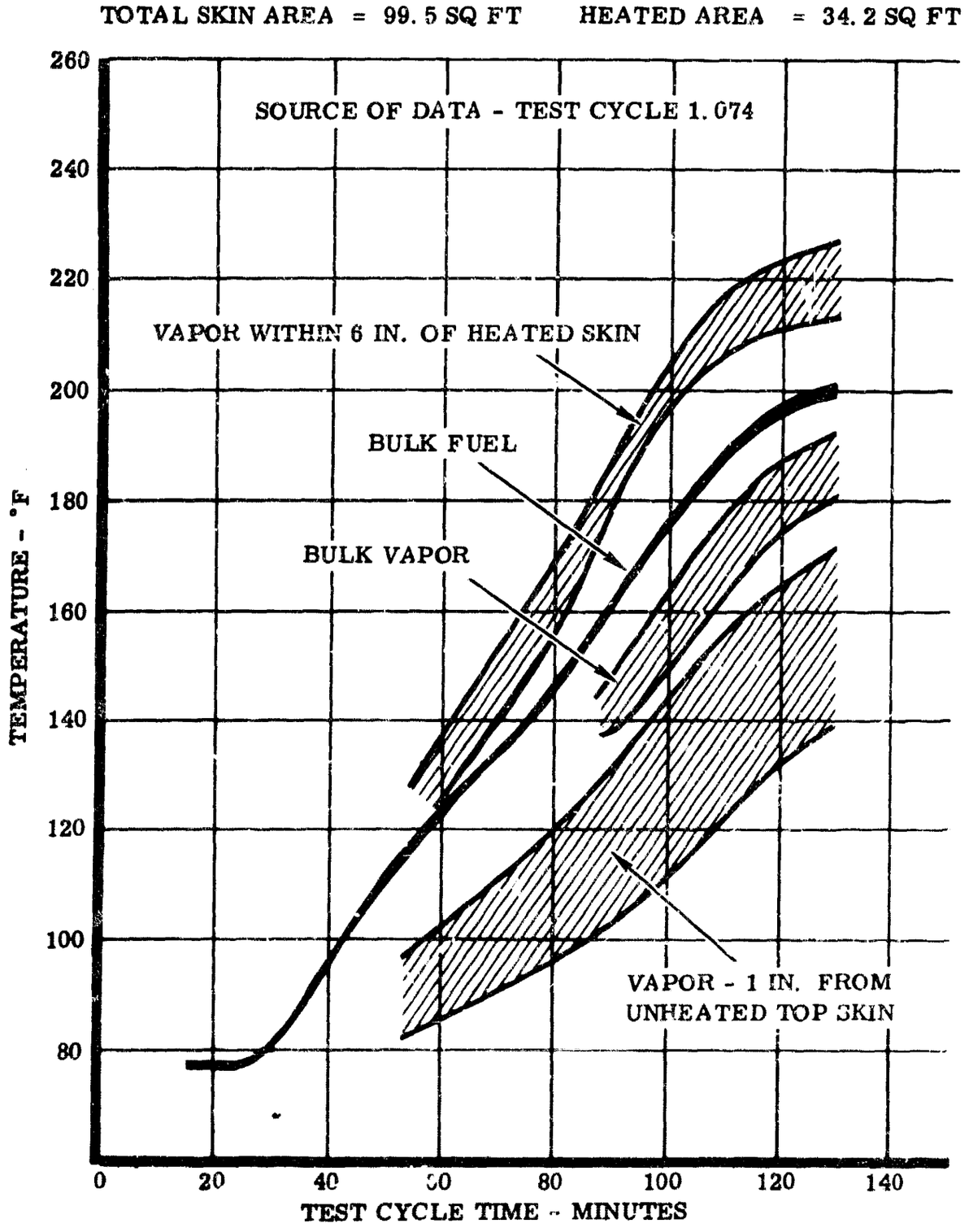

Figure 12. Time-Temperature History of Fuel and Vapor in Fuselage Tank

Results - The fuselage tank was opened and inspected upon completion of test cycle 1.048 and the first and second test series. It was noted that the entire tank was clean after the test cycle 1.048 and the first test series. At the second test series inspection it was found that the top four sections at each end of the tank bottom curved surface had a very slight discoloration. The vent area had a fainter discoloration. The remainder of the tank was clean.

A sample of the reserve fuel remaining in the fuselage tank after the second test series was tested on the gas drive coker. The fuel passed the 450/550 conditions and failed at 475/575 and 500/600. Fresh fuel had passed the 425/525 conditions, failed one out of three tests at 450/550, and failed all tests at 475/575 and 500/600. These results indicate that the reserve fuel was not adversely affected by the heating and replenishing cycles.

Altitude and Inerting

Operational Procedure and Results - Prior to test cycle start-up, the automatic altitude control solenoid valve and the vacuum pumps were energized and fuselage and wing tanks pressurized to 16.8 ± 0.3 psia with gaseous nitrogen. At test cycle start-up the altitude programmer was energized and automatically controlled the tank pressure as shown in Figure 3, to within ± 0.4 psi. The maximum rate of pressure reduction during simulated climb was 1.6 psi per minute. At 16 minutes after test start, the pressure of the tanks reached 3.6 ± 0.2 psi and this pressure was maintained. At 126 minutes after test cycle start-up, the pressure of the tanks was automatically increased by addition of gaseous nitrogen to 17.2 ± 0.2 psi at a maximum rate of 0.8 psi per minute.

Vent Heating

Operational Procedure and Results - At 16 minutes after test cycle start-up, the resistance heater tapes on the fuselage and wing tank vent lines were energized to simulate aerodynamic heating. An individual powerstat and temperature controller was used to attain a metal temperature of 495 ± 5°F at 47 ± 2 minutes after test start-up, and to maintain this temperature throughout cruise conditions. At 126 minutes after test start-up, the heater tapes were de-energized. The temperature of the vent lines then decreased at a linear rate to 310 ± 10°F at 159 minutes.

Upon completion of the two test series, the vent lines were inspected for deposits. The fuselage tank vent line was given a rating of 2 to 3 on the CRC Lacquer Rating Scale, Reference 3, for the first seven inches above the tank. The coating, which was very thin, decreased to a rating of 2 at the connection to the surge tank. The wing tank vent line rated 6 to 7 from the wing tank to the surge tank, and it was noted that the deposit was very thin.

Fuel Condensate

Operational Procedure and Results - Upon completion of each test cycle the condensate resulting from tank fuel boil-off was drained from the vacuum system condenser tank and measured. During the first 31 test cycles of the first test series, the amount of condensate ranged from 5 to 685 milliliters per cycle. From test cycle 1.009 to 1.031 the amount of condensate was greater than 270 milliliters. Based on previous testing, this amount of condensate is not unusual for the vent system design previously used. However, after test cycle 1.031, it is found that the wing tank reference pressure valve to the wing tank sump was closed. It is believed that this valve was closed from test cycle 1.009 to 1.031. When this valve is closed, the sump tank is not referenced, or vented to the wing tank, and the unpumpable fuel, five to six gallons, drains much more slowly into the sump tank. This leaves a greater amount of puddle fuel in the wing tank, and therefore results in a different temperature environment. After test cycle 1.031, the valve was lockwired in the open position to prevent inadvertent closure. From test cycle 1.032 through 2.100 (the remaining 169 test cycles) the amount of condensate exceeded 100 milliliters during seven test cycles (range 230 to 495 milliliter per cycle) and during the rest of the test cycles the average amount of condensate was 32 milliliters per cycle.

Booster Pump

Operational Procedure - Prior to the start of each test cycle both booster pumps were started under a no-flow condition and checked for proper operation. The fuselage boost pump was de-energized, and the wing boost pump was used to supply fuel during the first portion of the test cycle. At 15.0 ± 0.3 minutes after test start-up, the airframe system pressure rapidly decreased due to the low level of the fuel in the wing tank. The pressure decrease was immediately followed by a decrease in flow rate at which time the fuselage boost pump was energized and wing boost pump de-energized.

Results - The fuselage boost pump was replaced prior to test cycle 1.036 due to an impending bearing failure. The fuselage boost pump and mounting flange were not visibly discolored after the two test series. Deposits were evident on the wing tank boost pump and flange.

Airframe Filter

Operational Procedure and Results - Approximately 101,000 gallons of fuel ranging in temperature from 69 to 220°F passed through the 74 micron filter during the two test series. The pressure drop across the filter during each test cycle is shown in Figure13 for the climb condition. Based on the data obtained, there was no measurable increase in pressure drop.

This would indicate that the flow equivalent time base is at least 250 hours (ten times the minimum). The airframe filter was removed after the two series. Numerous particles were noted between the folds of the filter element. Particles were also found in the filter bowl and were filtered into a millipore. Visual observation indicates these are teflon, metal slivers, small black particles which may have been wing tank deposits and other miscellaneous debris. The overall color of the filter element was slightly darker than a new element and is shown in Figure 14. The weights of the filter element prior to and at the end of the test were 335.8 and 336.5 grams, respectively.

Airframe Heat Exchanger

Operational Procedure - A napthenic mineral oil was circulated through the shell side of the heat exchanger at a flow rate of 3.0 gpm. This oil was heated by an electrical heater, having a variable heat control, to simulate the heat rejected to the fuel by the various airframe subsystems. For each test cycle, the heat input to the oil was set according to a schedule established during the initial test cycles. The heater was energized at test cycle start-up and de-energized 126 minutes thereafter. The heat input to the fuel during this period reached a maximum of 640 BTU/minute. The average fuel temperature rise across the airframe heat exchanger during cruise conditions was 69°F, and a maximum fuel-out temperature of 270°F was reached during the test cycle.

Results - There was no apparent change in overall heat transfer coefficient and pressure drop of the airframe heat exchanger as shown in Figures 15 and 16. The heat exchanger units were removed after the two test series and inspected. The inlets were clean, and the outlets were a 2 to 3 on the CRC Lacquer Rating Scale, which is believed to be no darker than when they were installed.

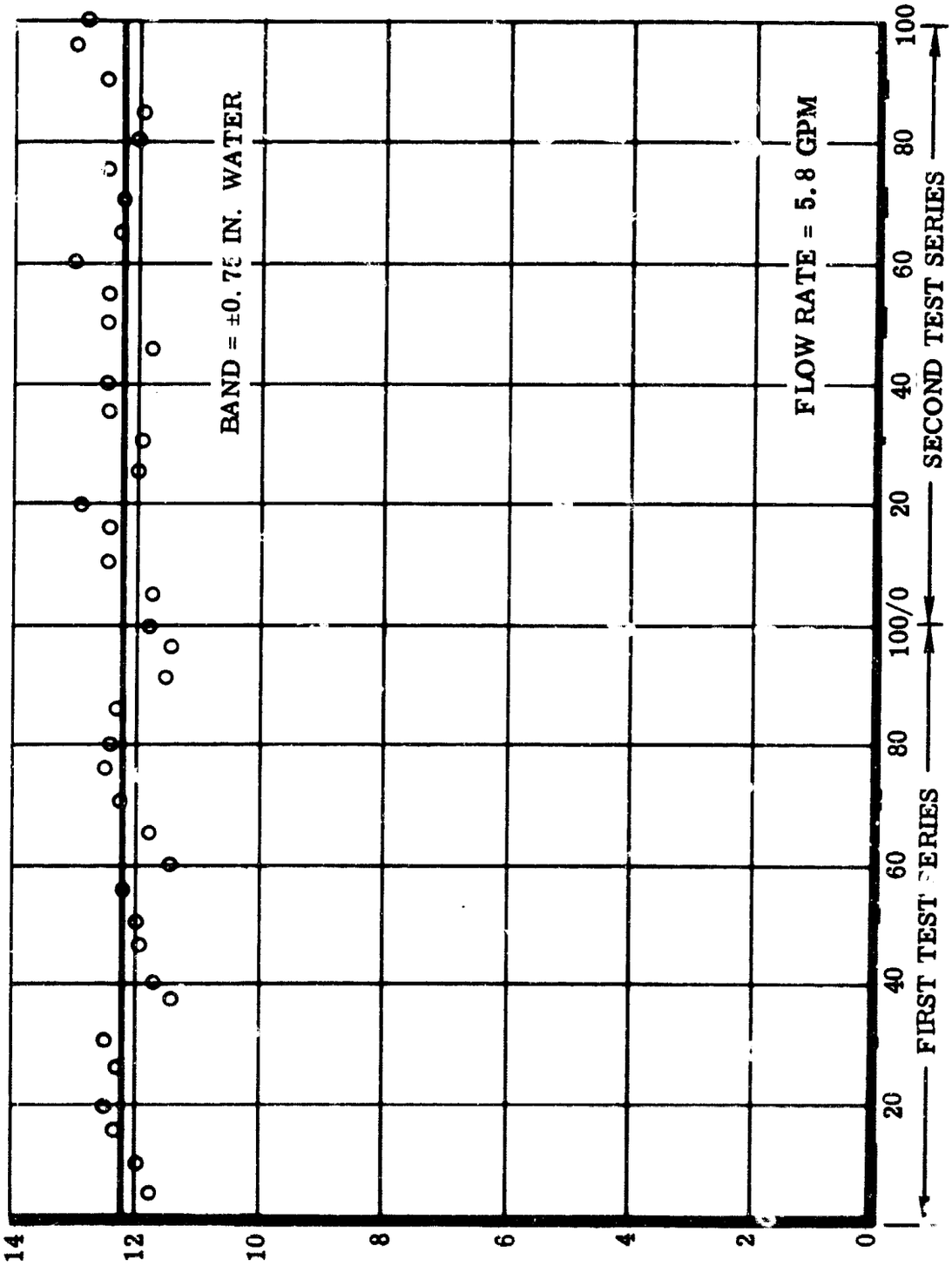

Figure 13. Pressure Drop Across Airframe Filter

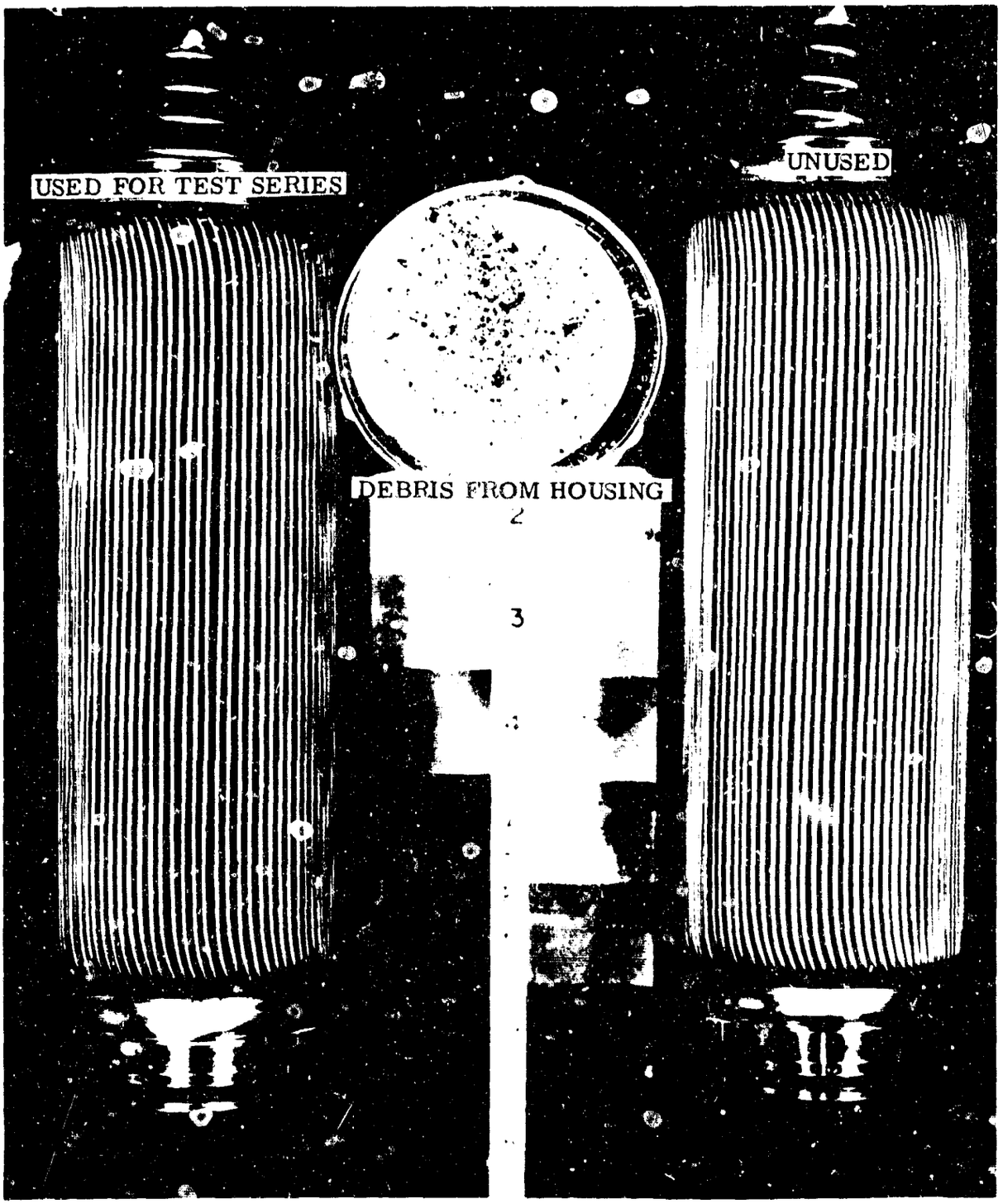

Figure 14. Airframe Filter Element

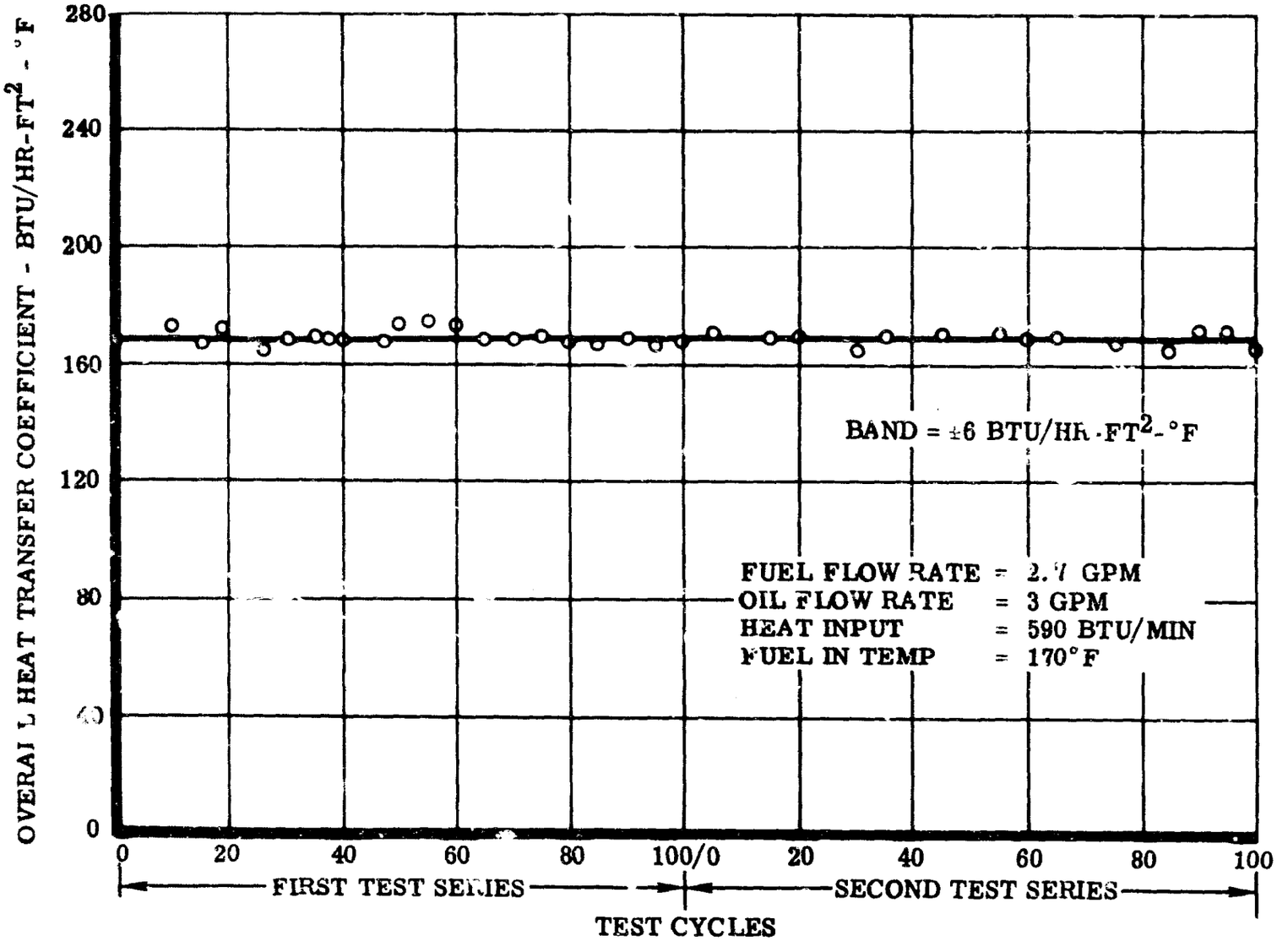

Figure 15. Overall Heat Transfer Coefficient of Airframe Heat Exchanger

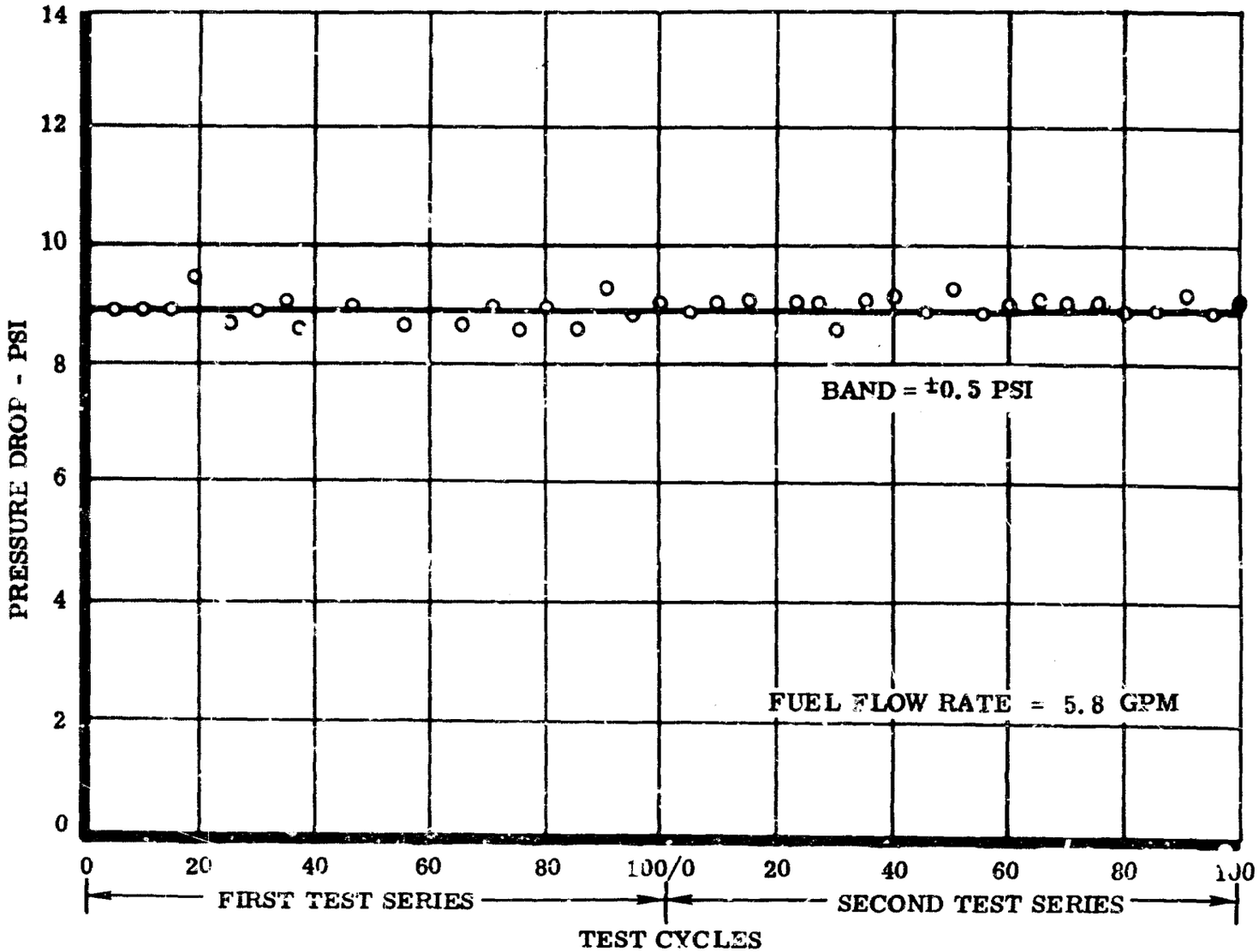

Figure 16. Pressure Drop Across Airframe Heat Exchanger

Engine Pump Subsystem

Operational Procedure - The pump speed and two throttling valves (main engine and bypass) were regulated during the test cycle to produce the specified temperature increase across the pump subsystem and the required fuel flow rate. The through-put flow rate was 5.8, 2.7, and 2.7 gpm during climb, cruise, and descent, respectively. The pump bypass flow rate was 0, 3.6, and 3.4 gpm during climb cruise, and descent, respectively. The increase in temperature across the subsystem was maintained at 5, 10, and 10°F during these conditions, respectively. The temperature of the fuel measured immediately downstream of the pump reached a maximum of 280°F during the test cycle.

During test cycles 1.006 and 1.017 fuel samples were taken downstream of the engine pump in order to analyze the engine pump wear products, if any. This was performed because the pump can greatly affect the results obtained in the engine system, see Reference 4. Also, the pump contained some objectionable materials (copper, silver, and cadmium) and though these are located where they are not subject to wear, it was advisable to make this analysis.

Results - The analyses, Reference 9, indicate that the amount of copper and iron is normal. The amount of silver and cadmium indicates that the silver or cadmium bearing materials in the pump are not releasing wear products into the fuel. The amounts reported for silver and cadmium are at the lower limits of detectability for these tests.

Upon completion of the first test series the engine pump outlet was inspected and found to be clean. The engine pump was removed from the system after the second test series and inspected. The inside of the inlet fitting (Figure 17) was coated with a very light tan, powdery deposit that could be wiped off easily. There was no deposit or discoloration evident on the outlet fitting. No spline wear was evident. This phenomenon of the inlet containing more deposit than the outlet occurred during the first test series of Reference 4 and is not unusual. It is hypothesized that this phenomenon is caused by a rapid decrease in Reynolds Number causing particulate matter to deposit from the bulk fuel. The deposition does not occur at the higher Reynolds Number. The pump was shipped to the manufacturer for disassembly and visual inspection. It was reported, Reference 10, that all pump components were in excellent condition. A very slight scoring was observed on the cylinder barrel outer stabilizing lands and on the corresponding surface of the port block face. This was reported as a normal condition resulting from the effects of the cylinder barrel pressure over-balance. No overhaul or parts replacement was necessary.

Figure 17. Engine Pump Fittings

Engine Filter

A 2 micron filter element was used for the engine filter in lieu of the more simulative 40 micron size. Based on past experience, Reference 4, it had been found that the filter reflected engine pump degradation rather than fuel coking. Therefore, in order to preclude possible pump contamination in the remainder of the engine system, a decision was made to use a 2 micron nominal (15 micron absolute) filter. As testing progressed, it was found that the 2 micron filter element performance was reflecting incoming contamination and not pump contaminants. It was decided to continue using this size so that the incoming contaminants would also not affect engine component performance.

Approximately 101,000 gallons of fuel ranging in temperature from 70 to 280°F passed through the filter assembly during the two test series. The 2 micron nominal (15 micron absolute) filter element was replaced 18 times during the two test series. The pressure drop, measured during climb conditions is shown in Figure 18. Replacement of the filter element due to excessive pressure drop varied from 2 to 27 cycles. The solids on the filter elements were analyzed and found to be inorganic material (Reference 11). Additionally, the engine filter element lasted longer after the fuel feed depth filter (2 micron nominal - 10 micron absolute) was changed. It was therefore, concluded that the engine filter elements reflected depth filter efficiency and system debris rather than fuel thermal degradation. This phenomenon was noted with respect to the airframe filter during the fourth test series of Reference 4.

Each engine filter element removed from the system was ultrasonically cleaned and reused. A total of three elements were used for the two test series.

Engine and Uni-Tube Heat Exchangers

Calibration Test Procedure - Prior to the first test series and after the second test series, the engine and Uni-Tube heat exchangers were calibrated under fluid flow and thermal conditions that produced heat transfer coefficients approximately twice those encountered during the normal test cycles. The purpose of these tests is to:

1. Determine more accurately the heat transfer efficiency loss by using higher heating capacity and flowrates.
2. Determine if a calibration shift has occurred.

The fuel was preheated in the fuselage tank to 186 ± 6°F and was recirculated through the heat exchangers. The oil was preheated to 470 ± 20°F while flowing through the engine and Uni-Tube heat exchangers at 5.46 ± 0.04 gpm and 0.5 gpm, respectively.

The fuel flow rate was then adjusted to 11.65 ± 0.05 gpm (71.1 lbs/min) through the engine heat exchanger; this produced a Uni-Tube fuel flow rate of 0.33 gpm. The Uni-Tube oil flow rate was then adjusted (0.54 ± 0.01 gpm) to produce a fuel-out temperature identical to that of the engine heat exchanger. After the fluid outlet temperatures had stabilized, the test was repeated with fuel flow rates of 8.73 ± 0.03, 5.85 ± 0.10, and 2.91 ± 0.01 gpm, and 0.24 ± 0.01, 0.16 ± 0.01, and 0.08 ± 0.01 gpm through the engine and UniTube heat exchangers, respectively.

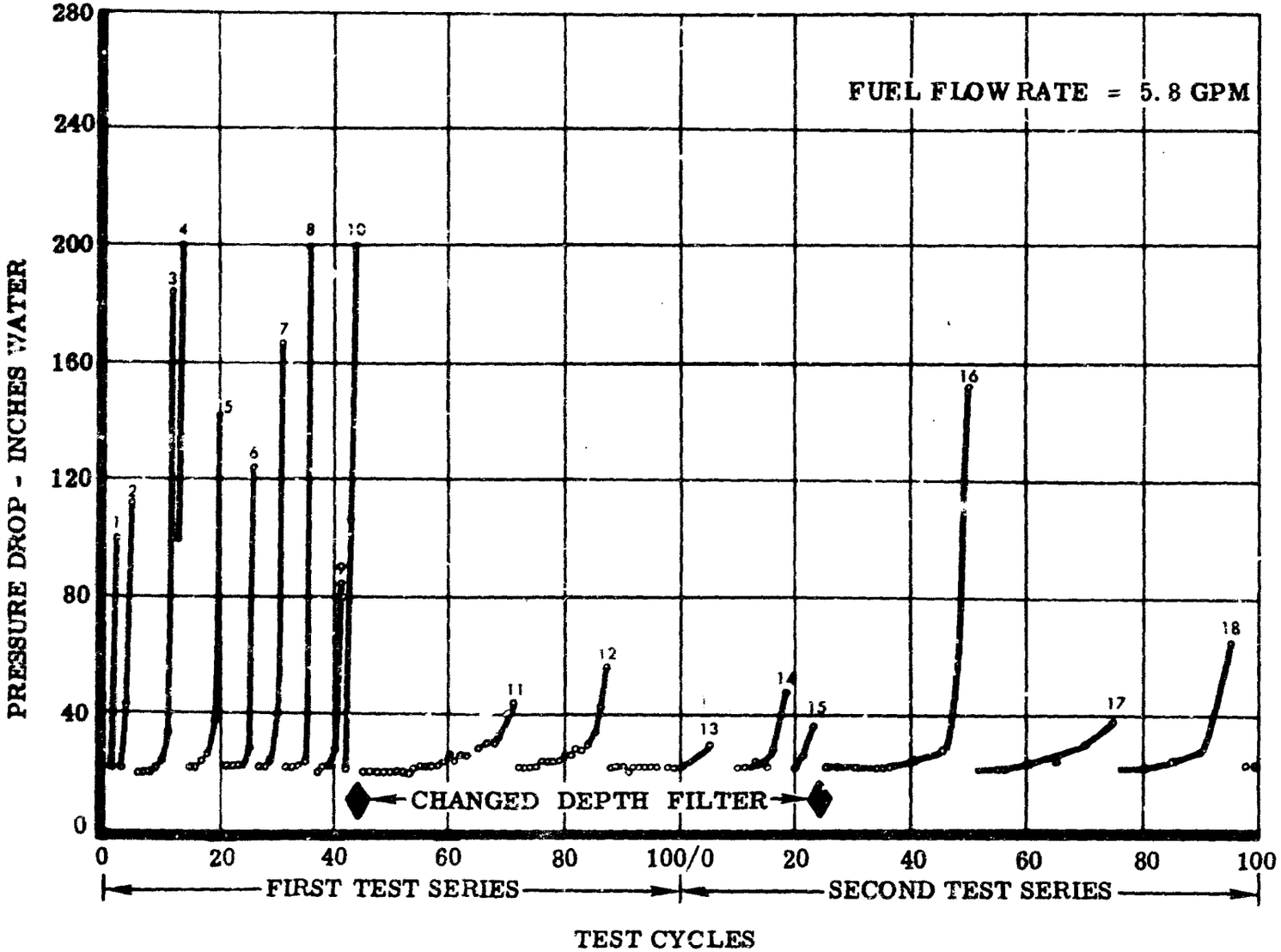

Figure 18. Pressure Drop Across Engine Filter

The Uni-Tube and engine heat exchanger oil flow rates were the same for all tests. The heat input for the 11.7, 8.7, and 5.9 gpm tests was 1670 BTU/Min. and for the 2.9 gpm test the heat input was 1340 BTU/min. The overall heat transfer coefficient of the engine heat exchanger and the fuel side heat transfer coefficients (outlet and average) of the Uni-Tube heat exchanger were computed from measurements of fuel flow rate and fuel, oil and tube wall temperature measurements. The overall heat transfer coefficient was corrected to an average fuel temperature in the heat exchanger of 210°F.

Normal Operating Procedure - The shell side fluid, a napthenic mineral oil, was circulated through the engine heat exchanger at a rate of 2.7 gpm and through the Uni-Tube heat exchanger at 0.3 gpm. This oil was heated by an electrical heater to simulate the heat rejected to the fuel by the engine lubrication and hydraulic systems. During each test cycle, the average heat input was controlled to 540 BTU/min. as established during the initial test cycles. This heat input resulted in an average fuel temperature increase across the heat exchanger of 25 and 60°F during the climb and cruise conditions, respectively.

At beginning of descent the heater was de-energized and the temperature rise during descent was that resulting from the residual heat in the oil system. The maximum temperature of the fuel out of the engine exchangers occurred at the start of descent and was 340°F. The measured maximum tube wall temperature on the Uni-Tube heat exchanger was 385°F.

Steady State Cruise Test Cycle Procedure - During the performance of the test cycles of the two test series, 20 "steady state cruise test cycles" were conducted approximately every 10 test cycles. The "steady state cruise test cycle" consisted of a normal test profile except that the fuselage tank heaters were de-energized to permit the temperature of the fuel entering the engine and Uni-Tube heat exchanger to stabilize (188 ± 5°F). During this stabilization period, the fuel, oil, and tube wall temperatures were measured with the more sensitive (lower scale) of a dual range recorder. These temperatures were then used to determine the overall heat transfer coefficient of the engine heat exchanger and the fuel side heat transfer coefficients of the Uni-Tube heat exchanger. Upon completion of this stabilized portion of the test cycle, the fuselage tank heaters were re-energized to simulate the profile during the remainder of the test cycle.

Uni-Tube Heat Exchanger Discussion - The purpose of the Uni-Tube heat exchanger is to obtain fuel side heat transfer information which can be used to determine the fuel side heat transfer efficiency loss of the engine heat exchanger. The design of the Uni-Tube heat exchanger is delineated in Reference 2. The two configurations (1 and 2) discussed therein were tested during the pre-test series calibration tests, and it was found that the tube wall thermocouples of configuration 2 were the most sensitive to tube wall temperatures and, therefore, more sensitive to fuel degradation. However, these thermocouples were not as sturdy as those of configuration 1, and four of the ten thermocouples were inoperative at the end of the calibration tests. The remaining six thermocouples produced temperature measurements which were internally consistent and agreed with measurements made during previous testing, Reference 4. Furthermore, the oil side heat transfer coefficient was calculated based on these temperature measurements and compared to the theoretical heat transfer coefficient for an annular tube in the laminar flow range. These values were within 5.3% of each other. Therefore, it is considered that the Uni-Tube instrumentation is reliable as a source of data for fuel degradation.

The flow rate in the Uni-Tube is not exactly the same as the average flow rate per tube of the engine heat exchanger. However, this deviation is such that the effect on the difference in tube wall temperature between the Uni-Tube and engine heat exchanger is calculated to be 5°F during the test cycle. Therefore, when the maximum measured tube wall temperature in the Uni-Tube is 385°F, the maximum tube wall temperature in the engine heat exchanger should be 380°F. Therefore, it is regarded that the Uni-Tube simulates the temperature environment of an average tube in the engine heat exchanger, and the engine heat exchanger fuel side heat transfer coefficient can be calculated from the fuel side heat transfer coefficient of the Uni-Tube heat exchanger.

Results - The calculated heat transfer coefficients for the engine and standard heat exchangers, obtained during the calibration tests, are shown in Figure 19. As evidenced by the decrease in the heat transfer coefficients of the standard heat exchanger, a calibration shift occurred between the tests. The engine heat exchanger calibration test results indicate the same decrease within the repeatability of the test results; 3% band. Therefore, it is concluded from the calibration tests that the overall heat transfer efficiency was not measurably affected by the fuel thermal stability.

The results of the Uni-Tube calibration tests are shown in Figure 20. These results indicate that the fuel side heat transfer efficiency was not measurably affected. Since this fuel side heat transfer efficiency on the Uni-Tube did not change and the overall heat transfer efficiency of the engine and standard heat exchangers decreased, it can be concluded that the oil side heat transfer coefficient decreased. Based on the results

shown in Figures 20 and 21, it has been calculated that the average oil side heat transfer coefficient measured during the calibration tests had decreased from 660 to 622 BTU/hr-ft^2-°F (average for all fuel flow rates since oil flow rate was the same). This decrease in oil side heat transfer coefficient caused the decrease in the standard and engine overall heat transfer coefficients. This is further evidenced by the results obtained during the test series, Figure 21.

As shown in Figure 21 the overall heat transfer coefficient for the first 75 test cycles of the first test series was 231 +3,-5 BTU/hr-ft^2-°F, and for the remaining 125 test cycles of the first and second test series, the coefficient was 225 ± 5 BTU/hr-ft^2-°f. Using the absolute values of oil side heat transfer coefficient obtained during the calibration tests, it was found that the ratio of the oil side heat transfer coefficient before and after the two test series was 1.05. It can be shown that this ratio is equal to that of the normal test cycles. Using the Uni-Tube fuel side heat transfer coefficient obtained during the test cycles, Figure 22, and correcting this value for the higher fuel flow rate in the engine heat exchanger, it was found that if the initial overall heat transfer coefficient is 231 BTU/hr-ft^2-°F, as was measured, and the ratio of initial and final oil side heat transfer coefficient is 1.05, then the overall heat transfer coefficient at the end of the test series will be 224 BTU/hr-ft^2-°F. This is within one unit of the actual average measurement. It is therefore concluded from the test series engine heat exchanger data that the overall heat transfer efficiency was not measurably affected by the fuel thermal stability. This is affirmed by pressure drop measurements shown in Figure 23 and visual inspection of the engine heat exchanger, Figure 24.

The fuel side heat transfer coefficient of the Uni-Tube measured during the test series is shown in Figure 22. The average and outlet values were 555 and 449, respectively. There appears to be a trend indicating that the outlet fuel side heat transfer coefficient decreased. This coefficient is measured at the location wherein tube wall temperature is the highest and, therefore, wherein deposition should be the greatest. It is considered that the outlet fuel side heat transfer actually decreased; however, this decrease is not significant with respect to overall heat exchanger performance.

Inspection of the engine heat exchanger after the series and before it was bisected indicated that the CRC color scale rating of the inlet and outlet was 0 and 2-3, respectively. The inlet and outlet mating fittings rated 2 and 8-9, respectively. Here again, as pointed out in the engine pump section, areas of low Reynolds numbers have greater deposits even though the temperatures are the same. The heat exchanger was then bisected and the outer shell removed. Three tubes from different locations in the heat exchanger were cut open and it was found that they were consistent in color. A photograph of half the exchanger and one bisected tube is shown in Figure 24. Inspection revealed that the oil side contained no deposits. The fuel inlet was discolored, rating less than 2 on the CRC Lacquer Rating

Scale. The deposits became more prominent toward the fuel outlet where the tube was rated a 3 on the CRC Lacquer Rating Scale. It is noted, for future inspection purposes, that this heat exchanger appeared to have a fuel side deposit brown in color whose intensity lay approximately midway between the second and third test series heat exchangers reported in Reference 4. These heat exchangers, Reference 4, were reported to have had no measurable loss in heat transfer efficiency.

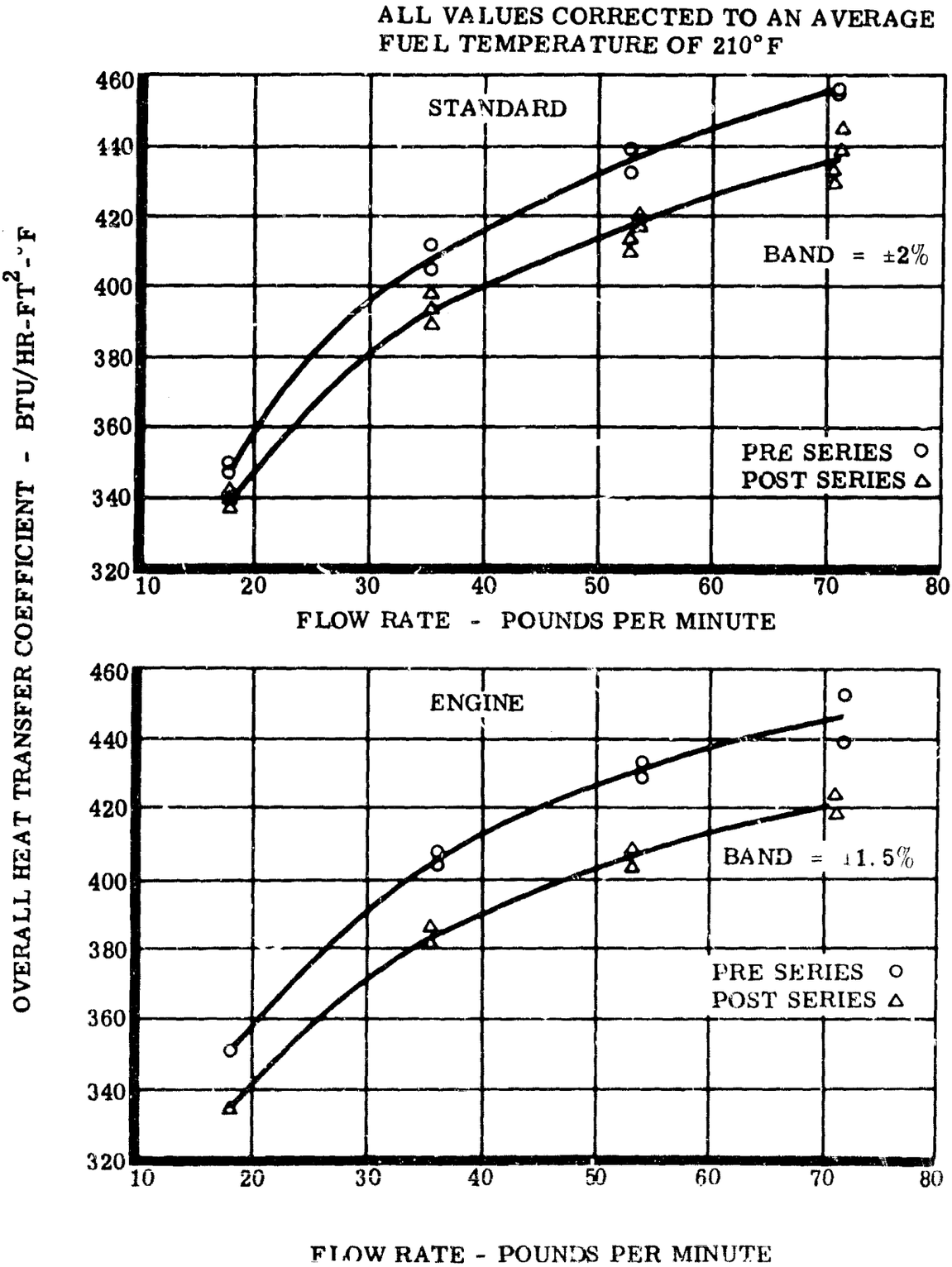

Figure 19. Engine Heat Exchanger Calibration Test Results

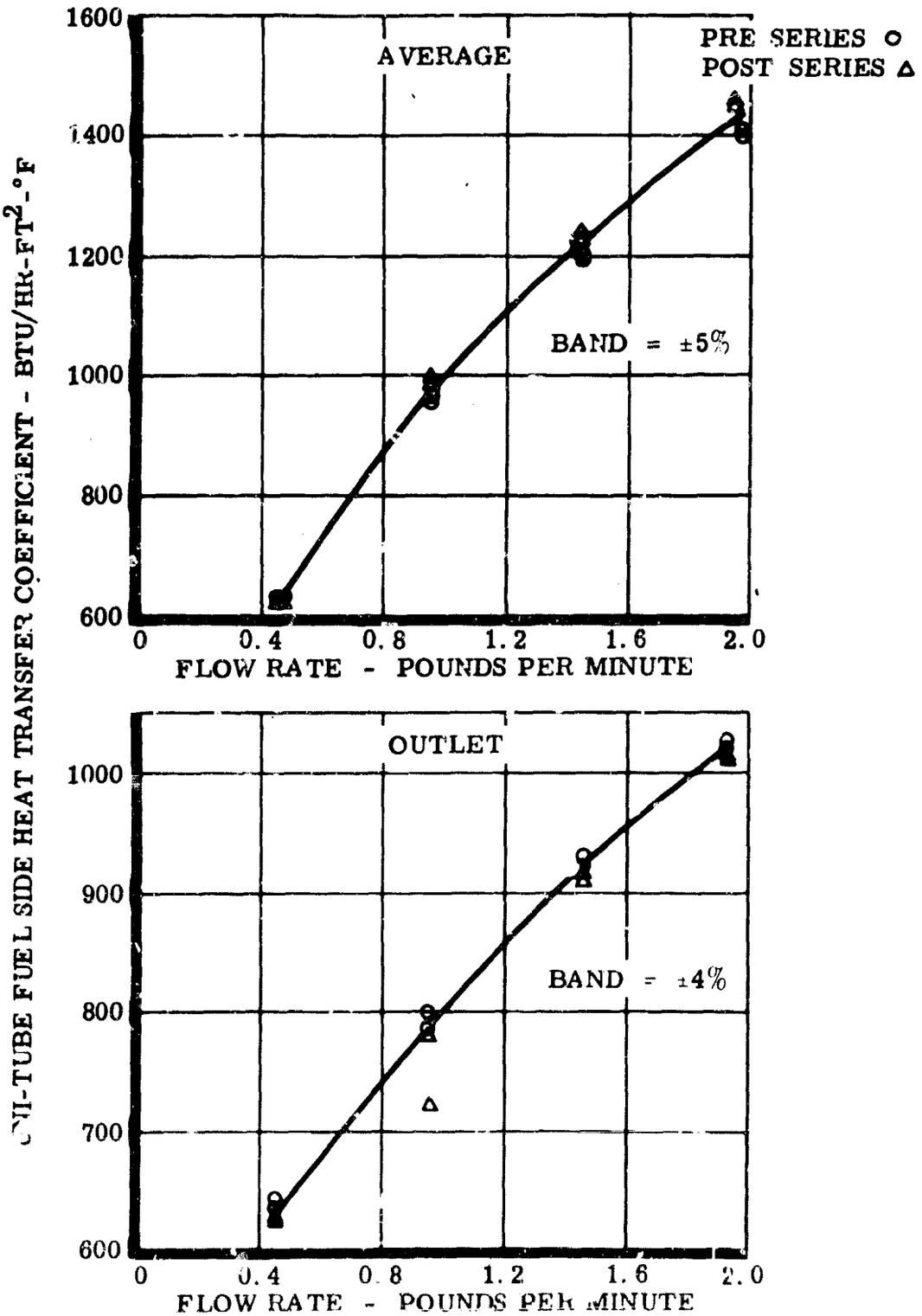

Figure 20. Uni-Tube Heat Exchanger Calibration Test Results

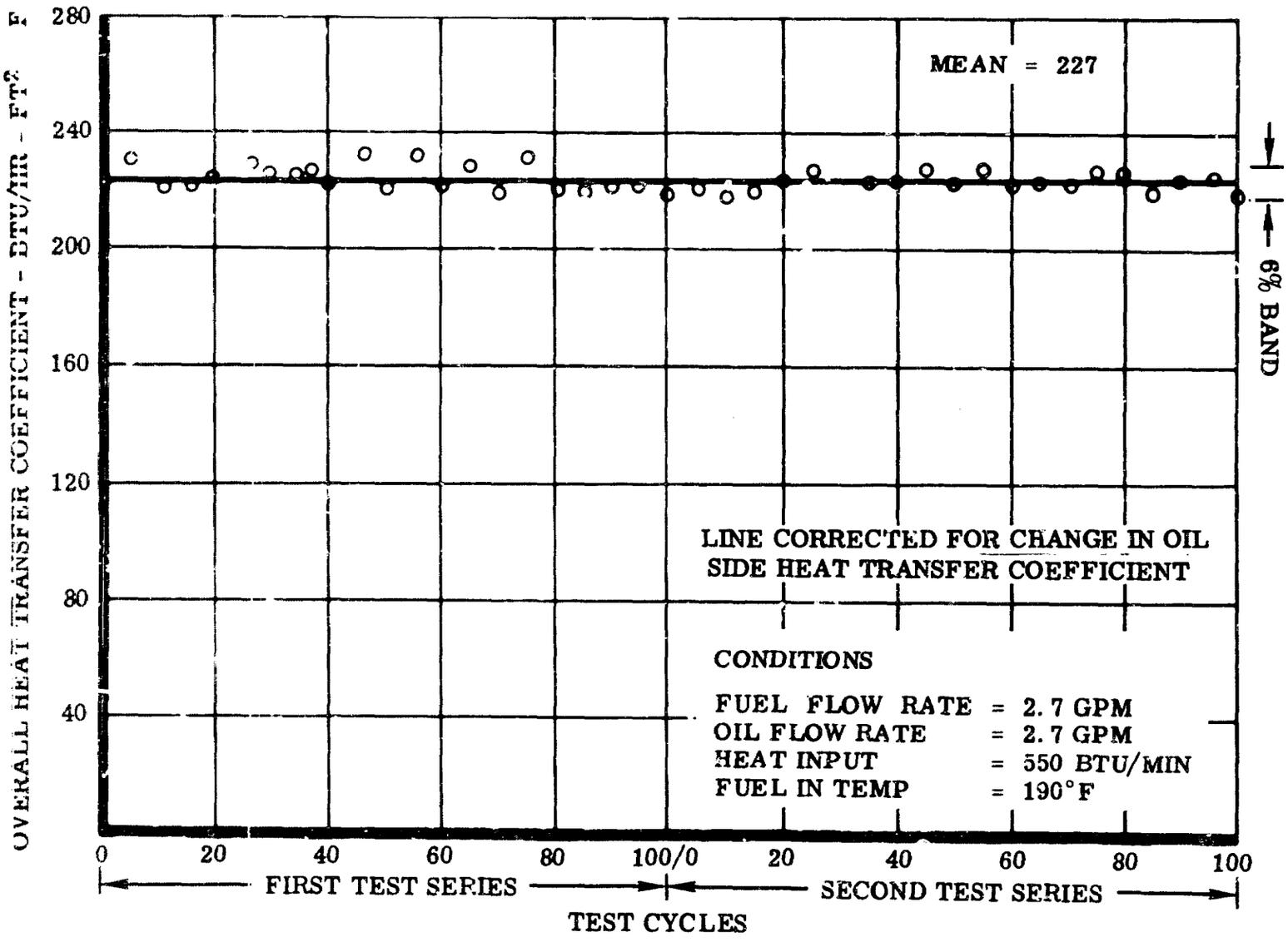

Figure 21. Overall Heat Transfer Coefficient of Engine Heat Exchanger

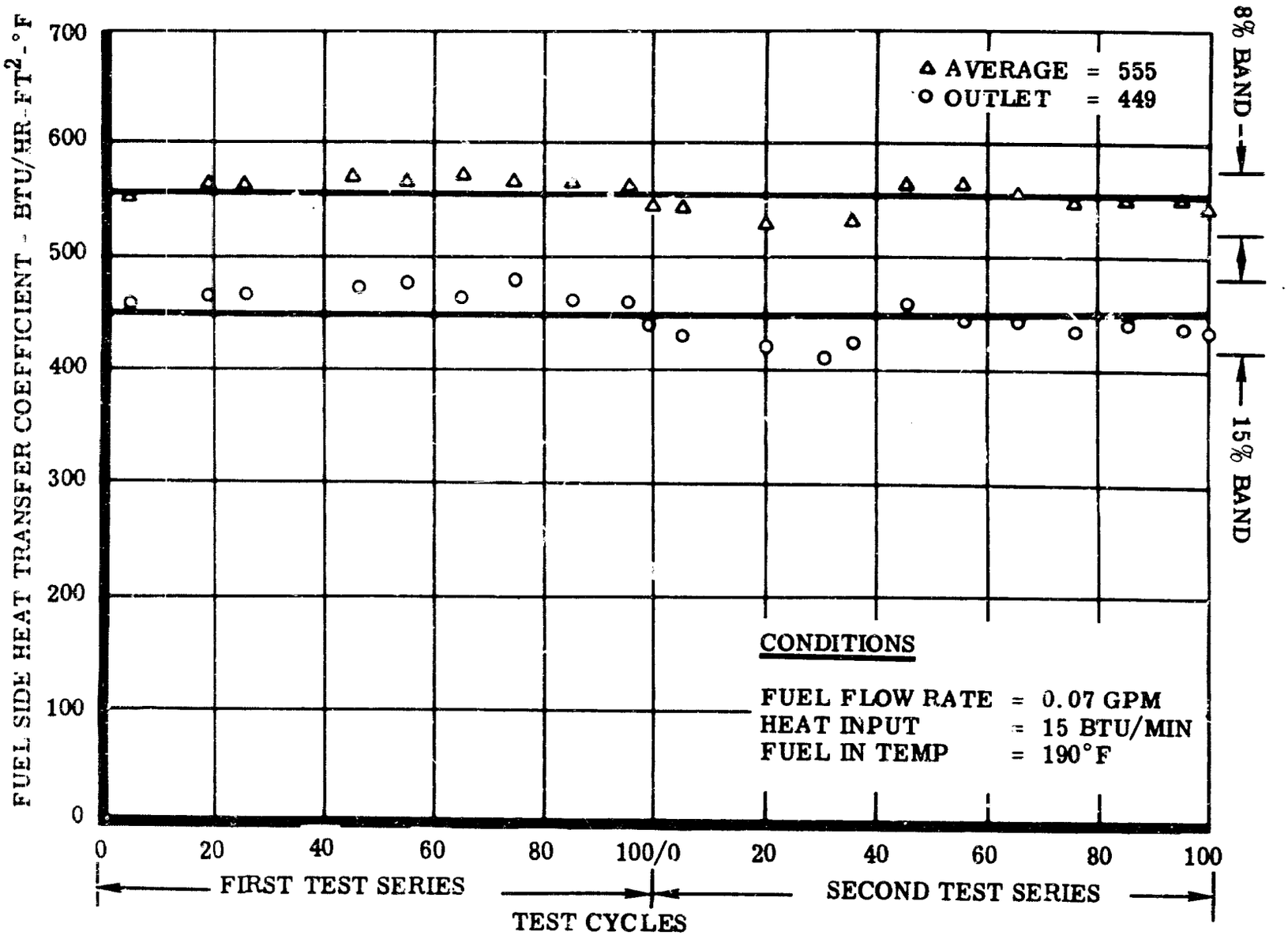

Figure 22. Fuel Side Heat Transfer Coefficient of Uni-Tube Heat Exchanger

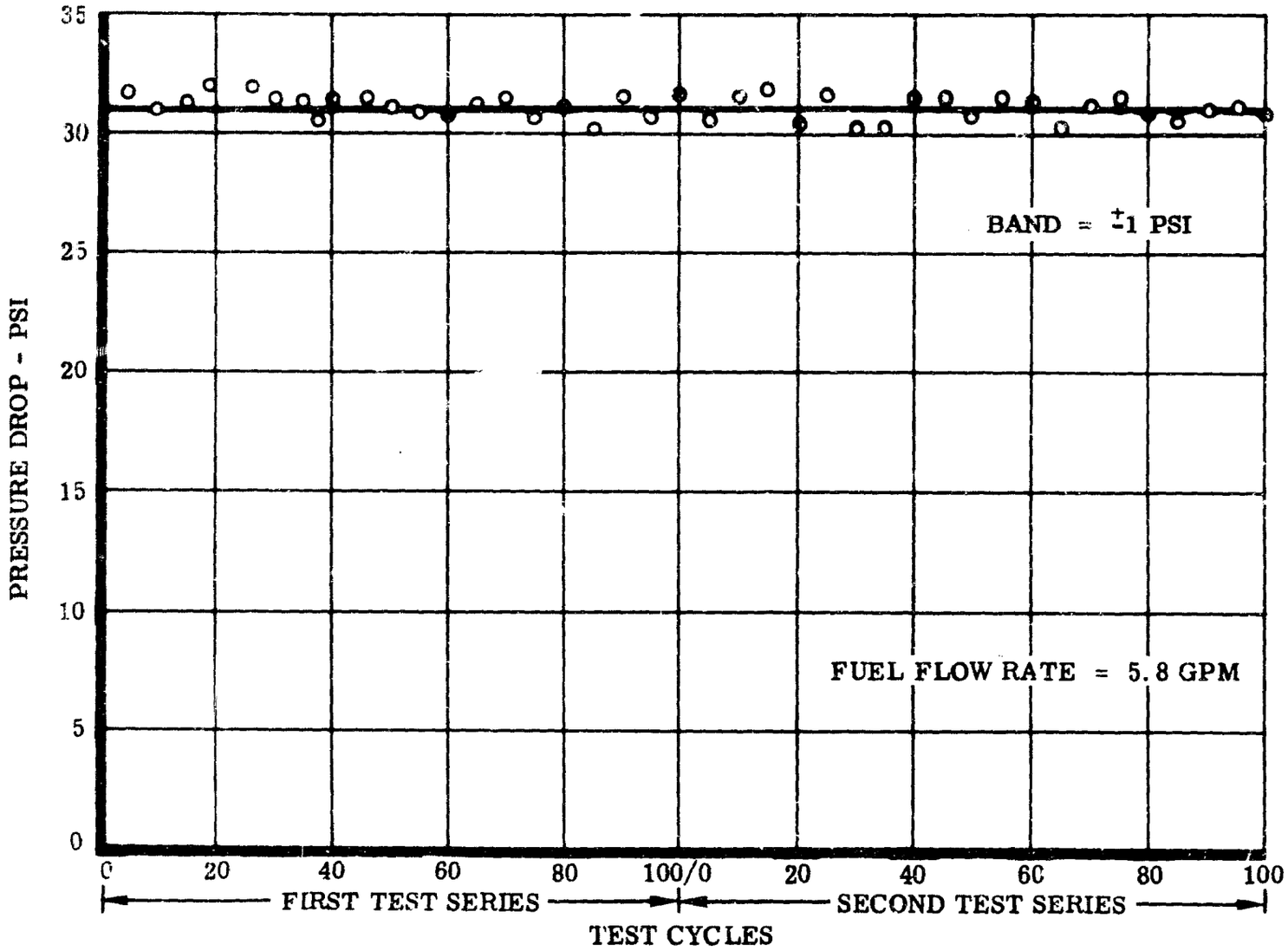

Figure 23. Pressure Drop Across Engine Heat Exchanger

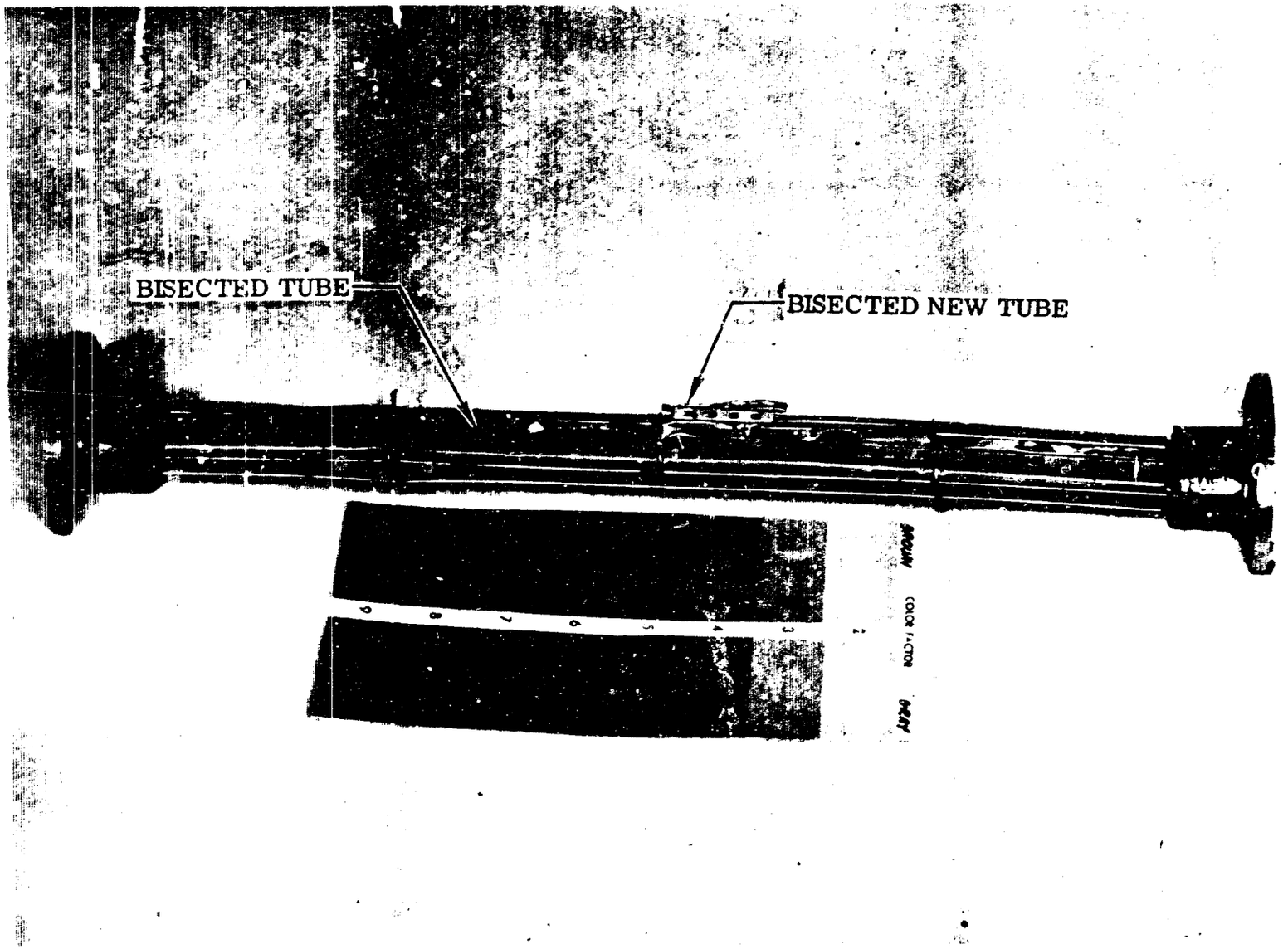

Figure 24. Engine Heat Exchanger

Manifold

Normal Operating Procedure - The manifolds used in both test series were 0.3125" O.D. x 0.028" wall 321 stainless steel tubing. Electrical connector tabs were welded to the center and ends of the manifold to permit terminal resistance heating. The manifold tubing adjacent to the tabs at the ends and center are relatively unheated. The heating power supply was energized at test start-up and the power output controlled to produce the fuel temperatures indicated below. This heat input is used for both climb and cruise conditions.

Test Series	Heated Length, In.*	Heat Input** BTU/Min.	Fuel Temp.** Increase, °F	Maximum Fuel Out Temp. °F
First	115	846	85 ± 2	600
Second	94	495	51 ± 1	500

*Distance between outer electrical connectors
**Fuel-in temperature = 290°F, cruise conditions, steady state test cycles

During descent when the fuel flowrate was decreased from 2.7 gpm to 0.68 gpm, the fuel outlet temperature increased to 600°F during the first test series and 500°F during the second test series. This maximum temperature is obtained within one minute and then is slowly decreased in accordance with the profile requirements by decreasing the power supply output.

Temperature Measurement Discussion

Six thermocouples were located on the outer wall spaced down the length of the manifold tube to provide a measurement of heat transfer coefficient which in turn would permit a determination of fuel deposits on the inner tube walls. The method of thermocouple attachment was investigated since it was evident that attaching the thermocouple directly to the tube wall would produce erroneous measurements. This error is caused by the thermocouple, and hence the temperature recorder, being subjected to a portion of d-c heating voltage applied to the tube. It was decided to use a method of thermocouple attachment reported, Reference 12, to be successful under these conditions. This consisted of electrically isolating the thermocouple from the tube with a thin sheet of mica. A narrow strip of glass tape was then wrapped around the tube over the thermocouple followed by a layer of asbestos, and a circular retaining clamp was used to hold the assembly on the tube. This method proved unsuccessful due to fracturing of the mica when the thermocouples were flexed during insulation of the manifold. It was decided to use one layer of glass tape instead of

the mica. This method was used in the first test series and proved to be unsuccessful. The temperatures measured were below the anticipated values; i.e., during cruise conditions there was a discrepancy of 20 to 40°F. The anticipated values had been calculated using the following equation:

$$t_w = t_f + Q/A \left(1/0.027 \frac{k}{D} N_{Re}^{0.8} N_{Pr}^{1/3} (\mu/\mu_w)^{0.14} + x_w/k_w\right)$$

where: t_w = outer wall temperature at a given distance from the inlet, °F

t_f = bulk fuel temperature at the same distance, °F

Q/A = fuel heat input flux, BTU/hr-ft^2

k = thermal conductivity of the bulk fuel, BTU/hr-ft^2-F/ft.

D = inner diameter of the tube, ft.

N_{Re}; N_{Pr} = Reynolds and Prandtl numbers, respectively, of the bulk fuel, dimensionless

μ/μ_w = ratio of the viscosity of the bulk fuel to the fuel film, dimensionless

x_w = manifold wall thickness, ft.

k_w = thermal conductivity of 321 stainless steel, BTU/hr-ft^2-°F/ft.

At the beginning of the second test series, other methods of thermocouple attachment were tried because of the discrepancy found in the first test series. The most accurate method found was the tack-welding of a stainless steel sheathed thermocouple directly to the tube and isolating the temperature recorder from ground. However, these thermocouples are a special order item (delivery in six weeks) and therefore, were not available for use in the second test series. The next best method was to tack-weld a constantan wire of an iron-constantan thermocouple around half the circumference of the tube and then tack-weld the iron wire on top of the constantan wire. A test cycle was then conducted and the difference between the anticipated (as calculated from the above equation) and measured temperatures were 0 to 9°F for the cruise conditions. This was considered acceptable since the discrepancy was within the National Bureau of Standards limit of error for the thermocouples.

Results - The deposit thermal resistance (x_d/k_d), which is discussed in Section IV, was calculated for each thermocouple location on the first and second test series manifolds. The values obtained for the deposit thermal resistance at each location are as follows:

Thermocouple Position	Maximum Fuel Film Temp., °F, for Test Series No.		Deposit Thermal Resistance (x_d/k_d), Mil-hr-ft^2-°F/BTU-ft, for Test Series No.	
	1*	2**	1***	2****
1	470	445	0.5	0.8
2	495	510	0.7	0.8
3	545	510	1.7	1.0
4	585	520	1.8	1.2
5	625	555	2.8	2.0
6	670	575	4.3	2.4

*Temperatures determined from metal temperatures measured during first steady state manifold test discussed in Section IV.

**Temperatures determined from metal temperature measurements during second test series.

***Determined from increase in metal temperatures during first test series.

****Determined from equation shown in Section IV.

The above values of deposit thermal resistance were converted to deposit thickness, in mils, by multiplying each value by a deposit thermal conductivity of 0.07 BTU/hr-ft^2-°F/ft. This choice of 0.07 is the average of 0.09 (the thermal conductivity of deposit-like materials) and 0.05 (the deposit thermal conductivity reported in Reference 13). These calculated deposit thicknesses for the first and second test series manifolds are shown in Figures 25 and 26, respectively.

Also shown in Figures 25 and 26 are calculated deposit thicknesses based on carbon analyses performed by NASA (Reference 14) and W-PAFB (Reference 15) laboratories on samples of the manifolds. The analyses conducted by W-PAFB were performed on a Laboratory Equipment Corporation (LECO) Model No. 734-200 Low Carbon Analyzer. The range of the instrument is 0.5 to 5000 ppm carbon for one gram samples. The sensitivity at the lower end of the range under proper conditions is 0.5 ppm carbon. The deposited manifold tubing samples (eight for each manifold) ranged in carbon content from 772 to 1515 ppm carbon for the first test series and 530 to 962 ppm carbon for the second test series. The deposits were removed from a sample of each of the manifolds and the stainless steel was analyzed for carbon content. The carbon content of these blanks (stainless steel alone) was found to be 717

and 547 ppm for the first and second test series manifolds, respectively. The carbon content on the deposit in each sample was calculated as the difference between the carbon content of the sample and the blank. The amount of deposit on each sample (micro-grams deposit per gram of sample) was reported as this value multiplied by 1.50 (assumes that deposit is 67 percent carbon). The analyses performed by NASA were conducted in much the same manner except that the carbon in the stainless steel did not have to be ascertained because their tests were conducted to give the carbon content only in the deposits on the samples. The reported deposit contents of the manifold tube (the first test series manifold was analyzed by NASA and W-PAFB and the second test series manifold by W-PAFB) were converted to deposit thickness by using 0.9 as the specific gravity of deposits. These calculated deposit thicknesses are shown in Figures 25 and 26. Also shown in these Figures are the results of a replicate analysis by W-PAFB(Reference 20).

Independent of this determination, AFAPL (Reference 16) calculated the increase in metal temperature that should result from the amount of deposits analyzed on the first test series manifold.

The calculated values were within 10 percent of those actually measured during the test series. The assumptions made in the calculations were as follows:

1. The change in temperature is caused by conduction only; therefore, the change in metal temperature is equal to the heat flux multiplied by the deposit thermal resitance.

2. The specific gravity is 0.9 based on the composition of deposits in tubes given in Reference 17 and a survey of organic compounds, Reference 18, relating to the deposit analysis.

3. The thermal conductivity is 0.1 BTU/hr-ft^2-°F/ft based on comparable materials to fuel deposits (i.e. powdered coke and paraffin wax).

The agreement between the calculated deposit thicknesses as determined by deposit thermal resitance and carbon analyses indicates that these may be reliable methods of determining the thermal stability of the fuel with respect to the manifold.

The pressure drop of the manifolds used in first and second test series is shown in Figure 27. There was insufficient amount of fuel deposit to cause a measurable increase in pressure drop. A photograph of each of the two bisected manifolds is shown in Figures 28 and 29.

In addition to the above performance parameters, the color of the deposits on the manifolds were rated with the CRC Lacquer Rating Scale. Since it is regarded that color is inferior to performance changes in quantifying deposits, the results of these reatings are not reported. However, an interesting relationship between the deposit thickness and the color ratings is shown in Figure 30. This plot was made by comparing the CRC Color Rating for each of the manifolds against the deposit thickness as determined in Figures 25

and 26 When the deposit thickness was 0.1 mil or greater, the manifold was rated a 9 or 10. In other words, above 0.1 mil the CRC Lacquer scale is insensitive to deposit thickness. Below 0.1 mil, the sensitivity of the color scale, i.e., the relative change in rating for a given change in deposit thickness, increases with decreasing deposits. It is most noteworthy that the relationship between the deposit thickness and color is not linear. This indicates that performance in terms of color cannot be indiscriminately extrapolated or interpolated on a linear basis. It is intended, during the next test series to make up a scale consisting of manifold tube segments whose deposit thickness can be determined and rating this scale with the CRC Lacquer Scale and the Tuberator, Reference 1. Thereby, a more detailed analysis can be made of the relationship of color and deposit thickness.

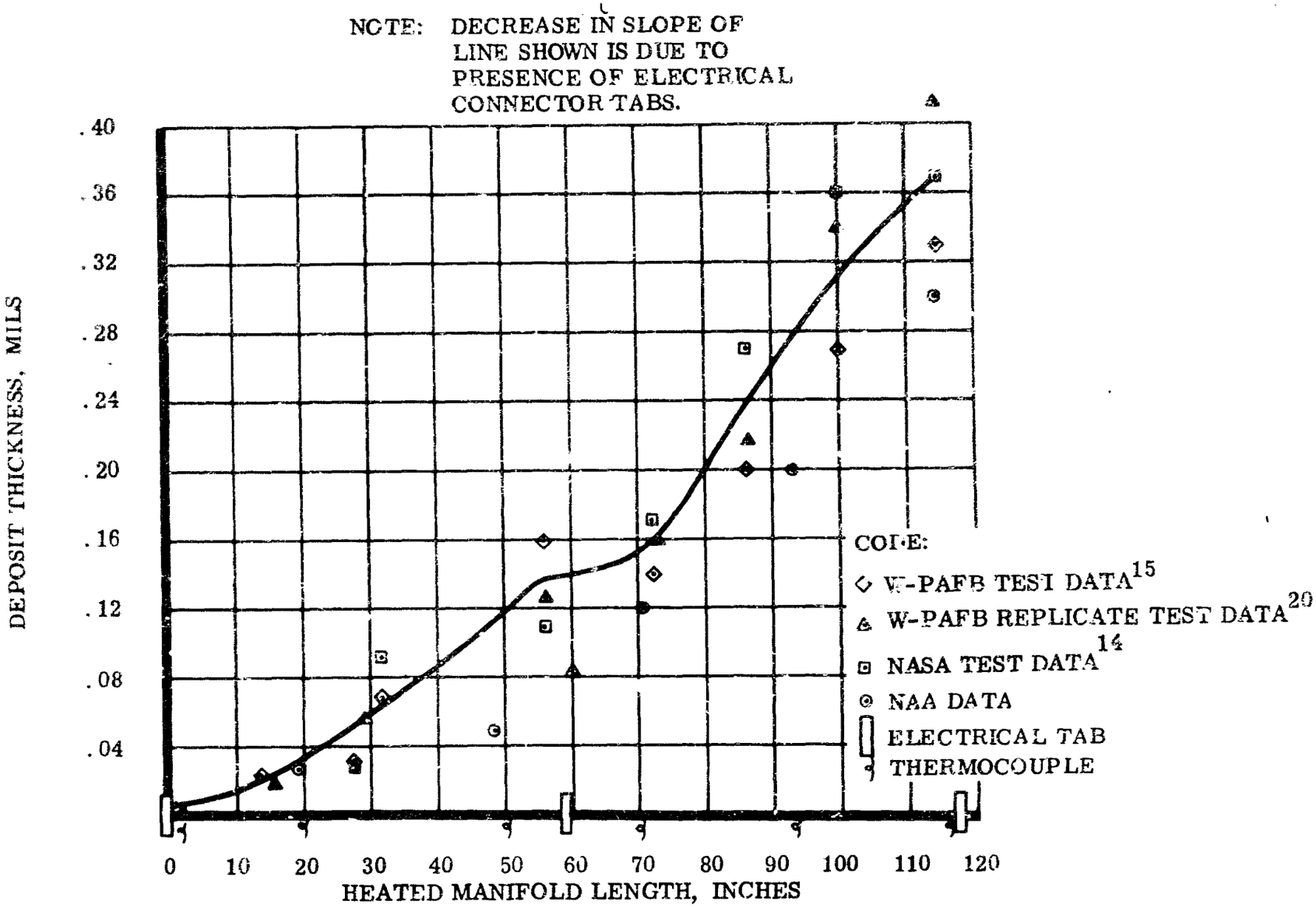

Figure 25. Manifold Deposit Thickness - First Test Series

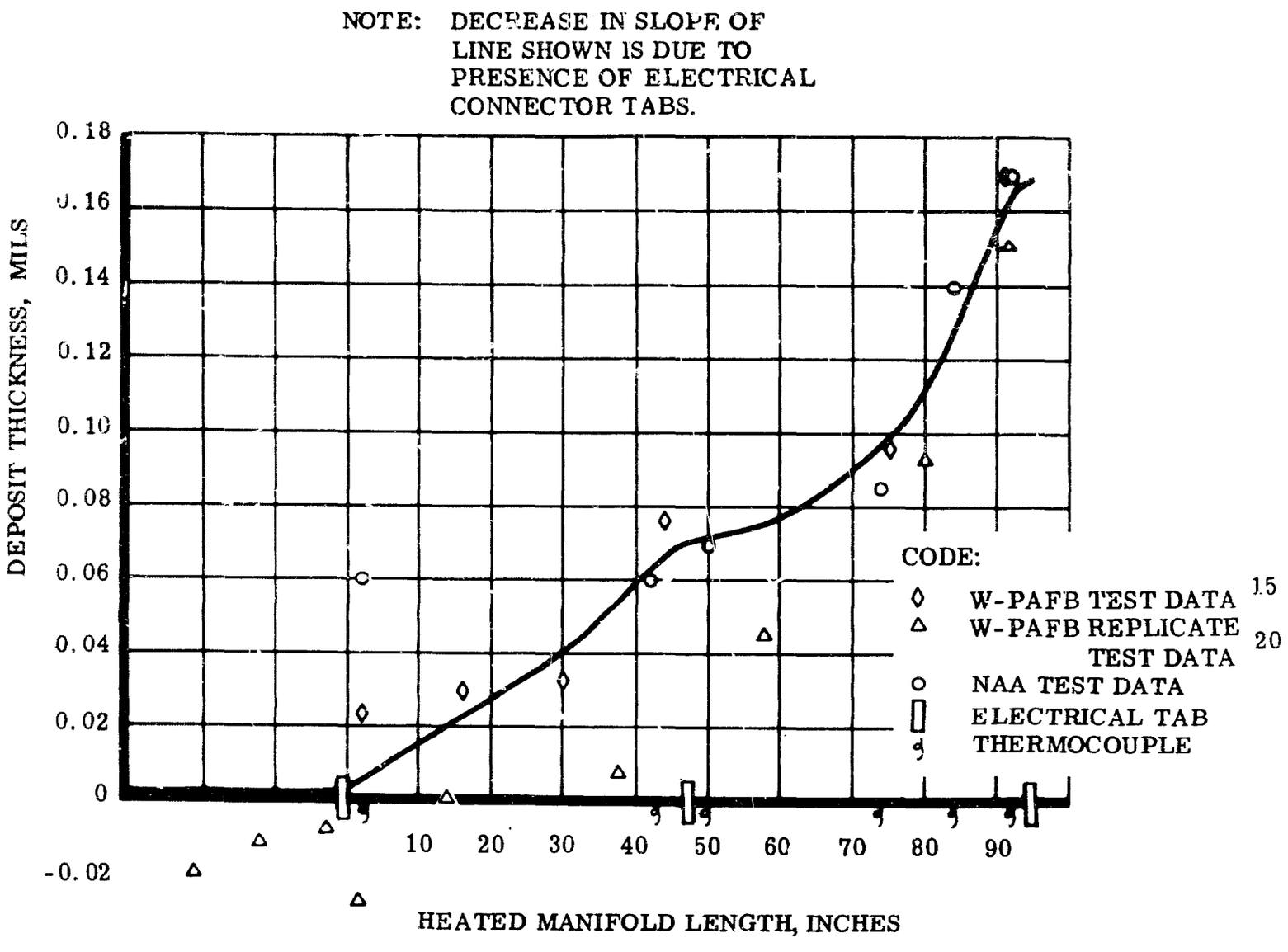

Figure 26. Manifold Deposit Thickness - Second Test Series

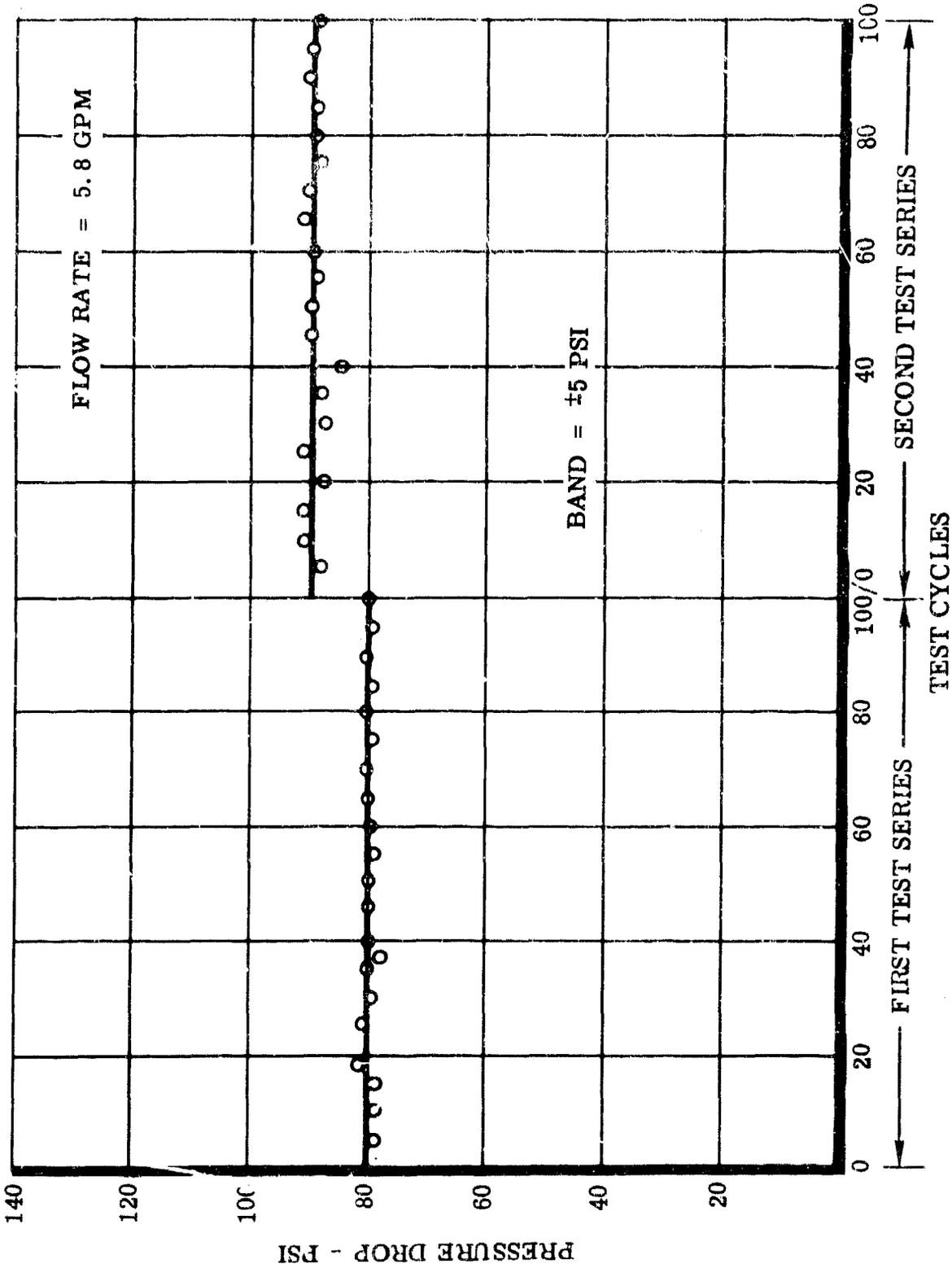

Figure 27. Pressure Drop Across Engine Manifolds

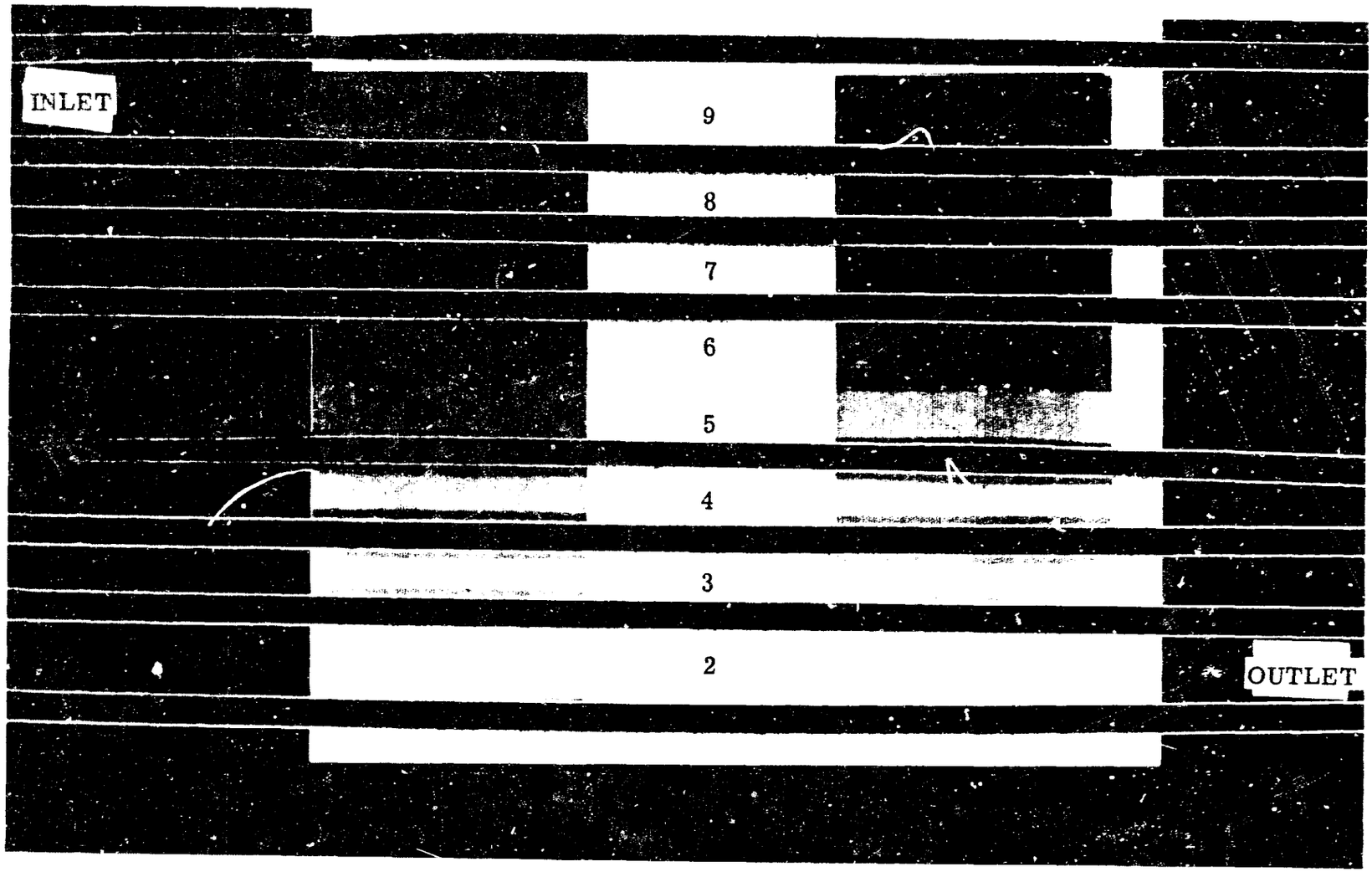

Figure 28. First Test Series Manifold

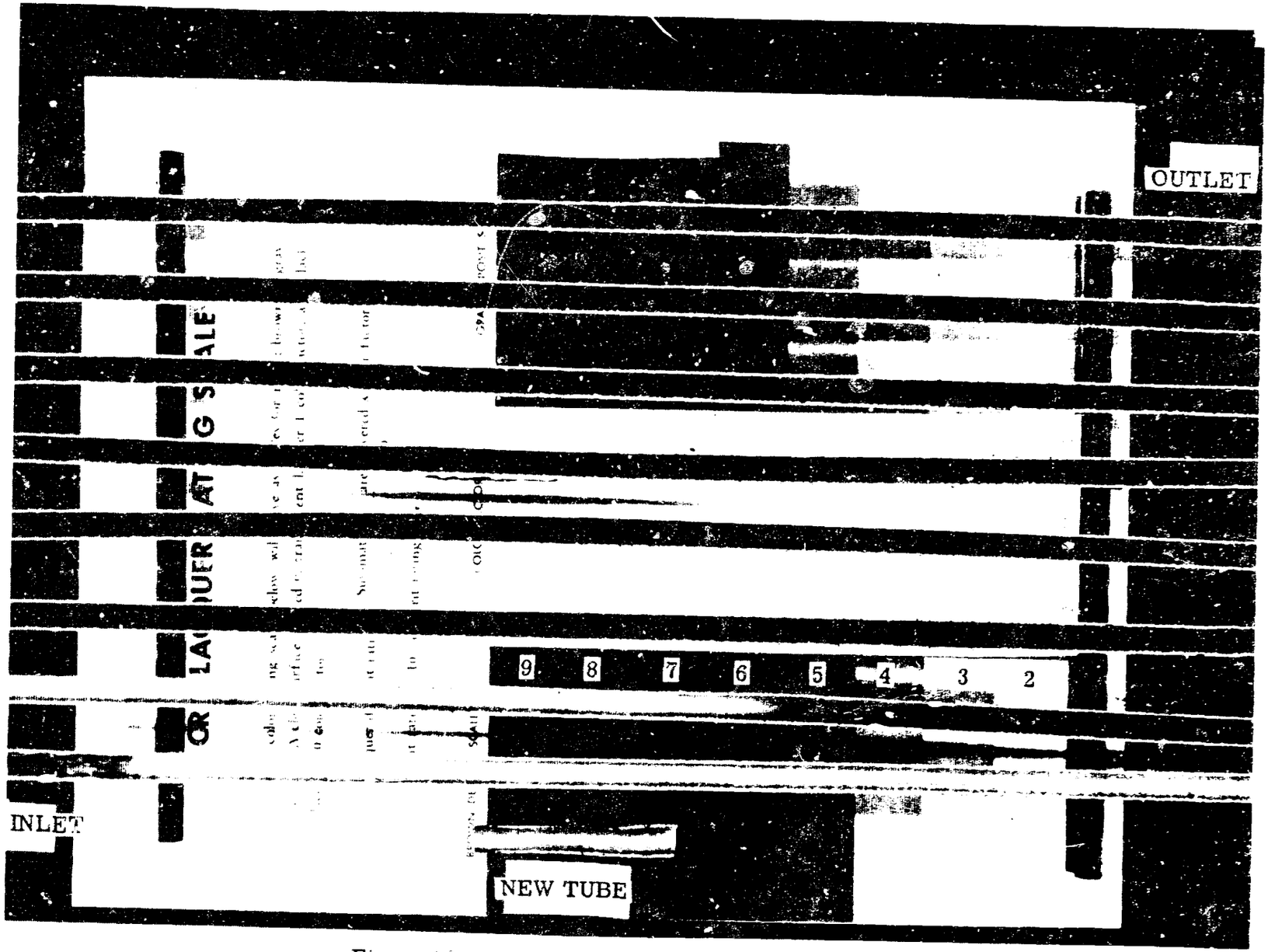

Figure 29. Second Test Series Manifold

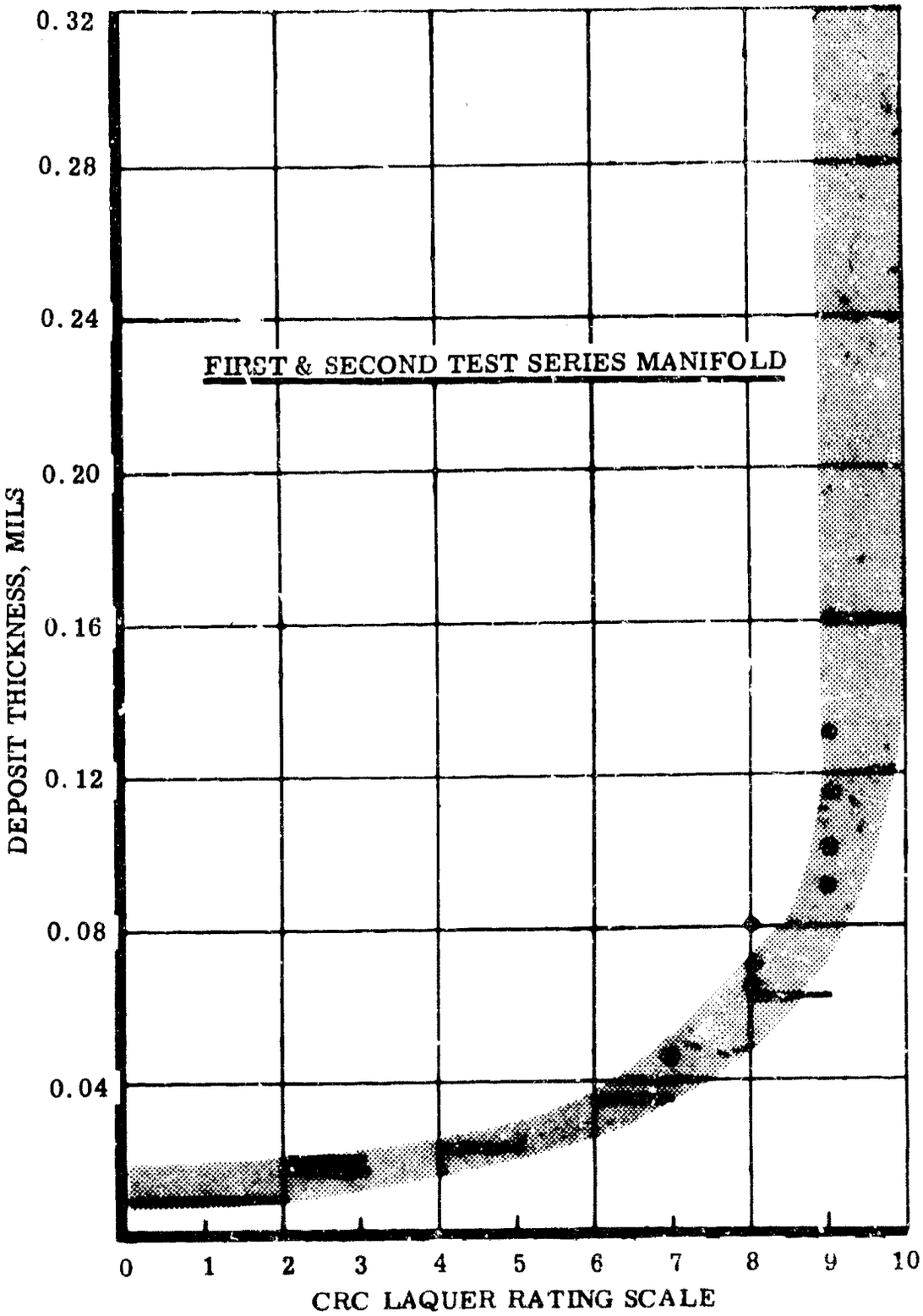

Figure 30. Comparison of Color Versus Deposit Thickness

Nozzle Subsystem

Operational Procedure - The nozzle heaters were energized at test start-up and the output controlled to produce a temperature rise of 2°F during the cruise condition and 8°F during the descent condition. The same heat input was used for the acceleration condition. The nozzle heater was de-energized at 159 minutes after test start-up. The temperature of the fuel into the nozzle reached a maximum of 600 and 500°F during the first and second test series, respectively. After the first test series, the nozzle was replaced because of the different temperature conditions of the second test series. Between selected test cycles a pressure drop-flow rate test was conducted to determine if plugging was taking place. This test was also conducted before and after each test series.

Results - The measurements of the pressure drop across the engine nozzles used during the two test series are shown in Figure 31. The pressure drop of the first test series nozzle increased from 352 to 370 psi, and the pressure drop of the second test series remained unchanged. In addition to these measurements shown in Figure 31, the pressure drop of the nozzles was determined prior to and after each test series. The pressure drop of the first test series nozzle increased from 692 to 725 psi at 2.7 ± 0.0 gpm, and the pressure drop of the second test series nozzle remained unchanged at 2.7 ± 0.0 gpm. Therefore, both the test series and pre- and post-test series nozzle pressure drop measurements indicate that the engine nozzle was not affected by the 500°F fuel temperature environment, but partial plugging occurred at the 600°F environment.

The test series nozzles were inspected after test cycles 1.048, 1.100, and 2.100 and following was noted:

CRC Lacquer Scale Rating

	Nozzle Face	Nozzle Screen	Outlet Adapter
1.048	8	9	8
1.100	10	10*	10
2.100	8	8	8

*A small amount of particulate matter was visible on the screen and appeared to be much larger than the screen pore size.

A photograph was taken of the two test series nozzle screens and is shown in Figure 32.

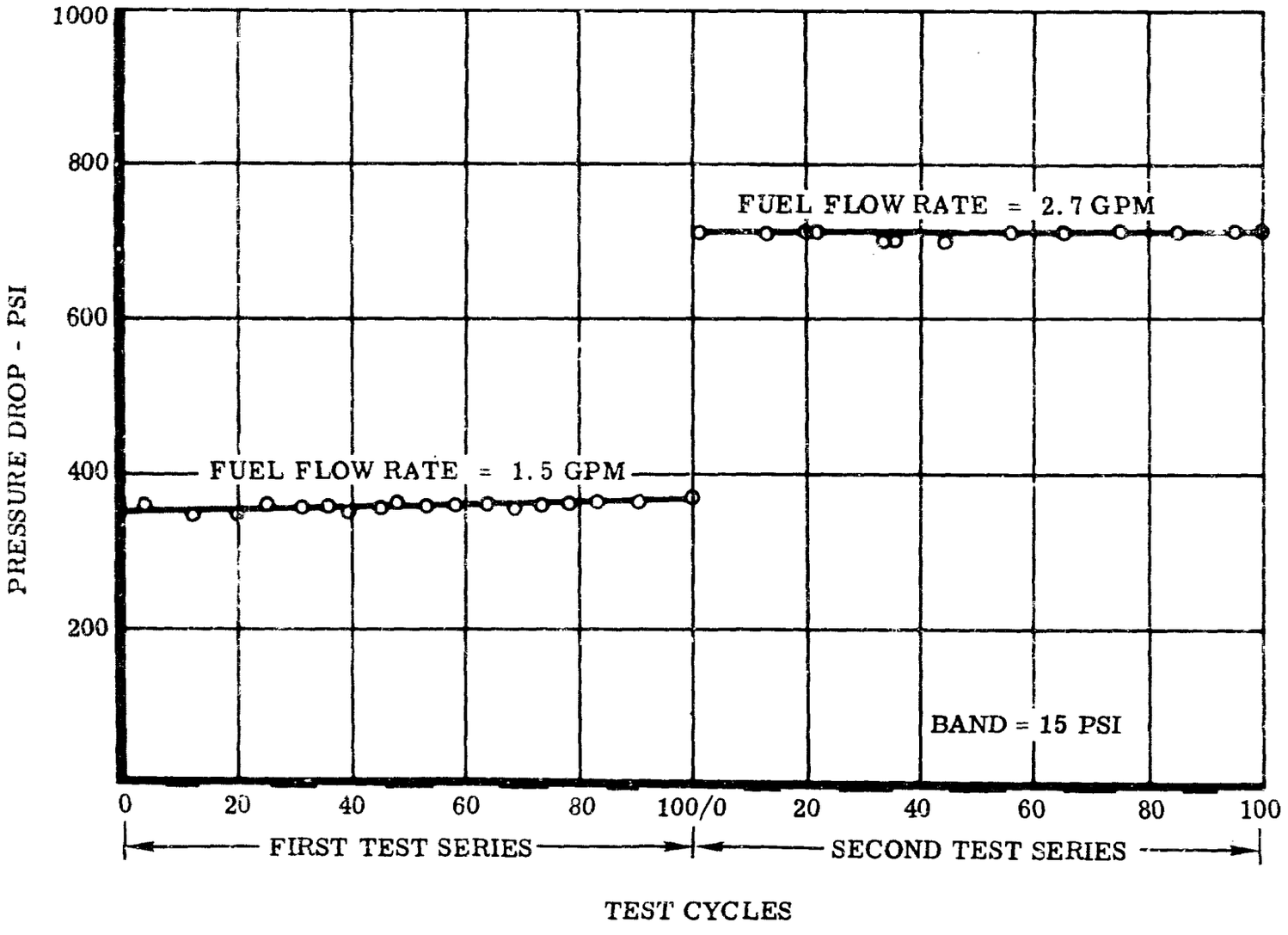

Figure 31. Nozzle Pressure Drop

Figure 32. Engine Nozzles

Additional Laboratory Analyses

In addition to the laboratory analyses described above in the appropriate sections, samples were taken for hydroperoxide number, oxygen content, and fuel threshold failure temperature determination.

Hydroperoxide Number - Fuel samples were taken of the fresh feed and the fuselage tank outlet, engine heat exchanger outlet, and manifold outlet at the beginning and the end of the cruise condition of test cycle 1.006. The hydroperoxide numbers were all the same (<0.05 milliquivalent of active oxygen per liter of sample), Reference 9. This value is reported as the lower limit of detectability. No further analyses were made because the data appeared to be of little value relative to its use.

Threshold Failure Temperature - The results are shown in Section V with other small scale thermal stability tests.

Oxygen Content -The dissolved oxygen in the fuel was measured during the first and second test series, Reference 19. Therein is a discussion and description of the equipment employed and the results obtained. The basic item of equipment used in these analyses is a Perkin Elmer 154D Vapor Fractometer. The results obtained are shown in Table III with each line of data representing one test cycle.

The levels of oxygen reported for the incoming fuel are typical for air saturated fuel. The drop from the saturated level to 10-15 ppm during cruise is probably the result of two mechanisms. Oxygen is evolved under reduced pressure in the fuselage tank and also oxygen is consumed by the fuel as temperature is increased. It has been shown in other testing, Reference 21, that dissolved oxygen does not begin reacting noticeably with a fuel until 350°F. Consequently, it is hypothesized that the drop in oxygen at the beginning of the cruise is due primarily to the evolution of gas when the tank is evacuated and the change from cruise level oxygen content to 3 ppm during descent is caused by the high temperature (500 to 600°F) reached by the bulk fuel.

Millipore Filtration

During test cycle 1.040, fuel samples were taken from the simulator and filtered through 0.45 micron Millipore filters. A photograph of these filters is shown in Figure 33. At a fuel temperature between 390 and 420°F a definite darkening of the filter is evident indicating particulate generation greater than 0.45 micron.

TABLE III - SIMULATOR OXYGEN CONTENT MEASUREMENTS

Condition	Before Test Start-up	Beginning of Cruise				End of Cruise				Descent
Time, Minutes	0	25				115				130
Sample Valve	3*	4	5	6	7	4	5	6	7	4
First Test Series Oxygen Content ppm	40	22	18	21	20	12	12	13	7	
	72	16	15	13	13	10	9	11	7	
	59	15	17	14	14	8	8	8	7	
	70	11	11	10	13	8	7	7	6	
	70	17	15	14	15	12	8	8	7	3
	57	14	14	16	14	8	9	7	9	3
	71	15	14	15	13	9	8	7	6	3
Second Test Series Oxygen Content, ppm	60					5	4	4	3	
		7	8	7	8	7	4	5	6	
	23	7	8	7	5					
		21	17	15	19	4	5	8	6	
	57	12	12	13	11	7	6	7	6	
	41	9	7	10	10	5	5	4	5	
		14	13	11	12	7	8	9	6	
		10	10	11	11	6	7	6	7	
	55	12	12	13	11	7	7	8	6	
										3
										2

Sample Valve No.*	Location
3	Simulator Refueling Line
4	Fuselage Tank Outlet
5	Engine Pump Outlet
6	Engine Heat Exchanger Outlet
7	Engine Manifold Outlet

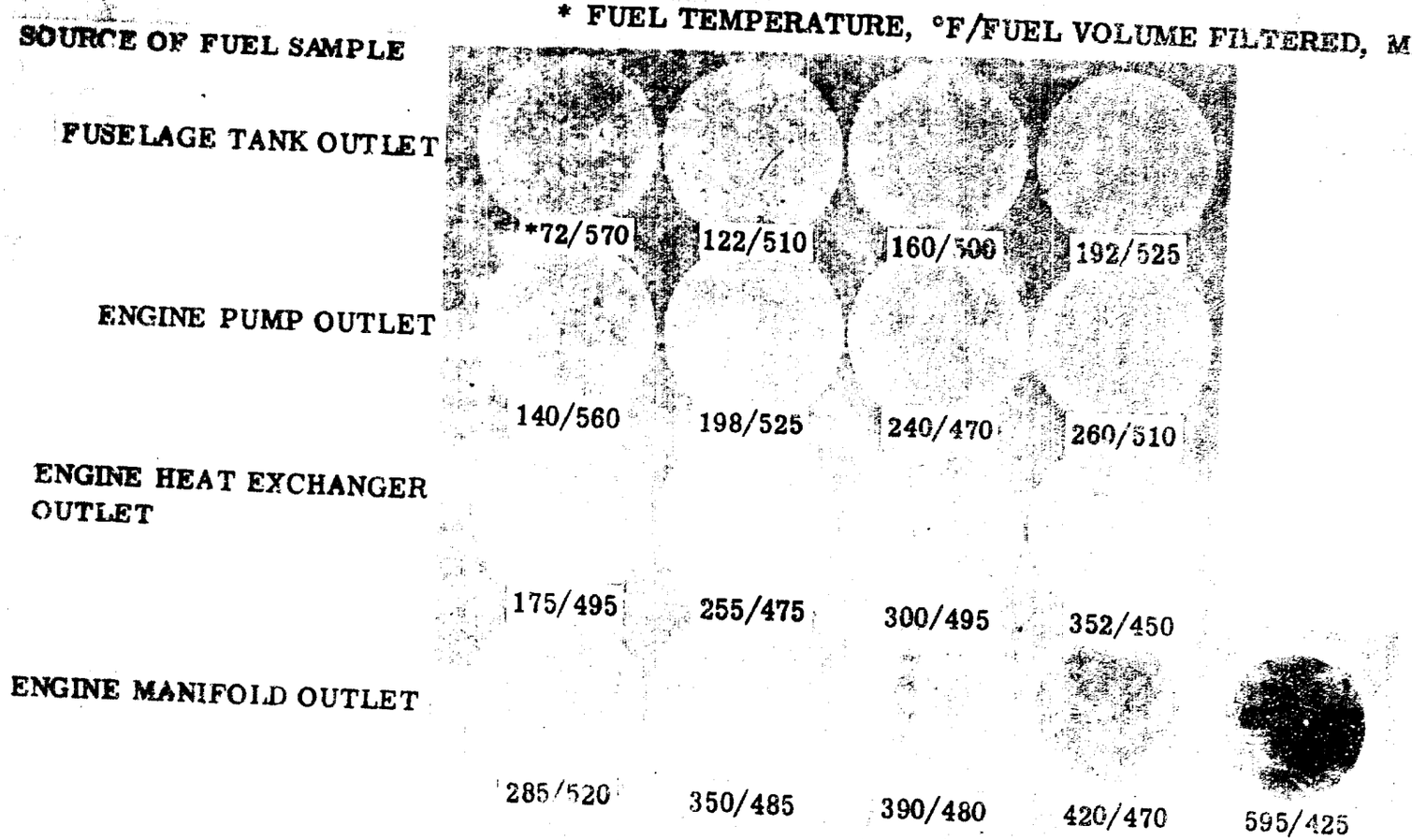

Figure 33. Millipore Filtrations - Test Cycle 1.040

SECTION IV

SIMULATOR STEADY STATE MANIFOLD TESTS

The purpose of the steady state manifold tests is to determine the rate of deposit formation of fuel AFFB-8-67 under constant temperature conditions. This data is compared to the data obtained during the cyclic tests and will be used to provide a basis of correlation to the small-scale tests which are operated in a steady state manner. The manifold was tested under steady state conditions because it was the only engine component which yielded quantitative deposit data during the cyclic tests. Two steady state tests were performed to cover the range of temperatures experienced in the first and second test series at the same heat flux. The more accurate sheathed thermocouples were used in the second steady state manifold test, and therefore, these data are analyzed more thoroughly in this section.

STEADY STATE OPERATIONAL PROCEDURE

Upon completion of the second test series, two steady state tests were conducted. The wing tank, engine nozzle, and Uni-Tube heat exchanger were not used in the system, and a new manifold substituted for the second test series manifold. The heated length of the manifold was 115 inches, as in the first test series, and 10 thermocouples were attached by the method used in the second test series. The steady state test consisted of running the simulator for 13.5 hours at the peak descent conditions of the first series. The fuselage tank was continuously refueled to replenish the 0.68 gpm flow rate out of the system. The fuel temperature into and out of the manifold was 340 and 600°F, respectively for the entire 13.5 hours.

The second steady state test was conducted using a new manifold and 10 sheathed thermocouples attached to the tube wall. The test was conducted exactly as above for 43.5 hours except the manifold fuel inlet was controlled to 200°F and the fuel outlet to 460°F. This test produced thermal degradation rates for lower metal or fuel film temperatures.

RESULTS

The fuel can be quantified with respect to its thermal stability in the manifold by a descriptor more useful than fuel side heat transfer coefficient. This is the deposit thermal resistance or the thickness of the deposit divided by the thermal conductivity of the deposit. It can be shown that the deposit thermal resistance for the manifolds used is defined by the following equation:

$$\frac{x_d}{k_d} = \frac{(t_w - t_f)\, 2\pi L}{7.8\, Q} - \frac{12\, D}{0.027\, k\, N_{Re}^{0.8} (N_{Pr})^{1/3}\, M^{0.14}} - \frac{0.253}{k_m}$$

where: x_d = thickness of deposit, inches

k_d = thermal conductivity of the deposit, BTU/hr-ft^2-°F/ft.

M = μ/μ_w

All other terms are defined in Section III.

The results obtained are shown in Figures 34 and 35. Figure 36 shows an actual computerized plot of the calculated values of x_d/k_d. The use of the deposit thermal resistance offers three advantages over the fuel side heat transfer coefficient. One, it can be directly compared to the deposit thickness measured at the end of the tests; two, it can be added to the inverse of the initial fuel side heat transfer coefficient, at whatever level it may be and determine the final heat transfer efficiency; and three, constant errors due to thermocouple and recording equipment error are minimized.

The equation given above is derived by assuming that the fuel side heat transfer coefficient does not change as the deposit builds up. The overall heat transfer efficiency decreases due to the thermal resistance of the deposit. This approach was used in Reference 13 and many textbooks on heat transfer. It is noted that this assumption would not be true if the ratio of deposit thickness to tube diameter increases to the point where the Reynolds Number is significantly increased. Using this assumption, a temperature profile of a radially cut tube would appear as follows for the same flow and heat input:

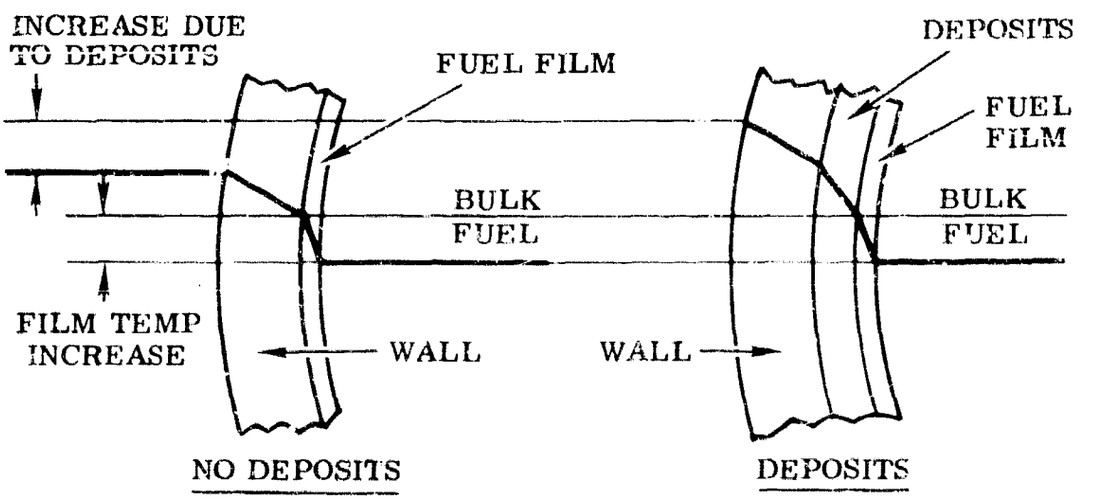

It is seen that the fuel film temperature is the same regardless of the amount of deposit. Therefore, it would be reasonable to assume that the rate of deposition, which should be dependent only on temperature, would be constant. However, the results obtained indicate that the deposit rate does not become constant until the deposit thickness reaches a certain level. This initial non-linearity may be attributed to a surface condition mechanism. As deposit builds up on a bare metal wall, the character and extent of the surface on which the deposit is forming is changing. It appears that deposition is occurring slowly on the stainless steel wall, and the rate increases as the wall adjacent to the film becomes deposited. At some finite deposit thickness, the entire wall will be coated with a porous deposit whose characteristics are not substantially changing and the deposition rate, thereafter, should be linear.

It appears from the results, shown in Figures 34, 35, and 36 that this theory of deposition maybe valid and the thermal stability of fuels tested in the simulator may be quantified by this method.

The amount of carbon in the steady state manifold tubes was analyzed (References 15 and 20) by W-PAFB laboratories in the same manner described in Section III. These values were converted to deposit thicknesses using the same conversion constants and are shown in Figure 37. Also shown in Figure 37 are the calculated deposit thicknesses determined by MAA from the deposit thermal resistance as described in Section III. The original data from W-PAFB on carbon content of approximately half the deposited tubes were lower than the blanks (stainless steel alone); therefore many of the data points plotted in Figure 37 are negative. It is not known at this time why the carbon analysis results of the steady-state manifolds are not in as good agreement with the thicknesses determined from deposit thermal resistance as those of the test series manifold. It appears from the visual observations of the tubes and the obvious fact that deposit thicknesses cannot be negative that the thicknesses calculated from deposit thermal resistances are more valid. It is noted that the deposit thickness of the first steady state manifold does not increase after the second electrical tab. This is attributed in part to erroneous temperature measurements caused by the less acceptable method of thermocouple attachment used on this manifold. Therefore, in the correlation which follows the data obtained on the second steady state manifold (instrumented with sheathed thermocouples) are used.

CORRELATION OF STEADY-STATE TO TEST CYCLES

The data obtained from the steady-state tests and the test series were analyzed with respect to each other. This was accomplished first for the second test series manifold (whose temperatures were more accurately measured) by determining from Figure 35 the slope of the deposit thermal resistance, x_d/k_d versus time, θ, for each temperature location on the second steady state manifold. This was determined for an x_d/k_d change of 2 Mils/BTU-ft/hr-°F-ft^2 because the second test series manifold experienced a change of this magnitude. The x_d/k_d θ was then plotted against the film temperature and is shown in Figure 38. A film temperature versus time plot was then made for each thermocouple location on the second test series manifold from the original test cycle data (metal temperature -15°F which allows for the temperature change across the metal wall). Based on this film temperature profile for each thermocouple and the x_d/k_d θ versus film temperature, a plot of x_d/k_d θ versus test cycle time was drawn for each thermocouple location. The area under each curve is the deposit thermal resistance accrued for one test cycle. The area below 375°F was neglected because it was demonstrated that the deposition is negligible below this film temperature. The values of x_d/k_d were multiplied by 90 test cycles and a thermal conductivity of 0.07 BTU/hr-ft^2-°F/ft (see Section III) to obtain the deposit thicknesses predicted on the basis of the steady state data (x_d/k_d θ = 15,600 $e^{-6500/T}$). These deposit thicknesses were then plotted against the average deposit thicknesses obtained from Figure 26. A plot of this comparison is shown in Figure 39. The above procedure was repeated for the first test series manifold, and the comparison is also shown in Figure 39.

The comparison obtained on the second test series is better than that of the first test series. It is considered that this is due to the more acceptable temperature measurement method used and the more applicable use of the deposit thickness prediction equation, i.e., within a x_d/k_d range of 0 to 2 mils/BTU-ft/hr-°F-ft^2 (or deposit thickness of 0 to 0.14 mil). As stated above, the equation derived from Figure 38 is applicable in the 0 to 0.14 mil region. Other equations have been derived for deposit levels in excess of 0.14 mil; however, they are not discussed herein, since there is little or no data to make a correlation. Also shown in Figure 38 is a change in slope at approximately 475°F. It is hypothesized that either the flushing rate (removal of deposit by its solution into the flowing fuel) is significant with respect to the deposition rate at the lower temperatures or the mechanism of deposit formation is changing at 475°F. The flushing rate plays an important role in comparing steady state to cycle tests because during the acceleration condition the fuel flowis eight times higher than the steady state tests. This may account for the deposit formation rate of the test cycles being more linear than the steady state tests.

CONCLUSIONS

Based on these data there appears to be an excellent correlation with with this fuel between the steady state and cyclic conditions on the basis of equal fuel film temperatures. The data indicate that the deposition rate of this fuel up to a deposit level of 0.14 mils be quantified in the engine system as $x_A/k_d\ \theta = 15{,}600e^{-6500/T}$ for film temperatures in excess of 375°F. Below 375°F, the deposition has been demonstrated to be negligible. It is also indicated that the deposit thickness in tubes can be quantified during a test by outer metal temperature measurements and also after a test by carbon analysis.

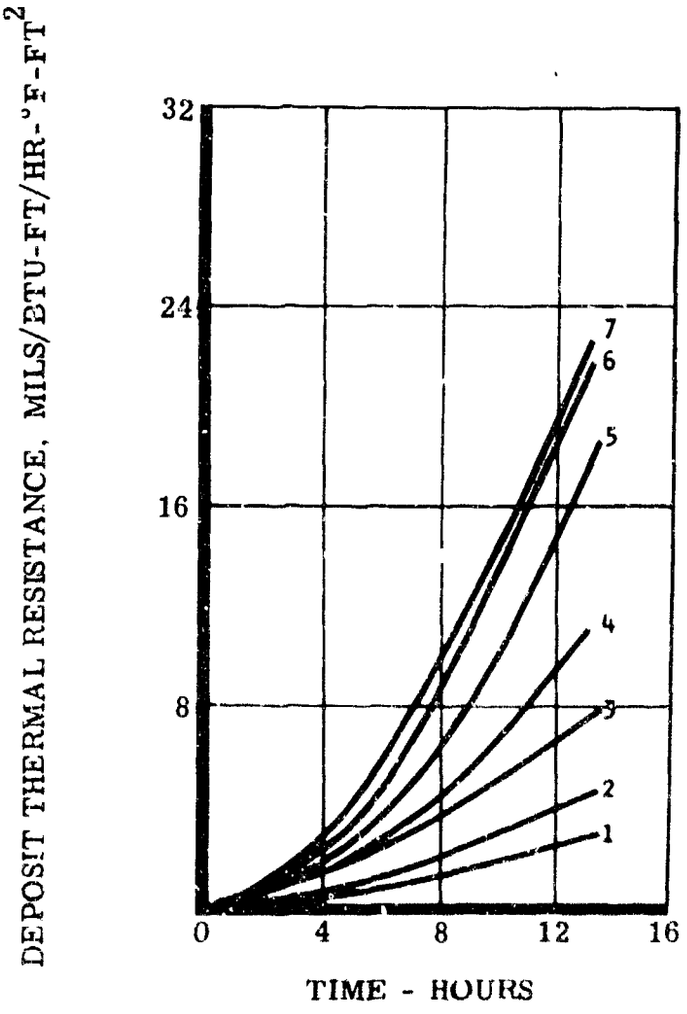

Figure 34. First Steady-State Manifold Deposit Buildup

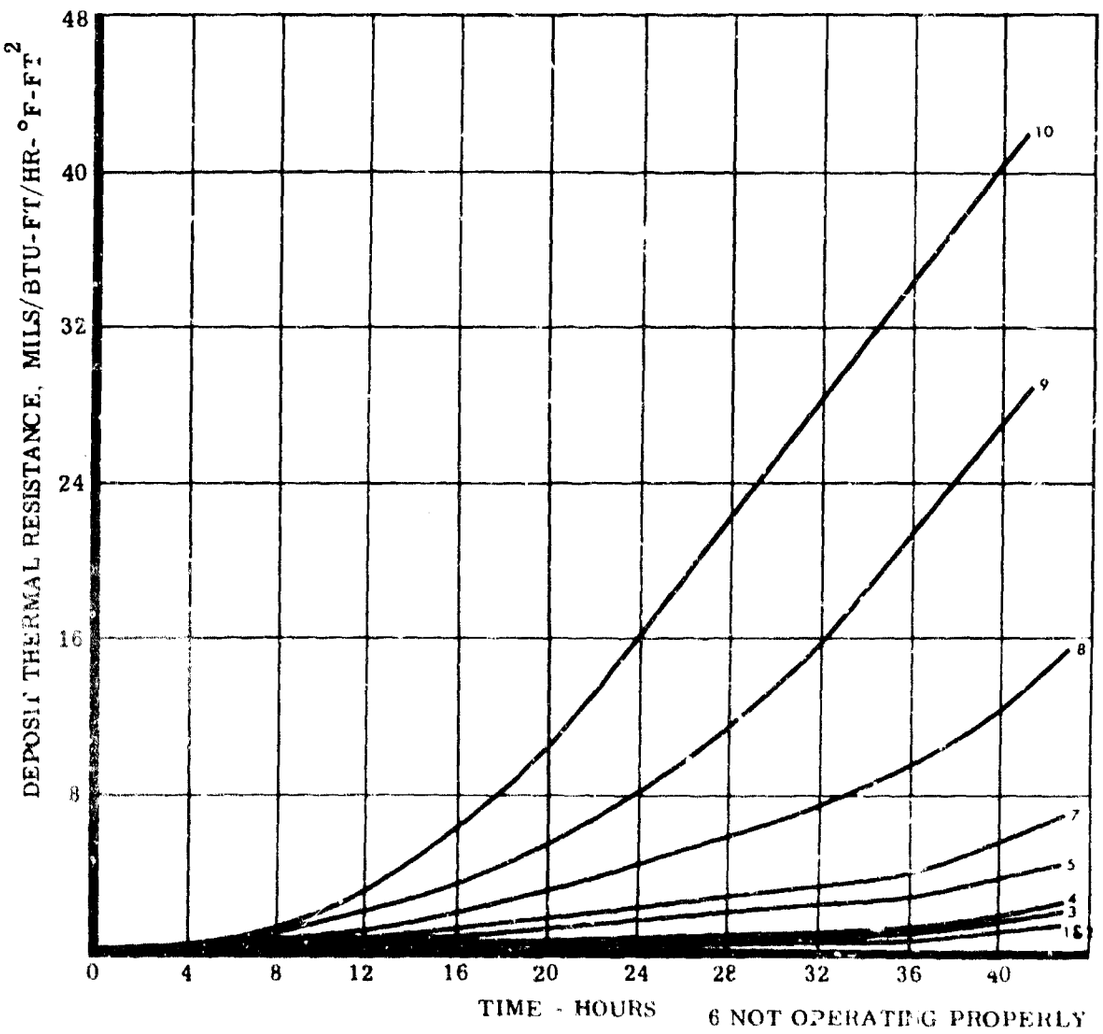

Figure 35. Second Steady-State Manifold Deposit Buildup

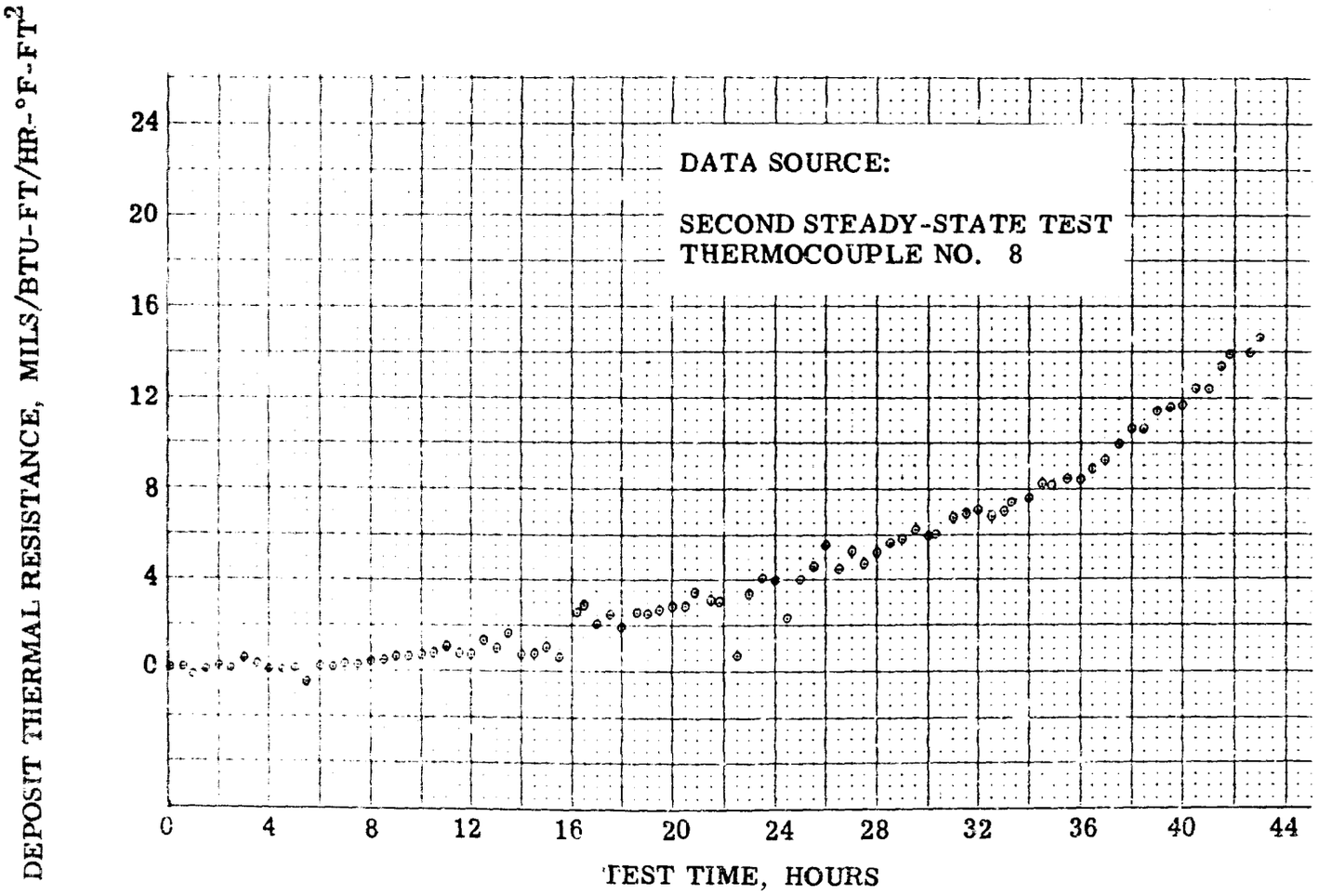

Figure 36. Actual Plot of Deposit Buildup

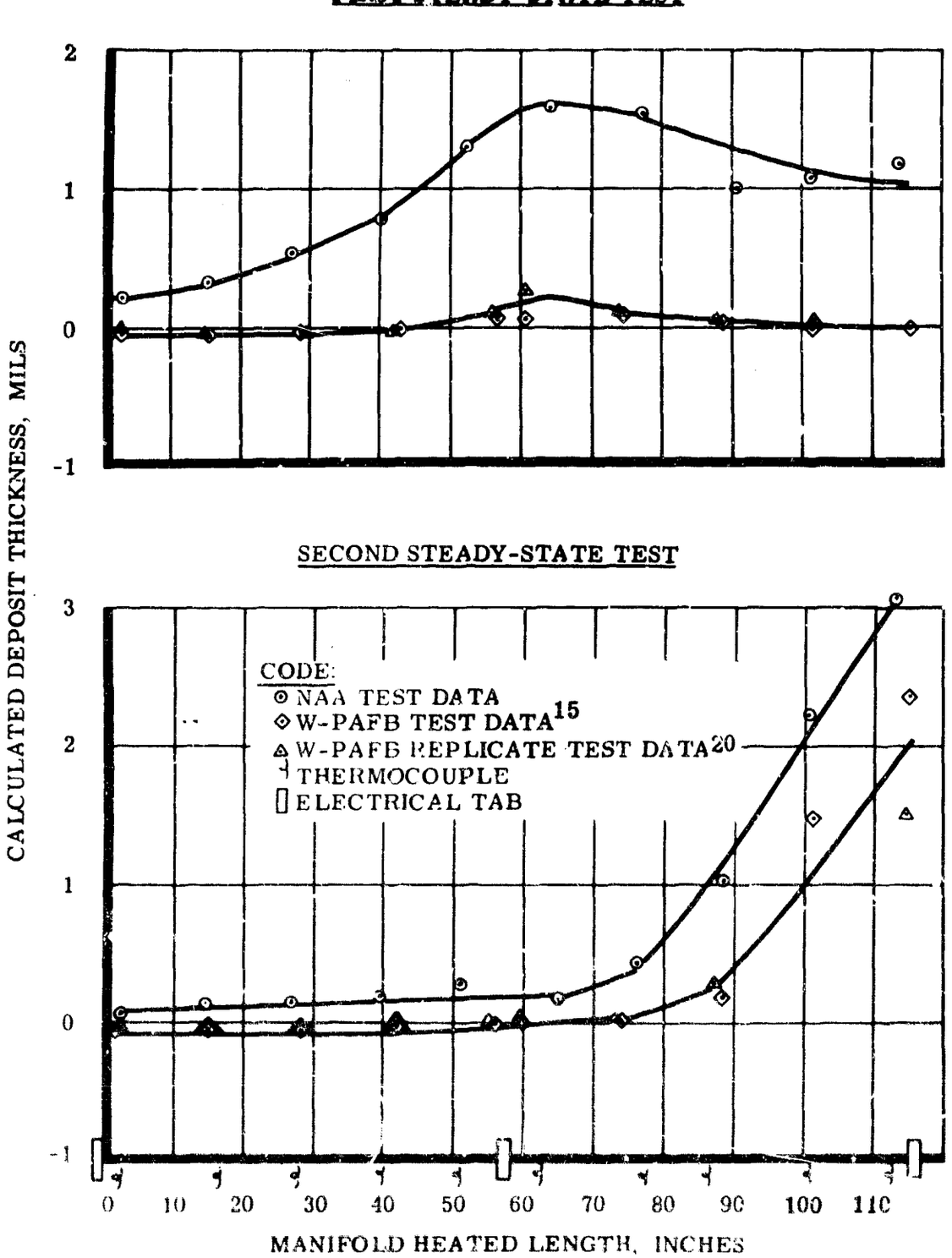

Figure 37. Manifold Deposit Thickness - Steady-State Tests

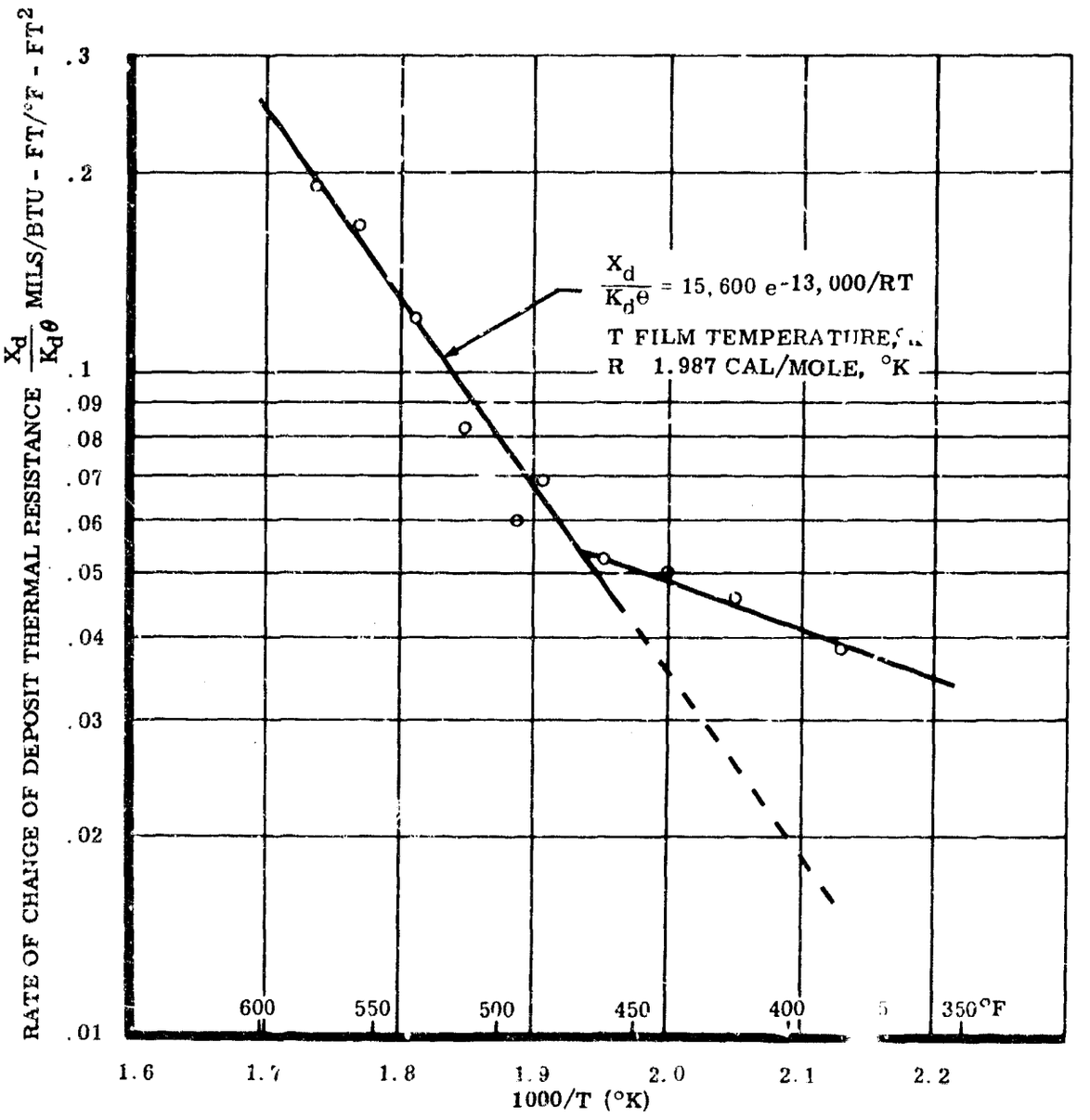

Figure 38. Manifold Deposit Build-up

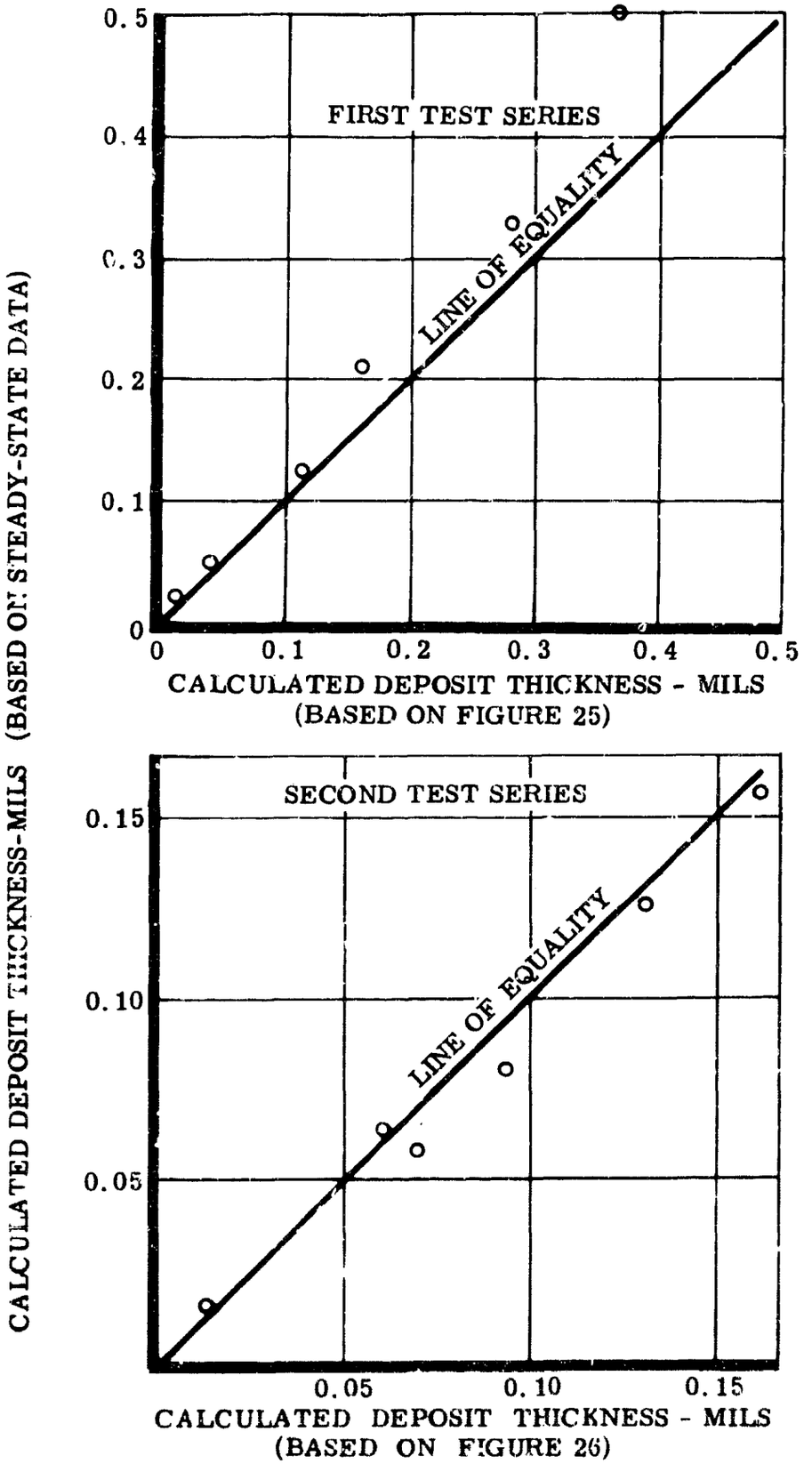

Figure 39 Comparison Between Steady-state and Cyclic Data

SECTION V

SMALL-SCALE TESTS

The purpose of the small-scale tests is to obtain data to determine if any of these devices ranks the fuels the same as the simulator and, further, if there is a quantitative relationship between the small-scale tests and the simulator. The data presented on fuel AFFB-8-67 in this section were obtained from the AF Aero Propulsion Laboratory which directed these tests conducted by the AF Materials Laboratory, University of Dayton Research Institute and Esso Research and Engineering Corporation. Also shown in this section are the small-scale test results of the four fuels tested in the SST Fuel System Test Rig reported in Reference 22. These data are included in this section so that the comparison to the simulator data which is made in Section VI may be more inclusive.

Samples of fuel AFFB-8-67 were taken from the storage tanks and tested in the following small-scale thermal stability devices:

Cokers
- Standard
- Gas
- Research
- Modified
- Micro

Minex

Thermal Precipitation Apparatus

5 ml Bomb

Esso's Standard Screening Unit

The results of these tests are shown in Table IV.

COKERS

The traditional methods and results of determining coker breakpoint are shown in Table IV. The definition of these bases of comparison is delineated in Reference 22. The data obtained on fuel AFFB-8-67 with respect to preheater tube temperature versus Tuberator deposit code is presented in Figures 40, 41, and 42. This concept of data presentation is discussed in Reference 13. In all these cases but one, the cokers gave large quantities of deposit at the 550°F tube wall temperature. The research coker gave a

lower breakpoint when a 300°F reservoir was used. It was reported in this effort that the fuel darkened in appearance under the 300°F conditions. It was also observed that the results of the standard, modified, and gas drive cokers were generally the same. This would indicate that pump wear does not significantly affect the coker results. Pump wear is considered to be a function of fuel lubricity which has been reported, Reference 23, to be dependent upon the aromatic content of the fuel.

The procedure for operating the standard coker may be found in Reference 1 and the modified and gas drive cokers in Reference 24.

MINEX

Two runs, shown in Figures 43 and 44, were made with this fuel; the first run started at 350°F and went up to 600°F in 20°F increments. During the first test, difficulty was encountered when steady flow control was attempted. The trouble was traced to the flow control orifice which appeared to be catching particulate contamination from the Minex rig. There was no definite breakpoint reached during this test. It is considered that even with the large amount of scatter, a definite buildup of deposits would have been detected by a large and consistent decrease in h_f^* and a simultaneous increase in pressure drop through the test section. The first test was stopped at 600°F because the three preheaters used to raise the temperature of the fuel flowing into the test section to the desired level were operating a full power, and therefore would not further increase the temperature. The points with a cross indicate that the temperatures changed by more than 1/2°F during the readings; these points should be disregarded.

A second run on this fuel was made after the Minex was thoroughly cleaned; a new jewel orifice was added, and one additional preheater was added. With the additional heating capability, it was possible to increase the temperature into the test section and consequently achieve 620°F fuel-out temperature. For the testing at 620°F the pressure in the test section was raised from 150 psig to 230 psig to prevent boiling in the test section. As the graph indicates, there is evidence of change in h_f^* at 600°F and a definite deposit buildup at 620°F. These two runs would indicate that the Minex breakpoint is 620°F. The data at 600°F are not conclusive enough to assign the breakpoint at this level.

The tubes used in these runs were analyzed for carbon content (see Section III for method) and transmitted by AFAPL, Reference 25, together with the conversion factor to deposit thickness for the Minex tube. The calculated deposit thicknesses were 0.011, 0.0099, and 0.011 mils for the inlet, middle, and outlet of the tube used in the first run and 0.037, 0.037, and 0.041 mils for the tube used in the second run. The following is a comparison of these data compared to that obtained from Figures 43 and 44.

	First	Second
Deposit Thickness (Based on Carbon Analysis), Mils	0.01	0.04
Deposit Thickness (Based on Loss in h_f), Mils	-0*(0.68)**	0.5**
Pressure Drop Increase, In.Hg.	4	1.5

*Determined by assuming that h_f has not decreased but has shifted for each temperature change.

**Determined by subtracting the inverse of the final h_f from the inverse of the initial h_f.

It can be seen from the above that the carbon analysis data is not consistent with the data obtained from Figures 43 and 44. These data are compared to the simulator data and discussed in Section VI.

THERMAL PRECIPITATION TEST

The procedure used for the thermal precipitation test is delineated in Reference 26 with the exception that weight measurements are deleted. The test was performed twice and a photograph of the filter papers are shown in Figure 45. Since this method has not been widely published, a summary of the procedure is given below.

Test filter papers (.45μ pore size, 47 mm diameter) are precleaned with naphtha by use of a vacuum filtration unit. The filter papers are then placed in an 180°F oven for 30 minutes and stored in a Petri dish. Two gallons of test fuel are then filtered with a filter paper and the fuel refiltered with another filter paper which is retained as the control filter paper. The fuel is then placed in a precleaned fuel reservoir and heated to 300 ± 5°F in 90 to 105 minutes and maintained at this temperature for 120 minutes. The fuel is then cooled to 80 ± 5°F in 30 to 45 minutes. One gallon of this test fuel is then filtered through the precleaned test filter. The color of the sample and control filter papers is then compared.

5 ML BOMB

Fuel samples from the simulator were tested in the Phillips 5 ml bomb. The procedure for this test is given in Reference 27 and the results are shown in Table IV. An oxygen sensitivity test of the fuel feed was also conducted using the 5 ml bomb. The procedure and results of this test are given in Reference 28. This oxygen sensitivity test is conducted in the same manner as the 5 ml bomb test except the test fuel is deaerated first with nitrogen. The fuel is deaerated by bubbling prepurified nitrogen with

a syringe through the fuel. The bomb apparatus is also purged with a continuous flow of prepurified nitrogen. The deaerated fuel is transferred to the bomb which is then purged for an additional 5 minutes. The results of this test are shown in Table IV.

ESSO STANDARD SCREENING UNIT

A sample of fuel was tested in the Esso's laboratory unit which is being used to study "vapor phase" deposits. This information appears in an Esso monthly letter, Reference 29. It was reported therein that the results indicate that fuel AFFB-8-67 is a poorer performer than anticipated from coker results. These tests are conducted in Esso's Screening Unit. The main section of the unit consists of a tubular reactor surrounded by five separate, independently controlled reactor heaters. The reactor is maintained on a slight incline, and liquid fuel flows down the reactor in the presence of flowing air (or nitrogen). The reactor heaters are controlled so that the fuel encounters a rising temperature sequence as it flows down the reactor. Weighed metal strips are placed in the center section of each heater zone and a thermocouple positioned in each zone. The test is conducted for four hours with a fuel flow rate of 125 cc/hour. The metal strips are again weighed after the test and the deposit weight versus temperature determined. The equation of these data is used to determine the relative activity of the fuel.

TABLE IV - RESULTS OF SMALL SCALE TESTS

TEST DEVICE	BASIS OF COMPARISON (CRITICAL CONDITION)	CRITICAL TEMPERATURE, F				
		RAF-176-64	RAF-176-63	FA-S-2A	FA-S-1	AFFB-8-67
MINEX	INITIAL CHANGE IN HF, FUEL TEMP.	390	EL355	EL350	EL300	600
MINEX	INITIAL CHANGE IN HF, METAL TEMP.	470	EL385	EL380	EL330	638
MINEX	ONE PERCENT LOSS IN HF/HR., FUEL TEMP.	479	440	437	392	620
MINEX	ONE PERCENT LOSS IN HF/HR., METAL TEMP.	509	470	467	422	658
MINEX	INITIAL DECREASE IN HF, FUEL TEMP.	390	EL355	405	EL300	600
MINEX	INITIAL DECREASE IN HF, METAL TEMP.	420	EL385	435	EL330	638
MINEX	RAPID DECREASE IN HF, FUEL TEMP.	500	480	445	450	620
MINEX	RAPID DECREASE IN HF, METAL TEMP.	530	510	475	480	658
BOMB	TWENTY-FIVE PCT. LOSS LIGHT TRANS.	384	386	440	348	403
BOMB	SAME BUT OXYGEN PURGED					487
COKER	3 IN. HG. MAX., FUEL TEMP.	375	G375	375-400	375	G450
COKER	12 IN. HG. MAX., FUEL TEMP.	G400	G375	G425	G375	G450
COKER	13 IN. HG. MAX., FUEL TEMP.	G400	G375	425	375	G450
COKER	CODE 2 MAX., FUEL TEMP.	375	350	425	325	400
COKER	CODE 2 AND 3 IN. HG. MAX., FUEL TEMP.	375	350	375-400	325	400
COKER	CODE 2 AND 12 IN. HG. MAX., FUEL TEMP.	375	350	425	325	400
COKER	CODE 2 SURVEY, METAL TEMP.	462	513	604	475	542
COKER	CODE 3 SURVEY, METAL TEMP.	331	382	512	382	545
COKER	TRANSIT, METAL TEMP.	467	406	517	398	516
R COKER	AMB., 3 IN. HG. MAX., FUEL TEMP.	375	375	450	G350	G450
R COKER	AMB., 13 IN. HG. MAX., FUEL TEMP.	375	G400	450	G350	G450
R COKER	AMB., CODE 2 MAX., FUEL TEMP.	350	350	450	325	375
R COKER	AMB., CODE 2 AND 3 IN. HG. MAX., FUEL TEMP.	350	350	450	325	375
R COKER	AMB., CODE 2 SURVEY, METAL TEMP.	467	481	571	463	500
R COKER	AMB., CODE 3 SURVEY, METAL TEMP.	452	483	570	399	500
R COKER	AMB., TRANSIT, METAL TEMP.	443	462	557	362	469
R COKER	200 F, 3 IN. HG. MAX., FUEL TEMP.	375	G350	L475	G350	375
R COKER	200 F, 13 IN. HG. MAX., FUEL TEMP.	375	G375	L475	G350	375
R COKER	200 F, CODE 2 AND 3 IN. HG. MAX., FUEL TEMP.	350	325	L475	300	375
R COKER	200 F, CODE 2 MAX., FUEL TEMP.	350	325	475	300	375
R COKER	200 F, CODE 2 SURVEY, METAL TEMP.	462	443	696	428	508
R COKER	200 F, CODE 3 SURVEY, METAL TEMP.	460	455	598	392	525
R COKER	200 F, TRANSIT, METAL TEMP.	443	443	627	376	521
R COKER	300 F, 3 IN. HG. MAX., FUEL TEMP.	300	L300	L275	L200	L375
R COKER	300 F, 13 IN. HG. MAX., FUEL TEMP.	325	350	L275	L200	L375
R COKER	300 F, CODE 2 MAX., FUEL TEMP.	425	325	275	325	EL375
R COKER	300 F, CODE 2 AND 3 IN. HG. MAX., FUEL TEMP.	300	L300	L275	L200	L375
R COKER	300 F, CODE 2 SURVEY, METAL TEMP.	542	428	490	443	405
R COKER	300 F, CODE 3 SURVEY, METAL TEMP.	541	443	305	455	430
R COKER	300 F, TRANSIT, METAL TEMP.	517	423	434	443	405
GAS COKER	3 IN. HG. MAX., FUEL TEMP.					400
GAS COKER	12 IN. HG. MAX., FUEL TEMP.					400
GAS COKER	13 IN. HG. MAX., FUEL TEMP.					400
GAS COKER	CODE 2 MAX., FUEL TEMP.					425
GAS COKER	CODE 2 AND 3 IN. HG. MAX., FUEL TEMP.					400
GAS COKER	CODE 2 AND 12 IN. HG. MAX., FUEL TEMP.					400
GAS COKER	CODE 2 SURVEY, METAL TEMP.					491
GAS COKER	CODE 3 SURVEY, METAL TEMP.					518
GAS COKER	TRANSIT, METAL TEMP.					NA
MOD COKER	3 IN. HG. MAX., FUEL TEMP.					G475
MOD COKER	12 IN. HG. MAX., FUEL TEMP.					G475
MOD COKER	13 IN. HG. MAX., FUEL TEMP.					G475
MOD COKER	CODE 2 AND 3 IN. HG. MAX., FUEL TEMP.					400
MOD COKER	CODE 2 AND 12 IN. HG. MAX., FUEL TEMP.					400
MOD COKER	CODE 2 MAX., FUEL TEMP.					400
MOD COKER	CODE 2 SURVEY, METAL TEMP.					521
MOD COKER	CODE 3 SURVEY, METAL TEMP.					491
MOD COKER	TRANSIT, METAL TEMP.					497
MIC COKER	CODE 1 MAX., FUEL TEMP.					313
MIC COKER	CODE 2 SURVEY, METAL TEMP.					525
MIC COKER	CODE 3 SURVEY, METAL TEMP.					525
ESSO UNIT RELATIVE ACTIVITY AT 375F			1.0	0.5*		1.3

* FUEL TESTED WAS ACTUALLY FA-S-2B

EL=EQUAL TO OR LESS THAN G=GREATER THAN L=LESS THAN

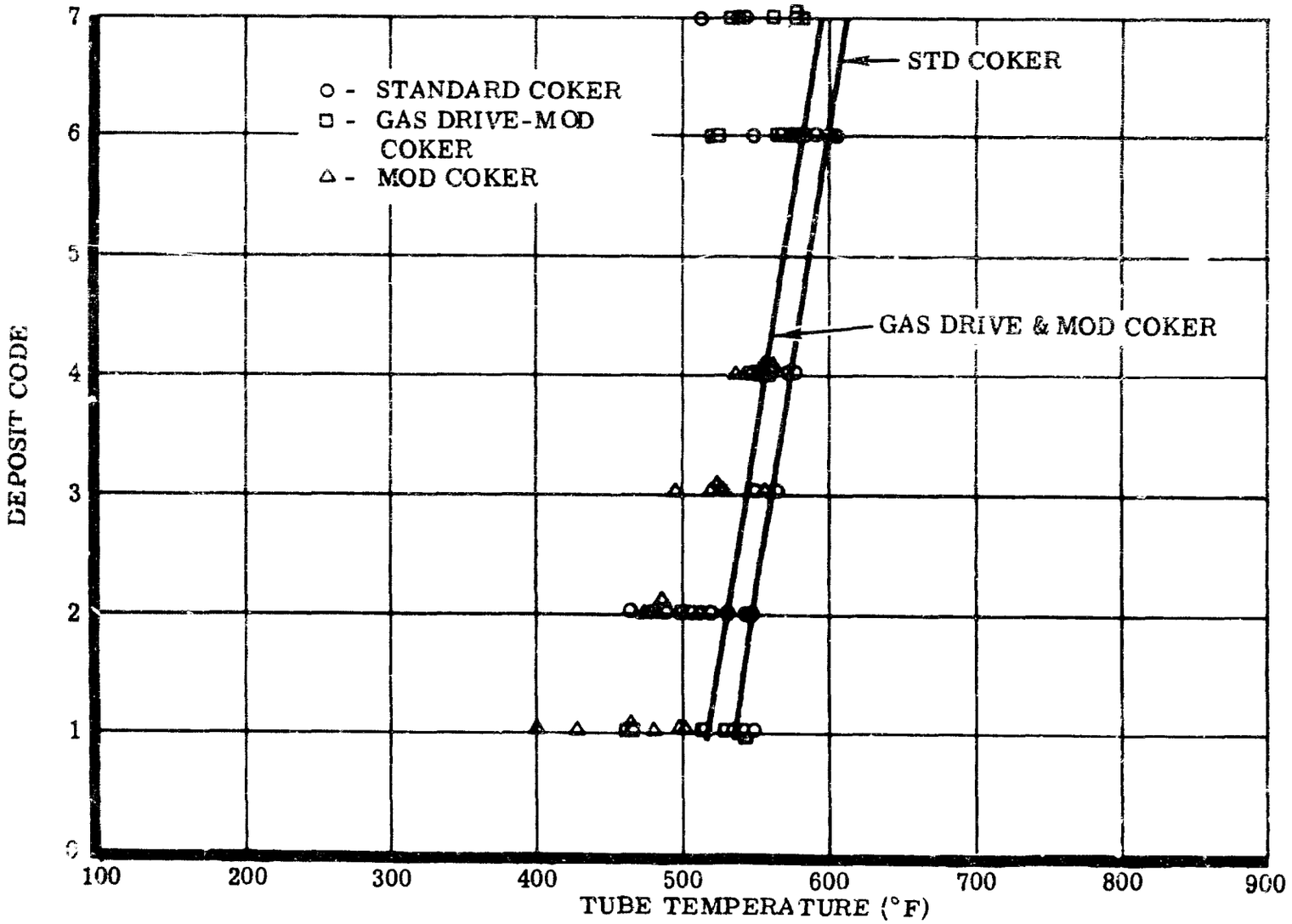

Figure 40. Standard, Gas, and Modified Coker Test Results

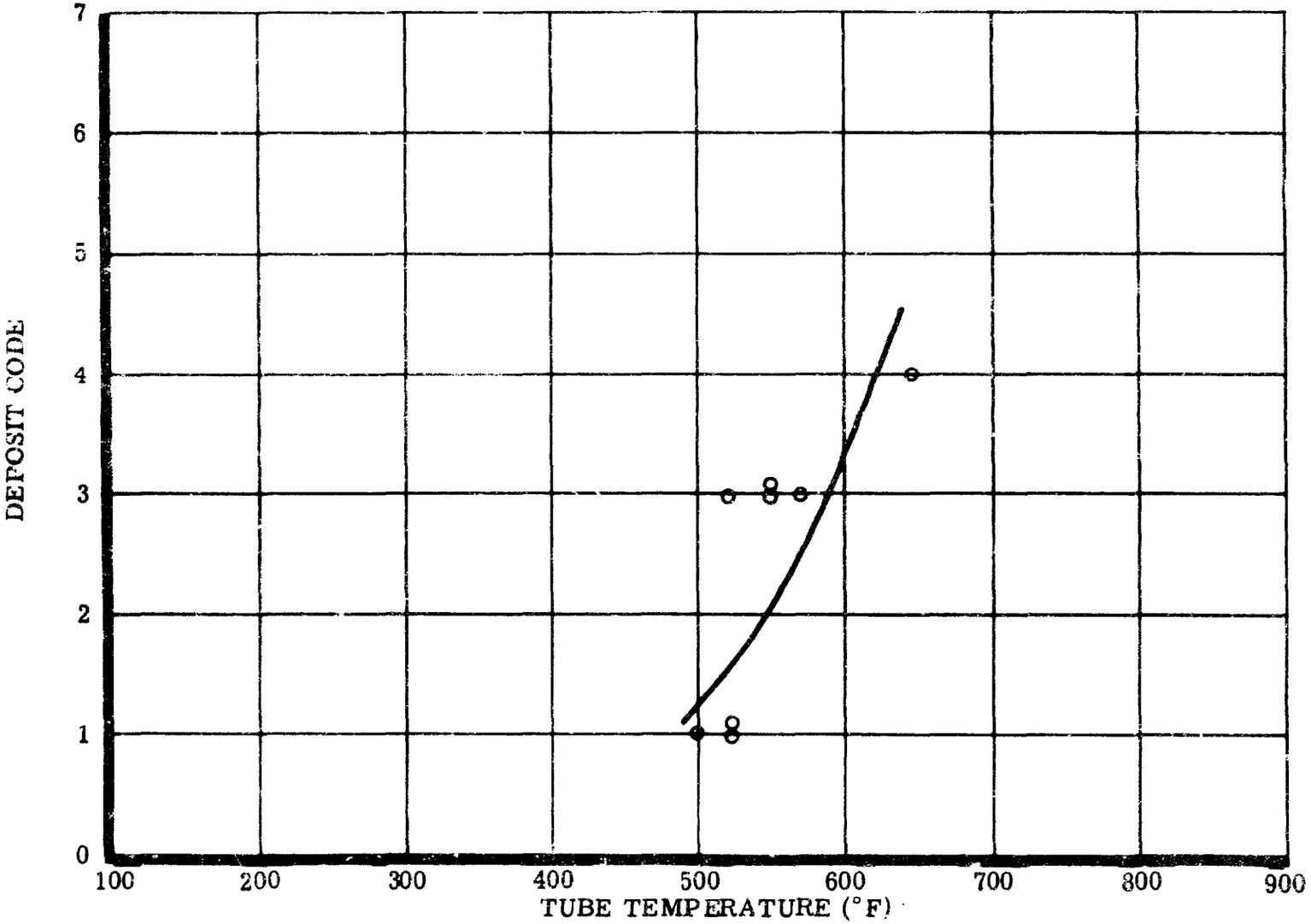

Figure 41. Micro Coker Test Results

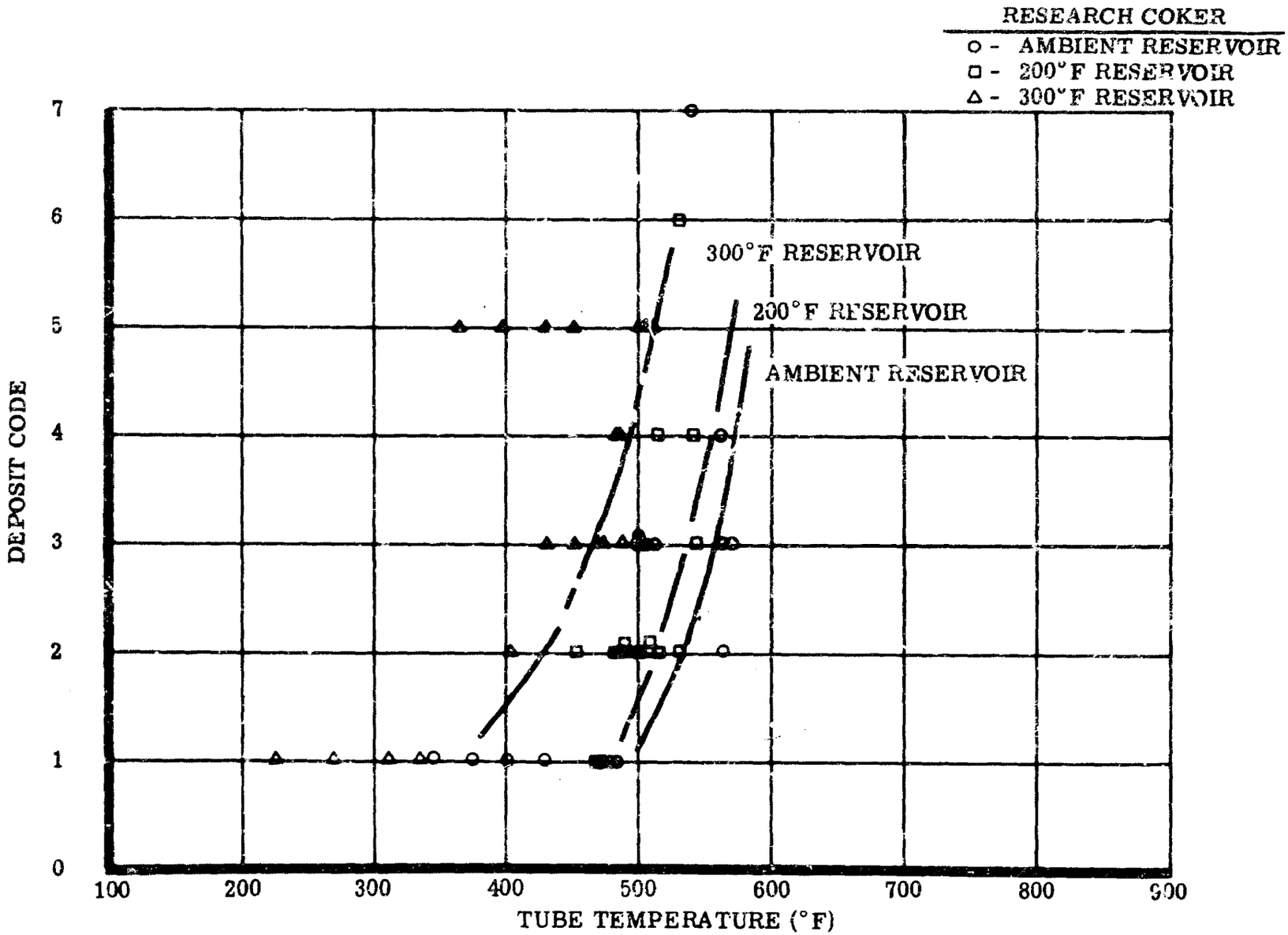

Figure 42. Research Coker Test Results

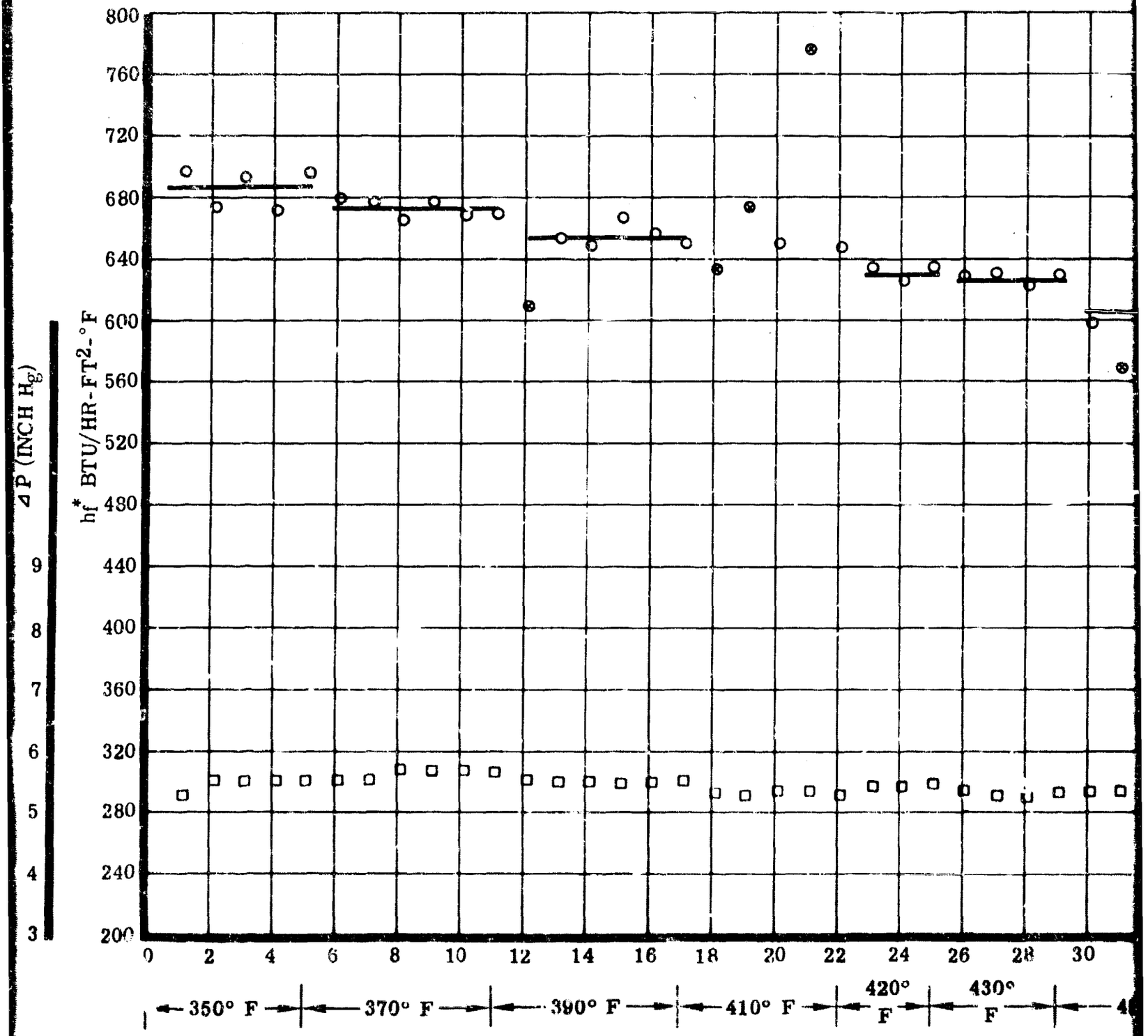
800
760
720
680
640
600
560
520
480
440
400
360
320
280
240
200
hf* BTU/HR-FT2-°F
ΔP (INCH Hg)
9
8
7
6
5
4
3
0
2
4
6
8
10
12
14
16
18
20
22
24
26
28
30
350° F
370° F
390° F
410° F
420° F
430° F

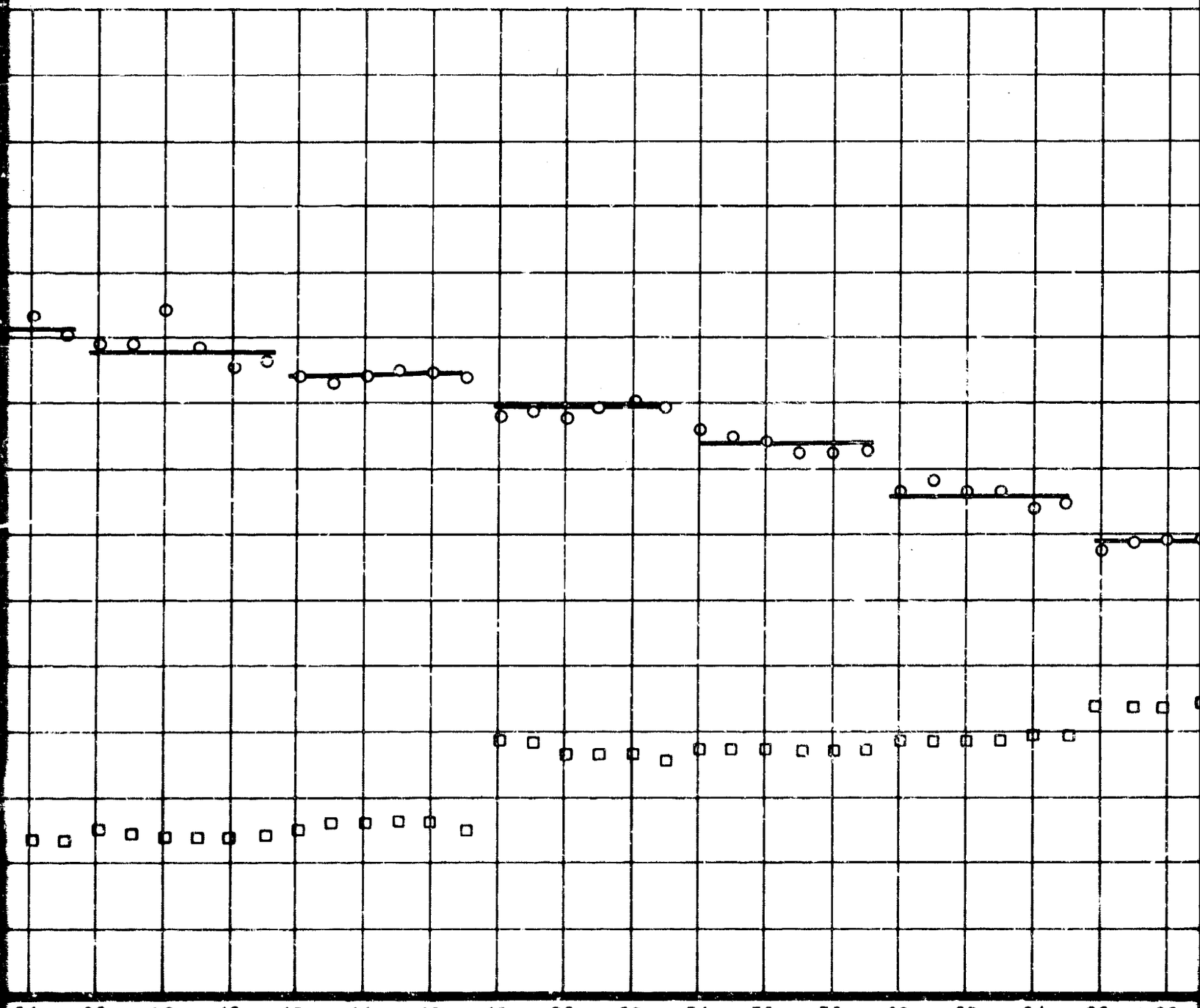
34
36
38
40
42
44
46
48
50
52
54
56
58
60
62
64
66
68
TEST TIME - HOURS
470° F
490° F
510° F
530° F
550° F
570°

2

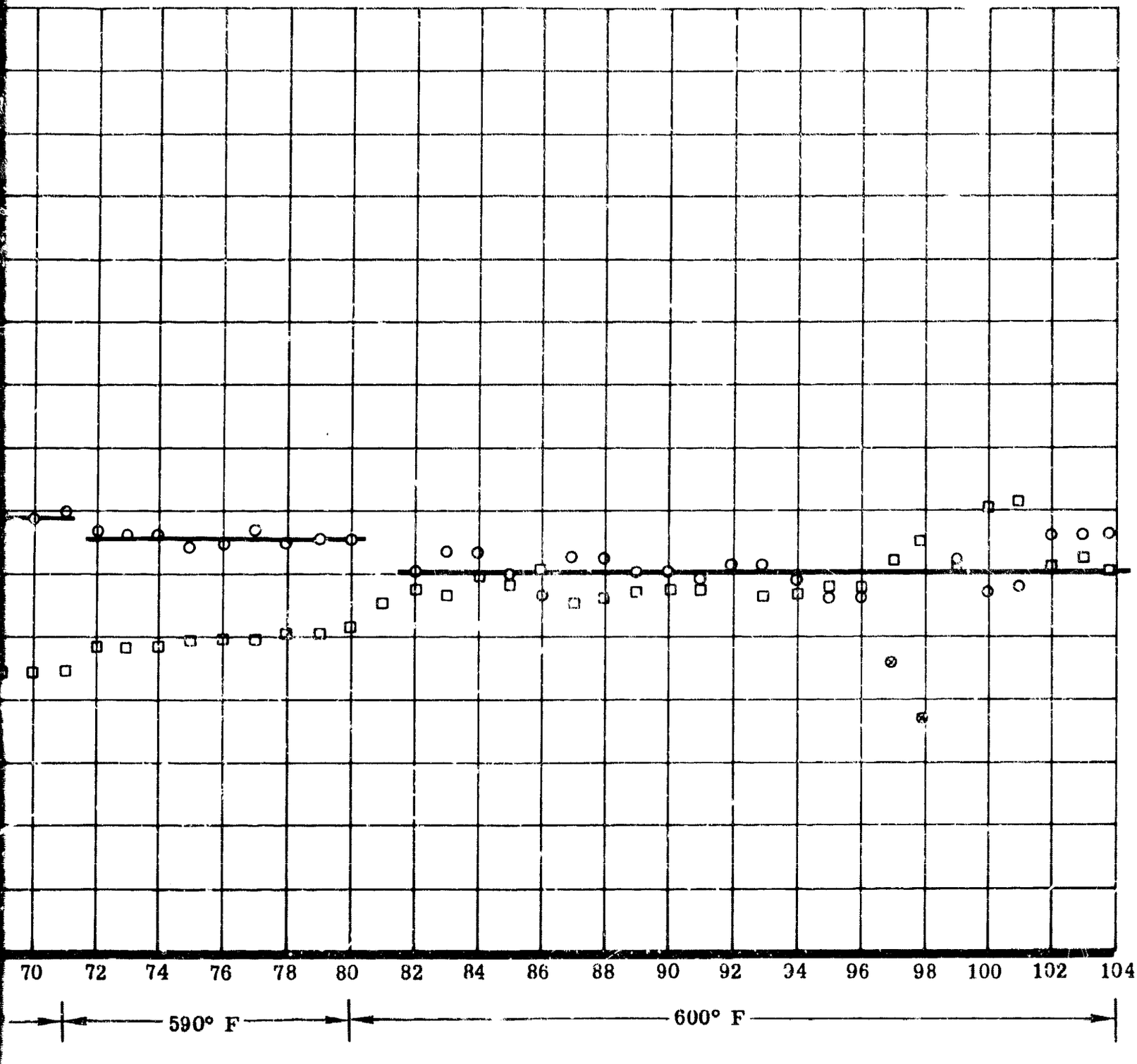

Figure 43. Minex Test Results - First Run

3

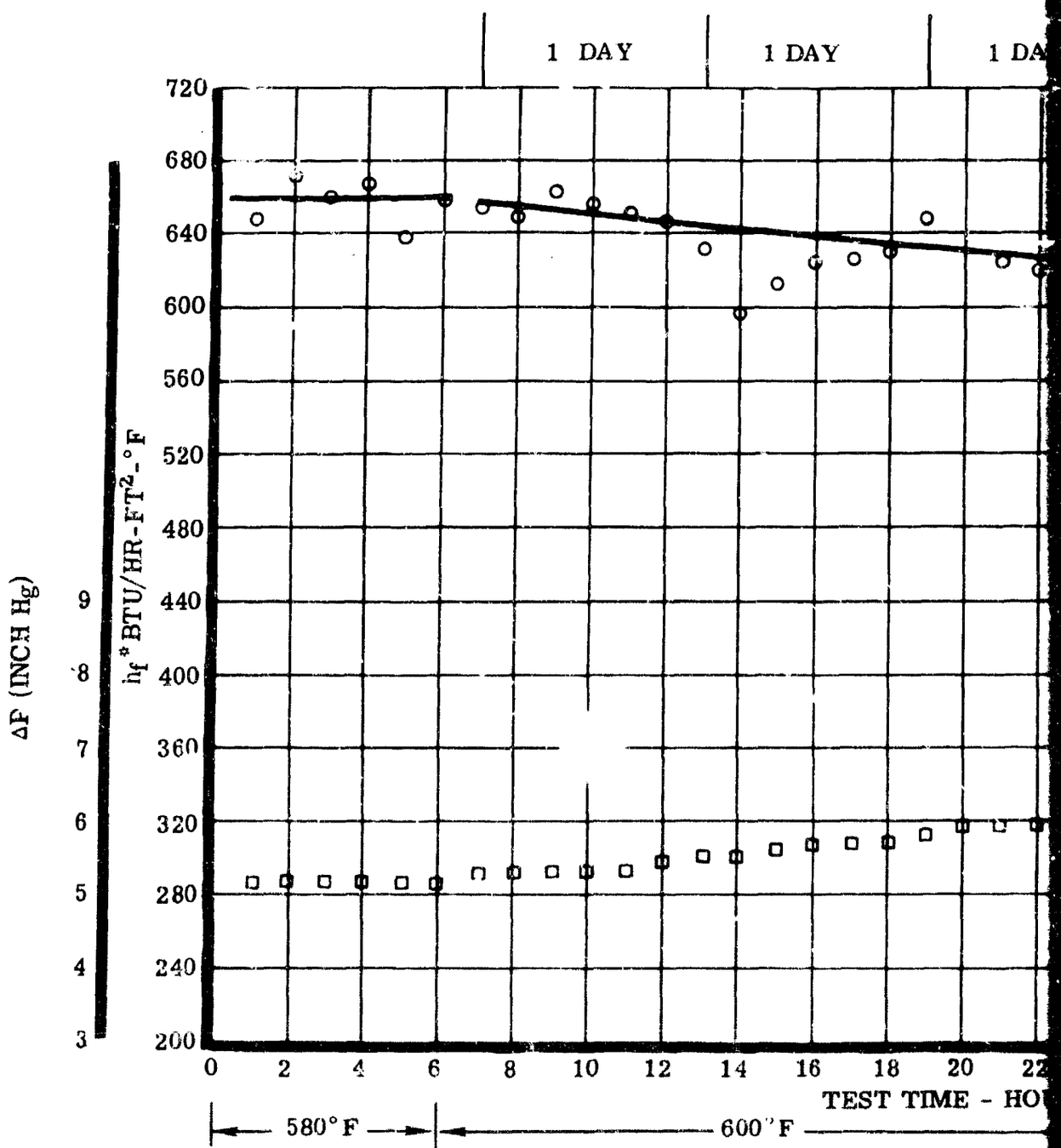
1 DAY
1 DAY
1 DA
720
680
640
600
560
520
480
440
400
360
320
280
240
200
h_f * BTU/HR-FT^2-°F
ΔP (INCH Hg)
9
8
7
6
5
4
3
0
2
4
6
8
10
12
14
16
18
20
22
TEST TIME - HO
580° F
600° F

Figure

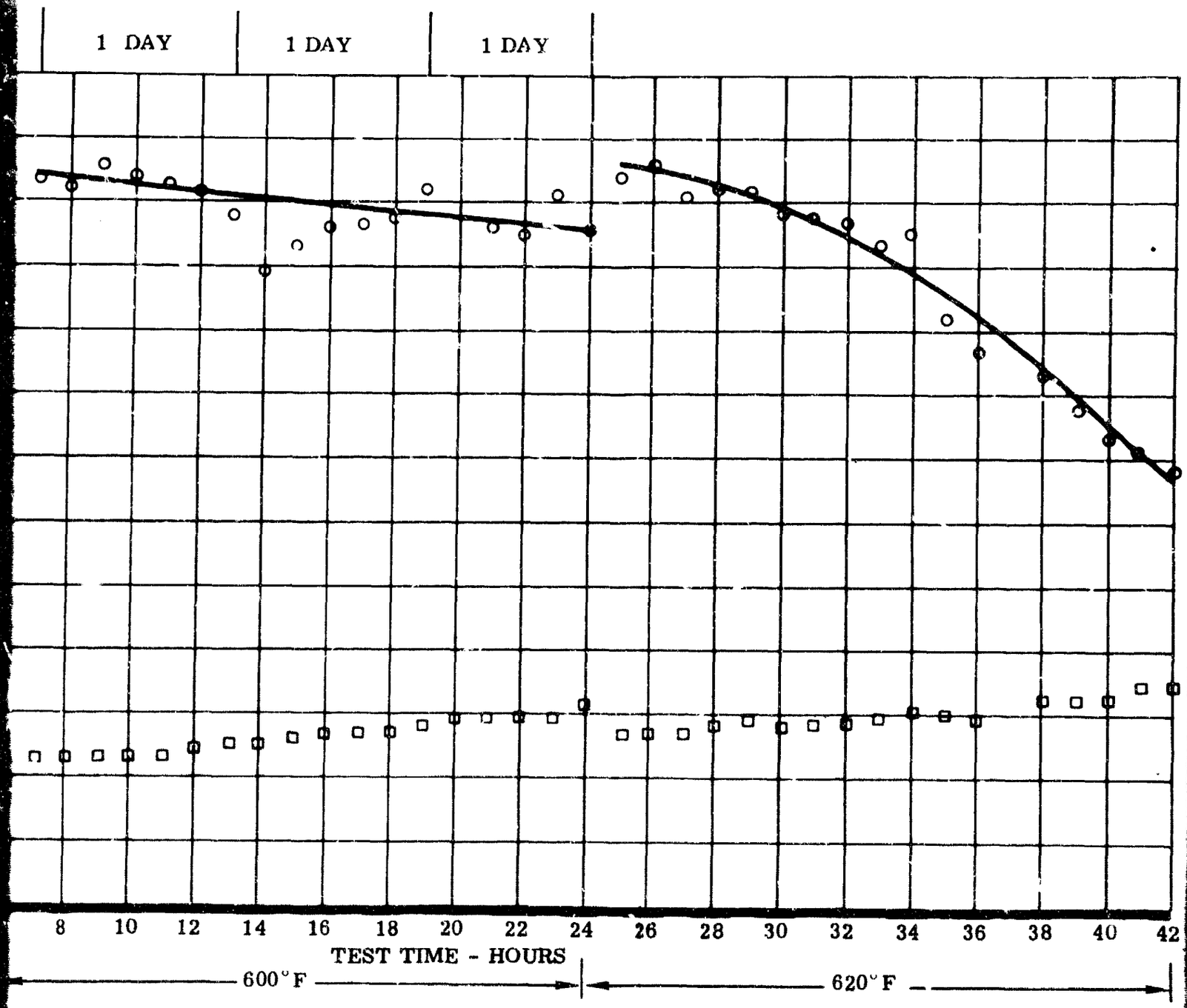

Figure 44. Minex Test Results - Second Run

2

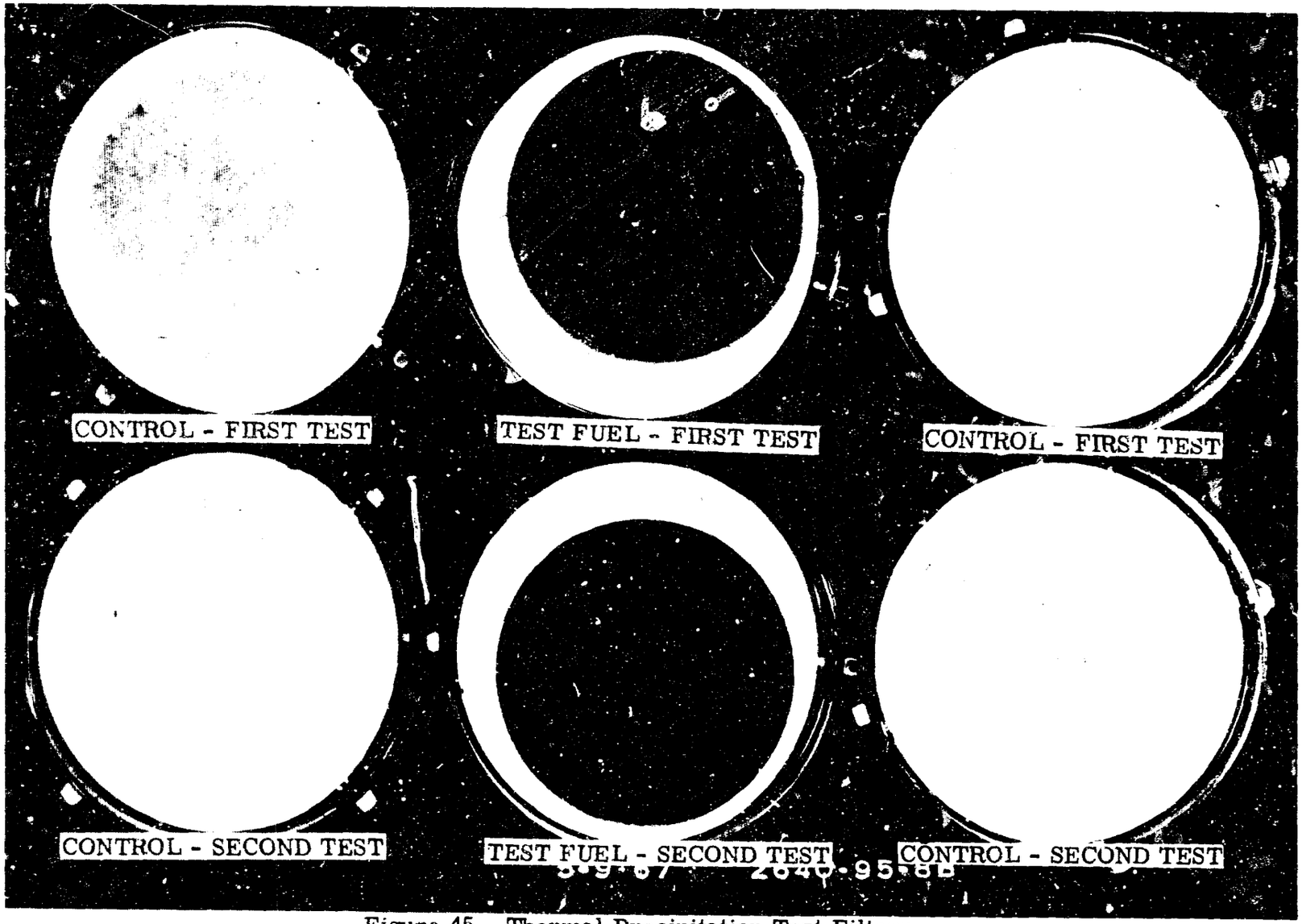

Figure 45. Thermal Precipitation Test Filters

SECTION VI

COMPARISON BETWEEN SIMULATOR AND SMALL-SCALE TESTS

The purpose of this section is to compare the simulator data to the small-scale test data. This will be a continuing effort in this program and additional fuels are to be tested; therefore, it is intended at this time to merely show correlation trends. Only one fuel (AFFB-8-67) has been tested to date in the simulator, and therefore, a comparison based on these data would not be indicative. Since other fuels have been tested in the small-scale devices and in the FAA-SST Fuel System Test Rig, which was modified into the simulator, these data are included in the analysis. A data correlation study carried out on the fuels tested in the FAA-SST Fuel System Test Rig is reported in Reference 22. Contained therein is the ranking of the fuels tested. Shown in Table V is the ranking of these fuels and AFFB-8-67 obtained by the same method. This table, along with Table IV, forms the basis of the discussion herein.

WING TANK

According to Reference 22, the ranking of the fuels tested in the FAA-SST Fuel System Test Rig in the order of increasing deposits was:

FA-S-2A
RAF-176-64
RAF-176-63
FA-S-1

The data used in obtaining this ranking was basically a comparison of the artist conception drawings of the deposits on the bottom of the wing tank. These fuels can be compared directly to the performance of AFFB-8-67 in the simulator because essentially the same environment and equipment were used. As additional fuels are tested in the simulator, the bases of comparison will be more quantitative than the use of drawings; i.e., the use of the probes, disk, disk, and thickness measurements. Applying the same approach (comparison of artist conception drawings) with fuel AFFB-8-67 the order of increasing deposits is considered to be:

FA-S-2A
RAF-176-64
RAF-176-63
AFFB-8-67
FA-S-1

Based on this ranking of the fuels in the wing tank, none of the small scale test devices that tested all five fuels ranked all five fuels in this order (2, 3, 1, 4, and 5). The Esso Unit (Vapor Phase Deposit Screening Unit) has ranked only three of the fuels (RAF-176-63, FA-S-2B, and AFFB-8-67). If it is assumed that FA-S-2B was the same fuel as FA-S-2A, then the Esso Unit ranking is the same as the wing tank ranking for the fuels.

This conclusion is to be anticipated since the Esso Unit is the only device which imposes environmental conditions (low pressure, presence of vapor, condensation, etc.) similar to the wing tank. The Minox and the cokers impose conditions (high pressure, all liquid phase, high flow, etc.) similar to the engine system.

It is to be noted that the above comparison is made on the basis of visual observations of the wing tank. As additional fuels are tested and quantitative data is obtained, the comparison will be made on a quantitative basis of the amount of deposit formed.

AIRFRAME SYSTEM

The wing tank discussed above was analyzed separately from the airframe system because the wing tank simulates a static system while the remaining airframe system, like the engine system, is dynamic. The fuselage tank is not discussed because no deposits were evident therein. The airframe system (excluding tankage) did not show any evidence of deposits. It is noteworthy that the SST Test Rig airframe heat exchanger did not exhibit performance change with any other of fuels after 290 test cycles at CRC Mach 3 conditions. This corresponds to a peak fuel temperature of 280°F and a peak metal temperature of 315°F. This is in agreement with the inlet of the engine and Uni-Tube heat exchanger where the maximum fuel and metal temperatures were 275 and 320°F, respectively. Therefore, it appears that the deposition of all the fuels tested in both programs is negligible with peak metal temperatures of 320°F. The results of the small-scale tests shown in Table IV are in general agreement with this finding.

ENGINE SYSTEM

The simulator results on AFFB-8-67 indicated that the fuel does not break (show visual signs of deposits in the order of a code 3 on the CRC Lacquer Rating Scale) until the peak film temperature was approximately 385°F in engine heat exchanger. The data obtained on the engine manifolds (both test cycles and the second steady state test) indicate that the rate of deposit formation can be quantified by $x_d/\theta = 15{,}600\ k_d\ e^{-6500/T}$ (see

page 65) where the deposit formation below a 375°F film temperature is negligible. As shown in Table IV, the critical metal temperature of the Minex is in the order of 200°F greater than this breakpoint, and the critical metal temperature of the cokers is in the order of 100°F greater than the simulator breakpoint. This apparent discrepancy in critical temperatures may be caused by a relative insensitivity of these tests to deposits. The only device which yields a critical temperature within 50°F of the simulator breakpoint is the Research Coker. This is on the basis of 300°F Code 2 Survey, 300°F Code 3 Survey, and 300°F Transit.

The Minex is the only small-scale device, similar in environmental conditions to the engine system, which yields quantitative data comparable to the simulator. Such data is shown on page 75. Using the deposition rate equation of fuel AFFB-8-67 determined from simulator tests and the Minex metal temperature profile (metal temperature in Minex is within 2°F of the film temperature) determined from Runs 1 and 2 shown in Figures 43 and 44, the predicted deposit thicknesses in the Minex tubes are 0.8 and 0.75 mils for the first and second runs, respectively. It can be seen from a comparison of these deposit thicknesses, based on simulator prediction data, to that data on page 75 that the data are in general agreement except for that based on carbon analysis. It was found that the carbon analysis test can give unrealistic values, i.e., in the steady state manifolds, page 64. Discounting the carbon analysis data, it appears that the simulator deposition rate equation may be valid for the Minex heat exchanger, and a correlation method is indicated.

In comparing fuel AFFB-8-67 to the fuels in the FAA-SST Fuel System TestRig extreme caution was used because of the difference in engine filter pore size and the performance of the engine pump. It was indicated in Reference 22 the data obtained downstream of the engine pump is in doubt because of the failures of this pump; such failures did not occur on the simulator engine pump. It was pointed out in Reference 4 that the effect of the pumps on the engine system components is considered to have decreased with each successive downstream component due to the filtering action of the components. Therefore, a comparison to the manifold and nozzle may be valid while the engine heat exchanger is questionable and the engine filter not worth discussing. The deposition equation, $x_d/\theta = 15{,}600\ k_d\, e^{-6500T}$, was applied to the film temperatures of the FAA-SST Test Rig - CRC - Mach 3 environment for the engine heat exchanger and manifold. This was done to predict how much deposits would have formed in the FAA-SST Test if fuel

AFFB8-67 had been tested therein. The results indicate that the engine exchanger overall heat transfer coefficient loss would not be measurable in 100 test cycles, and the manifold deposit thickness would be .001 to .002 mils per test cycle. Comparing these results to page 30 of Reference 4 it appears that AFFB-8-67 would rank higher than any of the fuels tested in the SST Test Rig. This would indicate that AFFB-8-67 is a better fuel in the engine system. This is not contradicted by a comparison of the engine nozzle performance.

Assuming that AFFB-8-67 is the better fuel, then it is evident that the fuels do not rank the same in the wing tank and the engine system. This phenomenon is to be anticipated since the environment and probably the deposit formation mechanisms are different. In general, (i.e., by summation of ranking in Table V, the Minex, Standard Coker, and Research Coker indicate that AFFB-8-67 is the best fuel, and the Esso Unit indicates that it is probably the third best fuel. This is in agreement with the above conclusion that the wing tank (similar to the Esso Unit) does not rank fuels the same as the engine system (similar to the Standard Coker, Research Coker, and Minex).

Therefore, based on these data, it appears that none of the small-scale devices singularly will predict the extent of deposition in both the static and dynamic system (i.e., "empty" wing tank and engine system). This suggests a need for using more than one of the above test devices or developing new small scale device. The success of the manifold data correlation obtained on the simulator to predict the thickness deposits in the manifold suggests a small scale device similarly designed to the manifold downstream of a device simulative of a wing tank.

TABLE V - RANKING OF FUELS

TEST DEVICE	BASIS OF COMPARISON (CRITICAL CONDITION)	RANKING				
		RAF-176-64	RAF-176-63	FA-S-2A	FA-S-1	AFFB-8-67
R COKER	300 F. CODE 3 SURVEY. METAL TEMP.	1	3	5	2	4
R COKER	300 F. TRANSIT. METAL TEMP.	1	3	5	2	4
R COKER	300 F. CODE 2 MAX.. FUEL TEMP.	1	3.5	5	3.5	2
R COKER	300 F. CODE 2 SURVEY. METAL TEMP.	1	4	2	3	5
R COKER	300 F. 3 IN. HG. MAX.. FUEL TEMP.	2	3	4	5	1
R COKER	300 F. CODE 2 AND 3 IN. HG. MAX.. FUEL TEMP	2	3	4	5	1
MINEX	RAPID DECREASE IN HF. FUEL TEMP.	2	3	4.5	4.5	1
MINEX	RAPID DECREASE IN HF. METAL TEMP.	2	3	4.5	4.5	1
MINEX	INITIAL CHANGE IN HF. FUEL TEMP.	2	3.5	3.5	5	1
MINEX	INITIAL CHANGE IN HF. METAL TEMP.	2	3.5	3.5	5	1
MINEX	ONE PERCENT LOSS IN HF/HR.. FUEL TEMP.	2	3.5	3.5	5	1
MINEX	ONE PERCENT LOSS IN HF/HR.. METAL TEMP.	2	3.5	3.5	5	1
R COKER	200 F. 3 IN. HG. MAX.. FUEL TEMP.	2.5	2.5	1	2.5	2.5
R COKER	300 F. 13 IN. HG. MAX.. FUEL TEMP.	3	2	4	5	1
COKER	CODE 2 MAX.. FUEL TEMP.	3	4	1	5	2
COKER	CODE 2 AND 3 IN. HG. MAX.. FUEL TEMP.	3	4	1	5	2
COKER	CODE 2 AND 12 IN. HG. MAX.. FUEL TEMP.	3	4	1	5	2
R COKER	200 F. CODE 2 AND 3 IN. HG. MAX.. FUEL TEMP	3	4	1	5	2
R COKER	200 F. CODE 2 MAX.. FUEL TEMP.	3	4	1	5	2
R COKER	200 F. CODE 2 SURVEY. METAL TEMP.	3	4	1	5	2
COKER	TRANSIT. METAL TEMP.	3	4	1.5	5	1.5
COKER	13 IN. HG. MAX.. FUEL TEMP.	3	4	2	5	1
MINEX	INITIAL DECREASE IN HF. FUEL TEMP.	3	4	2	5	1
MINEX	INITIAL DECREASE IN HF. METAL TEMP.	3	4	2	5	1
COKER	12 IN. HG. MAX.. FUEL TEMP.	3	4.5	2	4.5	1
R COKER	200 F. 13 IN. HG. MAX.. FUEL TEMP.	3.5	2	1	3.5	3.5
BOMB	TWENTY-FIVE PCT. LOSS LIGHT TRANS.	3.5	3.5	1	5	2
R COKER	AMB.. CODE 2 MAX.. FUEL TEMP.	3.5	3.5	1	5	2
R COKER	AMB.. CODE 2 AND 3 IN. HG. MAX.. FUEL TEMP.	3.5	3.5	1	5	2
R COKER	200 F. CODE 3 SURVEY. METAL TEMP.	3.5	3.5	1	5	2
R COKER	200 F. TRANSIT. METAL TEMP.	3.5	3.5	1	5	2
R COKER	AMB.. 3 IN. HG. MAX.. FUEL TEMP.	3.5	3.5	2	3.5	1
R COKER	AMB.. TRANSIT. METAL TEMP.	4	2.5	1	5	2.5
R COKER	AMB.. CODE 3 SURVEY. METAL TEMP.	4	3	1	5	2
R COKER	AMB.. 13 IN. HG. MAX.. FUEL TEMP.	4	3	2	5	1
COKER	3 IN. HG. MAX.. FUEL TEMP.	4.5	2	3	4.5	1
R COKER	AMB.. CODE 2 SURVEY. METAL TEMP.	4.5	3	1	4.5	2
COKER	CODE 2 SURVEY. METAL TEMP.	5	3	1	4	2
COKER	CODE 3 SURVEY. METAL TEMP.	5	3.5	2	3.5	1
ESSO UNIT RELATIVE ACTIVITY AT 375F			2	1		3

SECTION VIII

FUTURE WORK PLANNED

It is intended to continue testing fuels and analyzing the data in order to investigate the performance of hydrocarbon fuels under high Mach number flight conditions. As the quality of each fuel is quantified in the simulator, these values will be compared to small-scale test results. This will provide a basis for calibrating these devices for determining fuel suitability for advanced aircraft. Additionally, design criteria will be determined on the basis of the fuel performance and Air Force supplied design requirements for Advanced Aircraft.

The next fuel to be tested in the simulator will be of a poorer quality than AFFB-8-67. The environment will be the 600°F profile shown in Figure 5. This will permit the acquisition of a greater amount of performance degradation in a fewer number of test cycles. It is anticipated that the following fuel will be of the highest thermal stability quality attainable. This will permit a determination of the limit of use of available hydrocarbon fuels.

SECTION VIII

REFERENCES

1. ASTM D 1660-64 "Standard Method of Test for Thermal Stability of Aviation Turbine Fuels," adopted by ASTM, 31 August 1964

2. NAA Report NA-66-1380, "Advanced Aircraft Fuel System Simulator Modification and Performance Report," dated 27 December 1966

3. CRC Manual No. 5, "CRC Diesel Engine Rating Manual," page 36

4. NAA Report NA-65-247, "Performance of Current Quality Commercial Jet Fuel in the Supersonic Transport Airframe and Aircraft Engine Fuel System Test Rig," Final Report, Federal Aviation Agency Contract FA-SS-65-3, dated 14 May 1965

5. Esso Research and Engineering Company Quarterly Progress Report No. 2, AF33(615)-3575, 16 August - 16 November 1966

6. Monsanto Research Corporation Memo dated 15 February 1967, Job 2551-2

7. W-PAFB Air Force Material Laboratory Analysis Test Report on Wing Tank Deposits, dated 20 April 1967

8. W-PAFB Air Force Material Laboratory, Analysis Test Report on Wing Tank Deposits, dated 22 May 1967

9. Monsanto Research Corporation, Memo, dated 6 March 1967, Job 2551-2

10. Letter dated 17 May 1967 from R. T. Burgess of Pesco Products to R. P. Bradley of North American Aviation, Inc.

11. Monsanto Research Corporation, Memo, dated 15 February 1967, Job 2551-2

12. Rocketdyne Report RM 1084/362 "Study of an Endothermic Fuel for the Atlas Rocket Motor" dated 17 September 1967

13. Air Force Technical Report AFAPL-TR-64-154, "A Comparison of the Capabilities of a Fuel Coker and the Minor Heat Exchanger for Determining Hydrocarbon Fuel Thermal Stability," dated March 1965

14. Letter dated 11 May 1967 from R. R. Hibbard of the National Aeronautic and Space Administration to A. E. Zengel of Wright-Patterson Air Force Base

15. Letter dated 20 June 1967 from A. E. Zengel of Wright-Patterson Air Force Base to H. Goodman of North American Aviation, Inc.

16. Telephone call on 14 June 1967 between A. E. Zengel of Wright-Patterson Air Force Base and H. Goodman of North American Aviation, Inc.

17. Perry, R. H., et al; Chemical Engineering Handbook, McGraw Hill Book Co. New York, 4th Edition

18. Alberts, L., et. al. Handbook Chemistry and Physics; Chemical Rubber Publishing Company 46th Edition

19. University of Dayton Research Institute, Memo, dated 9 March 1967, FL67-9

20. Telephone call on 31 July 1967 between A. E. Zengel of Wright-Patterson Air Force Base and H. Goodman of North American Aviation, Inc.

21. L. Bagnetta, "Thermal Stability of Hydrocarbon Fuels," Technical Documentary Report APL TDR 65-89, Part II, Phillips Petroleum Co., June 15, 1965

22. NAA Report NA-65-753, "Data Correlation Study of Small-Scale Fuel Thermal Stability Test Devices and the FAA-SST Fuel System Test Rig," Final Report, Federal Aviation Agency Contract No. FA-SS-65-28, dated 30 November 1965

23. Esso Research and Engineering Company, Quarterly Progress Report No. 5, "Lubricity of Jet Fuels," AF33(615)-2828, 15 May - 15 August 1966

24. "Evaluation of Modified Fuel Coker for Measuring High Temperature Stability of Fuels for High Performance Aircraft," March 1966 (CRC Project No. CA-17-59)

25. Telephone call on 2 August 1967 between Tom Waddick of Wright-Patterson Air Force Base and H. Goodman of North American Aviation, Inc.

26. Pratt & Whitney Aircraft Division, Materials Control Laboratory Manual, Section Q-67, issued 3-31-66

27. "Thermal Stability of Hydrocarbon Fuels," APL TDR 64-89, Part II, Prepared by Phillips Petroleum Company under Contract No. AF33(657)-10639, August 1965

28. Monsanto Research Corporation, Memo, dated 26 April 1967, Job 2551-1

29. Esso Research and Engineering Company, Monthly Letter Report, dated 21 March 1967, "The Study of Hydrocarbon Fuel Vapor Phase Deposits," Contract No. AF33(615)-3375

UNCLASSIFIED

Security Classification

DOCUMENT CONTROL DATA - R & D

(Security classification of title, body of abstract and indexing annotation must be entered when the overall report is classified)

1. ORIGINATING ACTIVITY (Corporate author) North American Aviation, Inc. International Airport Los Angeles, California 90009	2a. REPORT SECURITY CLASSIFICATION Unclassified 2b. GROUP N/A

3. REPORT TITLE

High Temperature Hydrocarbon Fuels Research in an Advanced Aircraft Fuel System Simulator on Fuel AFFB-8-67

4. DESCRIPTIVE NOTES (Type of report and inclusive dates)

First Fuel Series Report, 3 January 1967 to 3 May 1967

5. AUTHOR(S) (First name, middle initial, last name)

Harold Goodman
Royce P. Bradley
Theodore G. Sickles

6. REPORT DATE	7a. TOTAL NO. OF PAGES	7b. NO. OF REFS
14 August 1967	vii + 91	29

8a. CONTRACT OR GRANT NO.	9a. ORIGINATOR'S REPORT NUMBER(S)
AF33(615)-3228 b. PROJECT NO. c. BPSN 6 (63 304801 62405214) d. BPSN 5 (68 0100 61430014)	NA-67-635 9b. OTHER REPORT NO(S) (Any other numbers that may be assigned this report) AFAPL-TR-67-116

10. DISTRIBUTION STATEMENT This document is subject to special export controls and each transmittal to foreign governments or foreign nationsl may be made only with prior approval of the Fuels, Lubrication, and Hazards Branch, Support Technology Division, Air Force Aero Propulsion Laboratory, Wright-Patterson AFB, Ohio

11. SUPPLEMENTARY NOTES	12. SPONSORING MILITARY ACTIVITY
	Air Force Aero Propulsion Laboratory Wright-Patterson AFB, Ohio

13. ABSTRACT

At elevated temperatures hydrocarbon jet fuels tend to form deposits that decrease heat exchanger efficiency and plug screens and filter elements. A small-scale device is required which has been demonstrated to be applicable to all qualities of hydrocarbon jet fuels and will quantify this tendency in terms meaningful to fuel system designers. In this report, the thermal stability of a fuel (AFFB-8-67) is quantified in terms of amount of deposit in an airframe and engine fuel system simulator. The data obtained from this first fuel series indicate that an expression, derived herein, in terms of time and temperature may predict the amount of deposits formed in any engine system using fuel AFFB-8-67.

Presently, the fuel's tendency to form deposits is determined by visual ratings of color. Two methods for determining the amount of deposits formed in a tube are discussed and a very favorable comparison results. A relationship is shown herein between these calculated values and the color of the deposits. It is shown that at certain levels of deposit thickness a color scale is insensitive to the amount of deposits. It is shown that at certain levels of deposit thickness a color scale is insensitive to the amount of deposits. In addition to fuel testing in the simulator, fuel AFFB-8-67 was tested in the Standard, Gas, Research, Modified and Micro Cokers, Minex, Thermal Precipitation Apparatus, 5 ml Bomb, and Esso's Standard Screening Unit.

(CONTINUED)

DD FORM 1 NOV 65 1473

UNCLASSIFIED

Security Classification

14. KEY WORDS	LINK A		LINK B		LINK C	
	ROLE	WT	ROLE	WT	ROLE	WT
Advanced Aircraft Fuel System Simulator						
Small-scale tests						
Thermal stability						
Fuel FTB-8-67						
Standard fuel coker						
Modified fuel coker						
Gas-driven coker						
Research coker						
Micro coker						
Minex						
Thermal precipitation apparatus						
5 ml Bomb						
Vapor phase screening unit						

ABSTRACT (continued)

Comparisons made to data obtained in small scale tests and the FAA-SST Data Correlation Study indicate that a static system (i.e., an "empty" wing tank) does not rank fuels the same as a dynamic system (i.e., engine system). Therefore, a dual type (static and dynamic) thermal stability device may be indicated. It was also indicated that the comparison criteria used in many of the small-scale tests yield breakpoints (initial deposition temperatures) 100 to 200°F below that indicated in the fuel system simulator.

This effort is continuing with the testing of additional fuel and Fuel Series Report will be released two months after completion of each fuel tested. The applicability of the above findings to these fuels will be reported therein.